Snowpack runoff formation processes during rain-on-snow events

PAR

Sebastian WÜRZER

ÉCOLE POLYTECHNIQUE
FÉDÉRALE DE LAUSANNE

Suisse
2018

Acknowledgements

Abstract

Rain-on-snow (ROS) events cause repeated flooding in many mountainous regions with a seasonal snow cover. The complex interaction of processes across spatial scales makes it difficult to accurately predict the effect of snow cover on runoff formation for an upcoming ROS event, often resulting in underestimating the flooding potential of a respective event. To improve predictability of such events, the present study aims to identify the dominant snowpack runoff formation processes at different spatial scales. Snow cover observations during natural ROS events and sprinkling experiments, as well as simulations of historical ROS events with the physics-based snow cover model SNOWPACK, lay the foundation for results presented in this thesis. The experimental work was a valuable way to gain hands-on experience of snow cover processes during ROS and collect data for model development and verification. The simulations of more than 1000 historical ROS events at station locations and 191 catchment-scale simulations, increased understanding of runoff formation processes for a variety of meteorological and snowpack conditions.

Meteorological forcing and initial snowpack properties were found to determine the temporal dynamics, intensities, and cumulative amount of snowpack runoff. Processes within the snowpack were found to modulate meteorological forcing such that runoff intensities were attenuated for intense and short rain events, but amplified for longer rain events. Although rainfall generally dominated snowpack runoff, individual events did have a significant snowmelt contribution. The analysis of spatially distributed snowpack simulations allowed identification of conditions leading to excessive snowpack runoff for whole catchments. These conditions include: a large snow-covered fraction, spatially homogeneous snowpack properties, prolonged rainfall events, and a strong rise in air temperature over the course of the event. A combination of these factors increases the probability of snowpack runoff occurring synchronously within the catchment, which in turn favours higher overall runoff rates. For both individual station locations and entire catchments, events with excessive snowpack runoff were more common during autumn and late spring, whereas winter snowpack usually retained part of the rainfall.

Lysimeter measurements during sprinkling experiments on cold and dry snowpack could not be reproduced in a satisfactory way using the two present water transport models in SNOW-PACK. This was attributed to the formation of preferential flowpaths. To address this problem, a dual-domain water transport scheme accounting for preferential flow was implemented in SNOWPACK. The presented approach was validated using an extensive dataset, comprised of meteorological and snowpack measurements as well as snow lysimeter runoff data for

more than 100 ROS events. Simulations of ROS on different initial snow cover conditions revealed that the new model was superior to existing approaches for conditions where field experiments found preferential flow to be prevalent.

The research presented in this thesis uses systematic analyses to identify meteorological and snowpack conditions which augment snowpack runoff formation during ROS. It further highlights the importance of correct meteorological forecasting and using detailed snowpack modelling for assessing the flooding potential of ROS in snow-affected catchments.

Key words: snow cover, liquid water transport, mountain hydrology, rain-on-snow, snowpack modelling

Zusammenfassung

Hochwasserereignisse im alpinen und subalpinen Raum werden oftmals durch Regenfälle auf eine Schneedecke, sogenannte „Rain-on-Snow" (ROS) Ereignisse, verursacht. Die Komplexität der beteiligten Prozesse erschwert es, den Einfluss der Schneedecke auf die Abflussbildung vorherzusagen und führt oftmals zu einer Unterschätzung des Hochwasserpotenzials. Um dieses besser abschätzen zu können, sollen in der vorliegenden Arbeit die jeweils dominierenden Abflussbildungsprozesse in verschiedenen Skalen identifiziert werden. Als Grundlage hierfür wurden Messungen während natürlicher Regenereignisse und Beregnungsversuchen, sowie Simulationen von über 1000 historischen ROS-Ereignissen an Stationsstandorten bzw. 191 Ereignissen über ganze Einzugsgebiete mit dem physikalisch basierten Schneedecken-modell SNOWPACK durchgeführt. Diese Kombination an experimentell erhobenen Daten und detaillierten Simulationen ermöglicht es zum einen, Schneedeckenabflussprozesse im Feld praktisch zu erfahren und Messdaten zur Modellentwicklung und -validierung zu gewinnen. Weiterhin konnten Schneedeckenprozesse nachgebildet werden, um allgemeingültigte Aussagen über den Einfluss äusserer Randbedingungen auf diese treffen zu können.

Menge, Intensität und die zeitliche Dynamik des Schneedeckenabflusses wurde dabei sowohl von meteorologischen Faktoren als auch von Schneedeckeneigenschaften bestimmt. So führen z.B. Schneedeckenprozesse zu einer Abschwächung der Schneedeckenabflussintensitäten für intensive und kurze Regenereignisse, jedoch zu einer Erhöhung für länger anhaltende Regen-fälle. Die Analyse räumlich verteilter Simulationen liess Verhältnisse identifizieren, welche insbesondere in gesamten Einzugsgebieten zu erhöhtem Schneedeckenabfluss führten: Diese sind ein hoher Flächenanteil der Schneebedeckung, räumlich homogen verteilte Schneedeck-eneigenschaften, längere Regenereignisse und stark ansteigende Lufttemperaturen. Eine Kombination dieser Faktoren ist wahrscheinlicher im Herbst und Spätfrühling, während im Winter ein Zusammentreffen der zuvor genannten Bedingungen eher selten ist. Sowohl an Stationsstandorten als auch in den Einzugsgebieten sind Ereignisse mit erhöhtem Schneedeck-enabfluss vor allem im späten Frühjahr und Herbst anzutreffen, wohingegen Winterereignisse meist einen gewissen Anteil an Regen zurückhalten. Die für die Schneeschmelze benötigte Energie wird primär durch turbulente Wärmeflüsse bereitgestellt.

Lysimetermessungen während Beregnungsversuchen auf eine kalte und trockene Schneedecke konnten mit den bestehenden Wassertransportmodellen in SNOWPACK nicht zufriedenstel-lend reproduziert werden. Dies wurde der Bildung präferentieller Fliesswege zugeschrieben. Um dieses Problem anzugehen, wurde SNOWPACK mit einem „dual-domain" Modell erweit-ert, welches die Bildung präferentieller Fliesswege berücksichtigt. Bei der Validierung mit

Lysimetermessungen von mehr als 100 ROS Ereignissen zeigte sich das Modell vor allem für kalte Schneedecken mit geringer Dichte überlegen, Bedingungen unter denen präferentielles Fliessen die Abflussbildung auch in Feldexperimenten dominierte.

Die Arbeit zeigt anhand systematischer Analysen verschiedene meteorologische Faktoren wie auch Schneedeckeneigenschaften auf, die eine verstärkte Abflussbildung während ROS-Ereignisse begünstigen und betont damit die Bedeutung verlässlicher meteorologischer Prognosen und detaillierter Schneedeckenmodellierung für die Hochwasservorhersage.

Stichwörter: Schneedecke, Regen-auf-Schnee, Gebirgshydrologie, Schneedeckenmodellierung, Wassertransport

Contents

Contents

List of Figures

List of Tables

1 Introduction

1.1 Motivation

Approximately 50% of the land area in the Northern Hemisphere is seasonally covered by snow (Armstrong and Brodzik, 2001). By releasing most of the winter precipitation during spring, snow constitutes an important part of the hydrologic cycle, and snowmelt dominates annual catchment runoff in many mountain regions and most regions higher than 45 °latitude (Barnett et al., 2005). Snowmelt provides fresh water for agriculture and human consumption for around one sixth of the world's population (Sturm et al., 2017) and constitutes an important source for hydro-electric power production (Winther and Hall, 1999). However, snow cover can also constitute a source of hazard. In particular, rain-on-snow (ROS) events can trigger a variety of natural hazards like flooding, landslides, and wet snow avalanches (Stimberis and Rubin, 2011), and these hazards can all occur at the same time. The frequency and characteristics of ROS events depend on the spatio-temporal variability of snow cover and meteorology and thus on the climatic and physiographic conditions of a respective region. Forecast systems can fail to predict the magnitude of runoff formation during ROS (Badoux et al., 2013), thus, research on the specific mechanisms that lead to unexpected peakflow is needed in order to improve runoff formation forecasting during ROS. Underforecasting peakflow generally results from inadequate meteorologic forecast data, limited process understanding, or insufficient process representation in hydrological models. Snow cover representation in hydrological models is usually limited to simple empirical models, and hence cannot be used for determining dominant snowpack processes during ROS. The flooding potential of a ROS event is an integration of a variety of processes at different temporal and spatial scales, which makes assessing the consequences of ROS a complex challenge for hydrological forecasting. In general, knowledge about processes during ROS is mostly based on case studies which primarily focus on the snowmelt energy contribution to runoff. To date, relatively little effort has focused on investigating the influence of snowpack properties on water transport and transient water storage during ROS. Particularly in Switzerland, ROS events have rarely been studied and most knowledge is based on the description of one individual event which occurred in October 2011 (Wever et al., 2014a, Rössler et al., 2014, Badoux et al., 2013). Given this limited

research based on individual events, it is impossible to make accurate deductions about the influence of external factors on runoff formation. This thesis focuses on the importance of initial snowpack properties and meteorological factors for snowpack runoff generation by systematically analyzing a large number of events at different scales. This allows us generate general assertions on ROS, which can hence be used to make predictions and improve snow cover models that are used operationally by hydrological services.

ROS events are a major cause of landslides in the Pacific Northwest of the USA (Osterhuber and Kattelmann, 1998, Harr, 1981) and Norway (Sandersen et al., 1997). Landslides are triggered when pore water pressures in saturated soils are increased due to high water input, such as that resulting from the combination of rapid melting and rainfall (Harr, 1986). Another type of gravitational mass movement often triggered during ROS are wet snow avalanches (Ferguson, 2000, Osterhuber and Kattelmann, 1998). The addition of liquid water in ROS can cause wet snow avalanches by either adding mass to the snow cover and increasing the stress on weak layers (Conway and Raymond, 1993) , or weakening bonds between grains and altering the snow texture (Brun, 1989, Conway and Raymond, 1993), therefore reducing the strength of a snowpack. Ice layers formed during ROS constitute another threat, since they hinder ungulate access to food resources and therefore cause widespread deaths (Putkonen and Roe, 2003, Vikhamar-Schuler et al., 2013, Forbes et al., 2016).

The focus of this work is the investigation of the hydrological implications of a snow cover experiencing rainfall, i.e., assessing the runoff potential of ROS events. Analyses on peak discharge show that ROS frequently contributes to high flows and ROS events often constitute up to 80% of annual peak flows (Il Jeong and Sushama, 2017, Merz and Blöschl, 2003, Sui and Koehler, 2001). Additionally, ROS events have shown the potential to generate some of the most devastating floods in many regions with seasonal snowpacks (e.g. Marks et al., 1998, Pomeroy et al., 2016, Kattelmann, 1997, Kroczynski, 2004, Rössler et al., 2014). In contrast, ROS events can also lead to reduced or delayed runoff generation and consequently result in reduced streamflow. Knowledge of the hydro-meteorological conditions that influence the flooding potential of a particular ROS event can be used to mitigate against the consequences of an upcoming ROS event.

1.2   Context

The following sections provide an overview of previous ROS research and snow cover processes governing snowpack runoff formation during ROS. First, the importance of a correct definition of what constitutes a ROS event, including an overview of former event definitions, is provided in Section 1.2.1. Whether the presence of a snow cover during rain augments snowpack runoff by generation of additional snowmelt or attenuates runoff generation by retaining rainfall is dependent on the energy available for melt, the initial energetic state of the snow cover, and on properties governing the transient storage of rainwater in the snowpack. The energy balance of the snow cover and the typical sources for snowmelt during ROS are discussed in Section 1.2.2.

Water storage and transport processes are discussed in Section 1.2.3. The governing processes influencing ROS runoff generation by processes determined by catchment physiography are described in Section 1.2.4. Section 1.2.5 points on the importance of large-scale meteorologic circulation patterns and atmospheric rivers on causing ROS. Finally, present knowledge on what factors lead to extreme flooding are summarized in Section 1.2.6.

1.2.1 Overview on literature and ROS event-definitions

Most studies on ROS focus on snowpack runoff formation with the motivation to improve flood forecasting and hazard assessment. This includes an extensive list of mostly point scale studies performing sprinkling experiments (Singh et al., 1997, Kohl et al., 2001, Eiriksson et al., 2013, Juras et al., 2016, 2017, etc.), assessing the mass balance by consecutive snow depth or SWE measurements (McCabe et al., 2007, Trubilowicz and Moore, 2017), lysimeter data (Berg et al., 1991, Jennings and Jones, 2015), or using models to assess the mass and energy balance changes during ROS (Wever et al., 2014a). Other studies have focused on ROS processes at the catchment scale (Garvelmann et al., 2015, 2014, Wayand et al., 2015, Freudiger et al., 2014, Rössler et al., 2014, Mazurkiewicz et al., 2008). Few case studies use retrospective hydrological modelling to identify the dominant processes governing runoff generation during ROS on the catchment scale (Rössler et al., 2014, Badoux et al., 2013). Kroczynski (2004) compared an event causing widespread flooding to an event with similar storm characteristics to identify snow cover characteristics leading to flooding. While most studies only assess total water available for runoff or snowmelt contribution, Berg et al. (1991) analysed 20 ROS events and conducted a regression analysis on storm and snowpack characteristics to identify predictors for measures concerning flood generation. While amount, duration, and intensity of snowpack runoff were all significantly correlated to their respective precipitation values, the time lag between onset of rain and snowpack runoff could not be explained by storm and snowpack characteristics. However, results of single studies are difficult to compare, since spatio-temporal characteristics of ROS events strongly depend on the region and the spatial and temporal scale and resolution of the respective study. The question of what constitutes a ROS event depends on the scientific focus, geographical perimeter, data availability, and technical restrictions of the respective study.

To assess the hydrologically relevant runoff formation processes at a catchment, the ROS event should be assessed from the start of rainfall till at least the peak of streamflow, if streamflow data are available. The boundaries of an event can be defined arbitrarily for single case studies, but otherwise one has to rely on correct assumptions about what constitutes a relevant ROS event for runoff formation. The number of event definitions for systematic investigations of a multitude of events are reflected by the number of studies and are usually chosen according to the purpose of the respective study. The most general definition of a ROS event is "rain falling on ground covered by snow". Commonly thresholds for rainfall totals within a given timeframe and snow depth or SWE are defined to identify hydrologically relevant events (Mazurkiewicz et al., 2008). Other studies require additional snowmelt derived by models (Freudiger et al.,

2014) or defined as a minimum decrease in snow depth or SWE (McCabe et al., 2007, Surfleet and Tullos, 2013, Wayand et al., 2015). With increasing spatial scale, averaging processes have to be taken into account, which is reflected by generally lower thresholds. For the major river systems of Germany, Freudiger et al. (2014) found thresholds of 3 mm of rainfall on a snowpack of at least 10 mm SWE suitable to detect potentially flood generating ROS events. If the perspective of a forecaster should be taken as a guiding principle, only thresholds of basic measures (rainfall totals and initial snow depth or SWE) should restrict the set of events to be able to generalize statements on what boundary conditions potentially form ROS floods. Such a broad definition allows for distinguishing snowpack and storm properties for events where snow cover might lead to attenuating conditions in contrast to flood events. As an example, with a cooling of air during the storm, a considerable amount of snowfall might lead to rising snow depth and SWE during the course of a ROS event. Berg et al. (1991) states that SWE values after ROS events don't differ considerably from pre-event conditions. Moreover, by focussing on peak flow events, it cannot be assure that similar meteorological and snow cover properties consequently lead to flooding. Even so, for a reliable qualitative prediction it is indispensable to assess how sensible runoff formation and flooding potential react to changes in meteorological parameters, snow cover properties, or catchment physiography.

1.2.2 Energy balance and snowmelt contribution

The augmentation of snowpack runoff relative to rain input is related to the energy input provided for snowmelt. Trubilowicz and Moore (2017) found snowmelt responsible for on average 25% of snowpack runoff at the point scale, which coincides with on average 27% snowmelt contribution found in Chapter 4. However, several studies found snowmelt contributions ranging from 7% to 70% at the catchment scale (Garvelmann et al., 2015, Sui and Koehler, 2007, Rössler et al., 2014, Wayand et al., 2015). The relative significance of snowmelt for snowpack runoff depends not just on snowmelt, but also on the amount of rainfall (Wayand et al., 2015). For higher total rainfall amounts, this implies that rainfall prediction should be prioritized when assessing a ROS event in advance (Wayand et al., 2015). Nevertheless, snowmelt contributions cannot be neglected since they can tip the balance to flooding, especially given the non-linear nature of runoff formation processes (Kirchner, 2009).

Assessing the exact snowmelt contribution during ROS requires the determination of single energy sources, displayed in the snowmelt energy balance (EB):

$$Q = Q_{sw} + Q_{lw} + Q_h + Q_l + Q_g + Q_p \qquad (1.1)$$

where Q is the total energy available to warm and melt the snowpack, Q_{sw} is the net shortwave radiative flux, Q_{lw} is the net longwave radiative flux, Q_h is the turbulent sensible heat flux, Q_l is the turbulent latent heat flux, Q_g is the ground heat flux, and Q_p is the energy advected by precipitation.

The relative importance of these terms is mainly governed by the meteorological conditions, but also by time of day, catchment physiography (elevation gradient, soils, etc.), and vegetation. Since meteorological conditions change over a certain period, their relative importance also changes with the length of the period under review. Net shortwave radiation depends on snow albedo and is most important during clear-sky conditions during the day, but completely absent during night. Net longwave radiation is primarily governed by incoming longwave radiation, which is mainly emitted from the lowest layers of the atmosphere in the absence of additionally emitting vegetation and terrain. It can therefore be estimated by the temperature and water vapour at typical sensor heights (Ohmura, 2001). The turbulent fluxes (sensible + latent) will both lead to increasing snowmelt as wind speed, temperature, or humidity increase. ROS events generally have positive air temperatures, overcast conditions, and are often accompanied by considerable wind speeds. These conditions limit the importance of shortwave radiative fluxes, but support increased incoming longwave radiative fluxes. Whereas turbulent heat fluxes typically compensate each other to some degree, during ROS conditions they usually both contribute to snowmelt and often constitute the dominant components of the snowmelt energy balance (Garvelmann et al., 2014, Marks et al., 1998, 2001). Heat advected by rain is an energy term unique to ROS events, however it contributes little to snowmelt (Singh et al., 1997). The ground heat flux is not dependent on the meteorological forcing and is usually of minor importance for shorter timescales. However, if snow falls on warm ground (e.g. during autumn), snowmelt can precondition soils for subsequent rain or melt events. It is commonly assumed that the snow cover must be isothermal at 0° C to allow for snowpack runoff. The initial heat deficit or cold content is than defined as the energy needed to heat up the snowpack to 0° C, sometimes expressed as by the water which needs to be refrozen to release that energy. The effect of vegetation on snowmelt will be depicted in Section 1.2.4.

There are two general concepts of snowmelt modelling: The temperature-index (TI) approach is based on the empirical relationship between air temperatures and melt rates (Hock, 2003, Ohmura, 2001). Full EB models, however, determine the single terms of the EB (Eq. 1.1) directly from measurements or use physics-based parametrizations. The TI approach was found to be sufficiently accurate for many applications in hydrology and is favoured for large-scale computations due to lower computational costs and the low data needs (Ohmura, 2001). However, standard TI models might underestimate snowmelt for ROS, since they do not account for wind and consequently fail for conditions where turbulent fluxes dominate snowmelt. This underpins the necessity of using full EB models like SNOWPACK to assess snowmelt under ROS conditions.

1.2.3   Liquid water transport and storage

Similar to the vadose zone, snow cover can be seen as a transient storage for liquid water (Webb et al., 2017). Snow cover can be represented by a three phase porous medium consisting of ice, liquid water, and air, with the hydraulic properties of snow changing with phase changes between the liquid and solid parts (Illangasekare et al., 1990). This section will give an overview

of the general concepts of water transport in snow. Details about the history of water transport models can be found in Chapter 2.

Despite the changes that occur in the ice matrix by snowmelt or refreeze processes, the mass balance of a snowpack during ROS is primarily governed by the transient storage of liquid water, which can lead to overall retention, and/or to a temporal offset between rain or snowmelt input and runoff leaving the snowpack. Once liquid water is introduced to the snow surface, a correct representation of water transport is crucial to predict the onset of snowpack runoff, which is of particular interest for assessing runoff formation at the catchment scale (See Section 1.2.4 and 6.2). Water transport is governed by the hydraulic conductivity of snow and therefore depends on physical characteristics like grain size. Analogous to soil, some liquid water in snow is held against gravity by capillary forces. The potential to retain water is often described as a fraction of pore space which has to be filled up to a certain threshold (called retention capacity or liquid water holding-capacity) before water is transported downwards. This retention capacity is empirically determined and expressed as a fraction of pore space, volume, or mass (Coléou and Lesaffre, 1998, Brooks et al., 2012, Garvelmann et al., 2015). Experiments show that the retention capacity (expressed as fraction of volume) of snow increases with snow density (up to ca. $600 \, \mathrm{kg \, m^{-3}}$) and decreases with grain size (Yamaguchi et al., 2012b). Since the introduction of rain leads to strong settling governed by wet snow metamorphism (Marshall et al., 1999), this process would suggest a higher retention capacity in snow (Yamaguchi et al., 2012b). However, the reduction of snowpack by melt will prevail for longer events, therefore lower the total retention capacity, and hence lead to additional snowpack runoff relative to the melt rate (Wever et al., 2014a).

Hydrological models such as PREVAH (Viviroli et al., 2009) or HBV (Bergstroem, 1995) use fixed or adjustable values for the retention capacity of snow cover. Until recently, physics-based snow cover models such as SNOWPACK and CROCUS (Vionnet et al., 2012) used solely such parametrizations for describing the amount of water held in respective snow layers. In soil science, the Richards Equation (RE, Richards, 1931), an approach accounting for both gravity and capillary forces, is widely used for describing water transport in unsaturated porous media. Especially at the onset of spring snowmelt and for hourly time-scales, implementing the RE in SNOWPACK led to a better reproduction of snowpack runoff measurements (Wever et al., 2014b, 2015). Recently, D'Amboise et al. (2017) also introduced a RE implementation in CROCUS. Although capillary forces in snow are rather small (Colbeck, 1974), they lead to water ponding on capillary barriers formed at distinct grain size transitions. This has been observed in laboratory experiments (Avanzi et al., 2016, Waldner et al., 2004) as well as in the field (Techel and Pielmeier, 2011, Eiriksson et al., 2013, and Chapter 2). Solving the RE enables the simulation of such features, which were found to support the formation of glide avalanches (Mitterer and Schweizer, 2013), ice layers (Pfeffer and Humphrey, 1998, Wever et al., 2016b), and preferential flowpaths (PFP) (Jordan et al., 2008, Eiriksson et al., 2013, Wever et al., 2016b). Further research in modelling water transport has been done by developing 3D water transport models that account for PFP in snow (Hirashima et al., 2014, 2017).
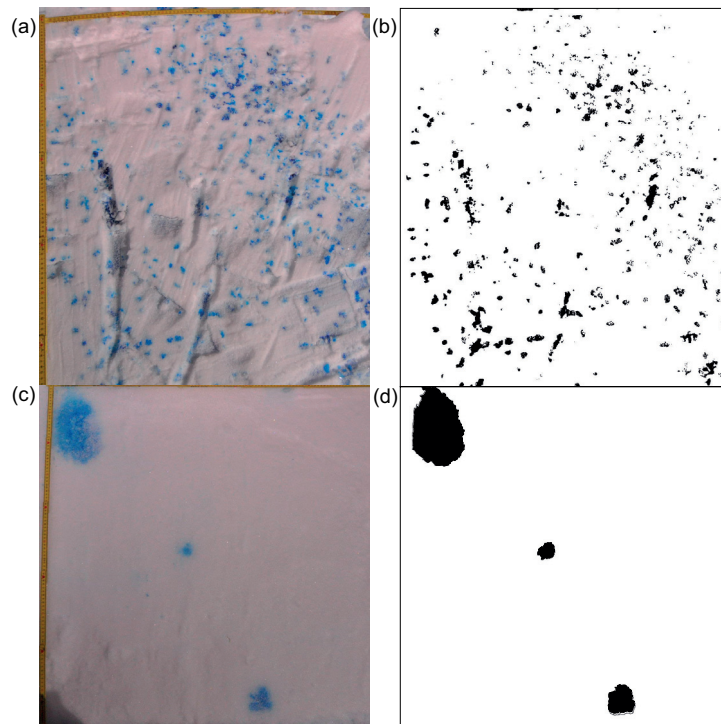
Figure 1.1 – (a,c) Photographs and (b,d) preferential flow areas identified by colour threshold analysis in different stratigraphic layers (a,b) near below the snow surface and (c,d) after a ponding layer.

The formation of PFP, in particular, was found to critically impact the timing of snowpack runoff during sprinkling experiments conducted for this thesis (Chapter 2) and Juras et al. (2017). By accounting for a relatively small amount of the snowpack volume, PFP put the concepts of retention capacity and cold content into perspective. Juras et al. (2017) show that percolation velocity under conditions promoting the formation of PFP is significantly increased. This shows that the effect of liquid water retention is more complicated and depends on snow conditions, thus, classical parametrisations lead to a significant overestimation of liquid water storage. Kattelmann and Dozier (1999) observed the formation of flow fingers of 1 cm diameter under spring melt conditions. However, abundance of PFP and the area taken up by PFP can vary significantly: Different studies found a large variety in the quantity of PFP ranging from 3 to 300 PFP m^{-2} (McGurk and Marsh, 1995, Williams et al., 2010, Albert et al., 1999). These numbers are within the range of numbers found in different stratigraphic layers of snow in experiments described in Chapter 2. Figure 1.1 shows 275 PFP m^{-2} (6% area) in a horizontal cut just below the snow surface and only 3 PFP m^{-2} (3% area) below a ponding layer. A vertical cut of typical profiles observed during sprinkling can be seen in Figure 2.1. There have been numerous observations of PFP (e.g. Gerdel, 1954, Marsh and Woo, 1984, Schneebeli, 1995), yet models used for operational purposes are usually not capable of accounting for such structures. The first implementation accounting for PFP in a physics-based 1D snow cover model was done in the companion studies presented in Wever et al. (2016b) and Chapter 2.

1.2.4 Catchment controls on runoff formation during rain-on-snow

Snow cover modulates precipitation input, so snowpack runoff can be regarded as a precipitation equivalent with divergent intensities and totals compared to rain input. Particularly for mountainous catchments, areas that retain, delay, or augment snowpack runoff usually coexist, and this can lead to significantly increased heterogeneity if compared to homogeneous rain input. Catchment physiography as well as individual storm characteristics determine the heterogeneity of energy input, mass, stratigraphy, and snow microstructure. For mountainous catchments spanning a wide elevational range, small uncertainties in temperature forecasts can cause a shift in snow line by several hundred metres and consequently increase the area affected by ROS. Wayand et al. (2015) found that hypsometry can cause variations in snowmelt contribution exceeding 100% when compared to when each elevation is assigned equal area. Blöschl et al. (1990) distinguished three states that the catchment snow cover can adopt. From low to high elevation these are: (1) saturated and runoff-producing (2) partly saturated and (3) dry snow (able to retain water) in upper elevations. Such variations in the state of snow cover were actually found to be decisive for the generation of flooding due to ROS (Kroczynski, 2004, Garvelmann et al., 2014, 2015). Despite fast snowpack ripening during ROS, variability in snow cover at the onset of rainfall will result in desynchronization of snowpack runoff generation (See also Sections 1.2.6 and 4). Since elevational gradients also determine storm characteristics such as the phase and amount of precipitation, storm velocity and the conditional rise in temperature will significantly influence synchronicity. Rössler et al. (2014) stresses the importance of full catchment scale simulations to be able to represent local orographic effects like seeder-feeder clouds, causing localized large amounts of rainfall. Such phenomena increase the risk of exceeding soil infiltration capacities and trigger local phenomena such as landslides and avalanches.

The presence of a forest canopy controls catchment snowmelt by significantly increasing incoming longwave radiation, but decreasing incoming shortwave radiation by shading. Both turbulent fluxes usually decrease with reduced wind speeds in forests (Garvelmann et al., 2014, Marks et al., 1998). Research on the impact of forest cover on runoff production during ROS is commonly focused on investigating the hydrological aspects of clear cutting. Generally, higher snowpack runoff is observed from open sites (Harr, 1986, Beaudry and Golding, 1983, Kattelmann, 1987a, Berris and Harr, 1987). Also, recent simulations by Wayand et al. (2015) suggest that catchment forest cover usually has a damping effect on snowmelt generation during ROS. However, some studies found no significant changes between open and forest sites (Berg et al., 1991, Garvelmann et al., 2015). Harr and McCorison (1979) did even find lower and delayed peakflows for a catchment after clear cutting. This was partly attributed to intercepted snow that experiences higher turbulent energy input and increased liquid water input to the snowpack during melting (Harr and McCorison, 1979). Additionally, snowmelt processes in small clearings might be affected by increased LWR input from nearby forest canopies (Seyednasrollah and Kumar, 2014).

Snow cover processes are tightly coupled to the hydrological system of the catchment. The
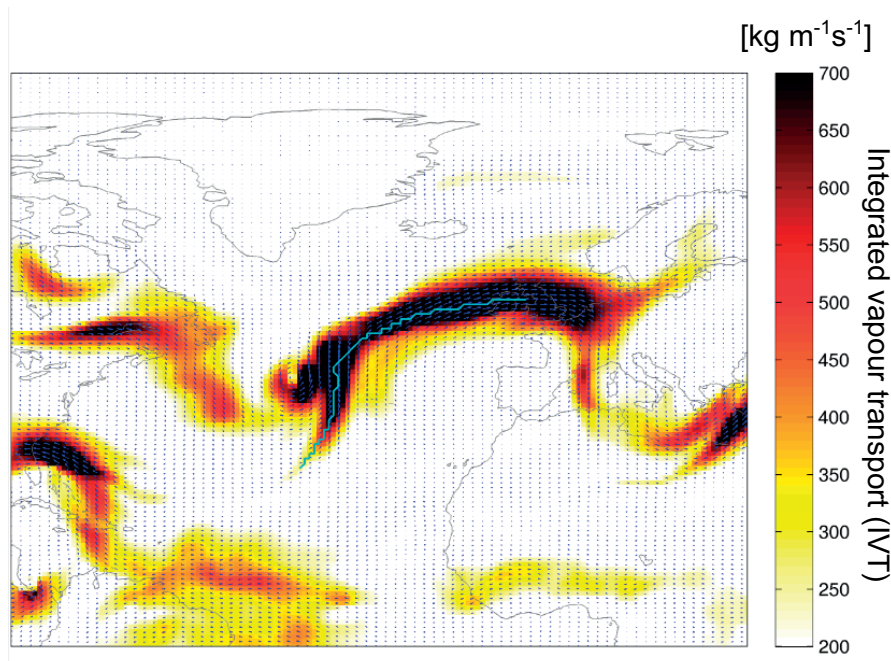
Figure 1.2 – Atmospheric river on October 2011, data and visualisation from Brands et al. (2017)

presence of snow cover was found to promote fast runoff processes by preconditioning the soil during snowmelt (Blöschl et al., 1990), or by forming basal ice layers (Stähli et al., 2001). Water travel times in snowpack were shown to substantially affect whole catchment travel times and eventually diurnal peak discharges (Lundquist et al., 2005, Lundquist and Dettinger, 2005). By shifting the storm meteorology of a ROS event to earlier or later periods in the year, Fang and Pomeroy (2016) show that peak flood discharge changes significantly with the state of the antecedent snow cover. The distribution of the snow cover is especially important for long-lasting events, since it determines the area contributing to snow melt (Garvelmann et al., 2015).

1.2.5 Large scale weather phenomena associated with rain-on-snow

The seasonality of ROS occurrence is strongly dependent on the region and elevation of the catchment. So called "Christmas floods" (Weihnachtshochwasser in German) are a common phenomenon in low elevation mountain ranges of Austria, Germany, and Switzerland (Merz and Blöschl, 2003, Sui and Koehler, 2001, Parajka et al., 2010, Caspary, 1995). They usually form when snowfall reaches down to low-elevation mountain ridges and a subsequent rise in temperature coincides with considerable rainfall. However, simulations conducted by Köplin et al. (2014) suggest that with a warming climate, mid-winter ROS events might become a more common phenomenon in currently cold climates and high alpine regions, where ROS floods are presently rather expected during the ablation period (Blöschl et al., 1990).

Caspary (1995) found that the three most extreme flooding events that occurred in two Black Forest catchments over 60 years feature this pattern. Moreover, these events, similar to all extreme winter flooding events, were caused by the large-scale circulation pattern called "west cyclonic" (Wz). An increase in frequency and persistence of the Wz circulation system led to an almost simultaneous increase in annual peak flows for the study region. Moreover, Parajka et al. (2010) found the Wz circulation caused over 50% of the annual precipitation maxima along the main Alpine ridge in Austria, the central Alps, and the Jura region in Switzerland, and that annual maximum floods in pre-alpine areas were found to be caused by ROS.

An atmospheric river (AR) is a long, narrow corridor of vapour-rich air and strong winds (Gimeno et al., 2014). The heavy precipitation observed during the October 2011 event was caused by such an AR (Rössler et al., 2014, Piaget et al., 2015). Figure 1.2 shows this AR for 11. October 2011 (Brands et al., 2017). If ARs hit mountainous terrain, forcing the air upwards, orographic enhancement of rainfall can lead to extreme precipitation and eventually flood events (Ralph et al., 2006, Gimeno et al., 2014). These types of floods are commonly observed in mountainous coastal areas such as the coastal regions of western North America (Ferguson, 2000). Moreover AR can support small scale enhancements in meteorological forcing in rough terrain, e.g. due to seeder-feeder effects (Rössler et al., 2014). In Europe, AR mainly hit the Iberian peninsula, northern France, great Britain, and the Norwegian coast (Brands et al., 2017), whereas they account for just 5% of winter precipitation in the northern ridge of the Alps and the Swiss Plateau (Lavers and Villarini, 2015). Lavers et al. (2011) found that the 10 largest winter floods of Britain since 1970 were associated with AR. Eiras-Barca et al. (2017) states that AR might not be the main source for floods; however, with rainfall increased by about 200% compared to non-AR rainfall, they form the majority of severe cases. Ralph et al. (2011) showed that the majority of quantitative precipitation predictions are biased low, particularly for greater lead times. However, it was shown that water vapour transport has higher medium-range predictability compared with precipitation (Lavers et al., 2014). When the presence of an AR is known in advance, hydrological forecasters should account for this under-prediction of quantitative precipitation forecasts by numerical weather models and hence adapt their flood predictions.

1.2.6 A recipe for extreme flooding

Generally speaking, the total rain- and meltwater leaving the snowpack must lead to sufficient soil infiltration or overland flow to cause flooding. Several studies conclude with some sort of "recipe" to outline the importance of the initial snow cover properties on controlling extreme ROS floods. These recipes include a significant amount of (intense) rainfall, a ripe snowpack with persistent snowmelt (indicating soils are near saturation), the synchronization of snowmelt and rainfall over most or all parts of the catchment (Jones and Perkins, 2010, Kroczynski, 2004, Jennings and Jones, 2015), and for the catchment to be fully snow covered (Jones and Perkins, 2010). Additionally, Kroczynski (2004) mentions that the "catalyst meteorological event" should provide warm air and dew-point temperatures as well as strong winds

for a considerable time. The fact that not all studies mention storm controls might display the limited significance of snowmelt amount on ROS flood generation. It is instead expected that processes promoting synchronous snowpack runoff control for catchment flood generation (Jones and Perkins, 2010, Jennings and Jones, 2015). However, Jones and Perkins (2010) state that it is still unclear how snowpack characteristics promote runoff synchronicity and how this synchronicity precisely contributes to extreme ROS floods. Experiments from Juras et al. (2017), however, suggest that a non-ripe snowpack leads to a quicker response due to PFPs. The large ROS event that occurred in October 2011 did not incorporate all the "ingredients" mentioned above to form an extreme flood. Snow cover was not in a ripe state for large parts of the catchments. However, the event supports the statement of Horton (1915) that suggests that the formation of a fresh, homogeneous and shallow snow cover followed by a warm heavy rain often results in flooding. Even if the total amount of snowmelt is not the main cause of extreme floods, it still supports flooding by augmentation of precipitation.

1.3 Summary of contents and research outline

The preceding sections provided a brief review of ROS literature (Section 1.2.1), snow cover processes at the point scale (Sections 1.2.2 and 1.2.3), their variability (Section 1.2.4) and their relevance for flooding potential during ROS (Sections 1.2.6). Despite an already wide range of literature on various issues regarding runoff formation during ROS, there are a number of gaps in knowledge that result from the design of those studies. Most studies are case studies or such that only focus on extreme flooding events, so it is difficult to draw general conclusions about dominant snow cover processes during ROS, specifically for regions with different climatological and physiographic conditions than those of the case studies. The goal of this work is to increase understanding of snow cover processes and their influence on snowpack runoff formation during ROS conditions at a variety of spatial scales and under different snow cover conditions. Eventually, a better process-based understanding will improve the assessability of runoff generation before ROS events, and help plan mitigating measures.

To be able to assess the range of relevant runoff formation processes, a combination of extensive field work and detailed modelling was chosen. Snow cover observations during natural ROS events and sprinkling experiments provided a hands-on experience of snow cover processes during ROS and model verification, whereas simulations of historic ROS events allowed for making general statements about runoff generation processes during ROS under a variety of meteorological and snowpack boundary conditions. Each of the three analysis chapters presented in this thesis focuses on the relevant processes at different scales: Chapter 2 uses measurements of mass balance during natural and experimental ROS events to investigate the importance of PFP on snowpack runoff formation and validate a dual-domain water transport model for the 1D model SNOWPACK that accounts for PFP. Chapter 3 investigates snowpack runoff formation on a vast number of point simulations at station locations. Chapter 4 focuses on identifying dominant snowpack runoff formation processes at the catchment scale and tests the transferability of assertions made in Chapter 3. In Chapter 5,

three publications which were conducted in close collaboration with this dissertation project are presented shortly. The final chapter, 6, discusses the conclusions and findings from the three analysis chapters and provides an outlook on procedures for future research.

The first analysis chapter (Chapter 2) focuses on the correct representation of water transport within the snowpack and seeks to determine the effect of preferential flow on runoff formation with respect to different initial snowpack conditions, representing either midwinter or spring snowpacks. To be able to account for the formation of preferential flow paths observed during field experiments, the SNOWPACK model was extended with a dual-domain water transport model based on the Richards' Equation. The new water transport model was validated against an extensive dataset of over 100 ROS events from several locations in the European Alps. This dataset, comprised of meteorological and snowpack measurements as well as snow lysimeter runoff data, allowed for testing the model under a variety of initial snowpack conditions, including cold, ripe, stratified and homogeneous snow. The goal of this study was to (1) investigate if accounting for preferential flow leads to improved snowpack runoff representation during ROS if compared to just matrix flow and (2) observe if the performance of this approach specifically benefits from certain snowpack or meteorological conditions. Results show that the model that accounts for preferential flow demonstrated an improved overall performance, where, in particular, the onset of snowpack runoff was captured more accurately. While the results were ambiguous for experiments on isothermal wet snow, improvements were pronounced for experiments on initially dry and cold snowpacks with low density. Sprinkling experiments with dye tracer identified preferential flow to be especially prevalent under such conditions. However, during initially wet conditions, accounting for preferential flow does not enhance model performance, which is attributable to the limited importance of preferential flow during such conditions. As a result of this study and a companion paper (Wever et al., 2016b), SNOWPACK now provides a better process representation for liquid water transport in cold snow.

In the second analysis chapter (Chapter 3), data of simulations of a vast number ROS events in the Swiss Alps were used to identify the dominant snowpack runoff processes. The focus of this study was to identify (1) the main contributing energy balance terms for different magnitudes of rain-on-snow events, (2) meteorological conditions associated with an amplifying, damping and/or delaying effect on snowpack runoff generation and (3) the influence of the initial snowpack conditions on the evolution of snowpack runoff generation. A strong seasonal and elevational dependence of snowpack and meteorological conditions was reflected by the characteristics of snowpack runoff generation. As a result, events with intensified snowpack runoff were most common during the late snowmelt season, with several such events also occurring in late autumn. Temporal dynamics, intensities and the cumulative amount of snowpack runoff were mainly determined by initial snowpack conditions like liquid water content (LWC) and snow depth, as well as by rainfall intensities. In particular, events with high initial LWC were associated with high runoff excess and short time lags. Meteorological forcing is modulated by processes within the snowpack, leading to an attenuation of runoff intensities for intense and short rain events, and an amplification of runoff intensities for

longer rain events. The results further confirmed that latent and sensible heat fluxes provided most of the snowmelt energy for individual events. Based on the results in Chapter 3, it can be assumed that a homogeneous and initially wet snowpack would support augmented catchment snowpack runoff by synchronizing catchment snowmelt. This study created the foundation for the hypotheses investigated in Chapter 4.

The final analysis chapter (Chapter 4) investigates (1) how meteorology, initial snowpack properties, and catchment characteristics jointly control runoff formation during ROS events and (2) if there are particular combinations of storm, snowpack, and catchment characteristics that entail an increased risk of excessive runoff and subsequent flooding. Spatially distributed SNOWPACK simulations allowed for identification of key factors that increase the likelihood of synchronous runoff formation, increased runoff intensities, and in turn high flooding potential. These are: (1) a high fraction of the catchment covered by (2) preferably shallow snow with (3) spatially homogeneous and (4) wet snow cover conditions, as suggested in Chapter 3. Important meteorological factors are (5) high or increasing air temperatures over the course of the ROS event and (6) long lasting rain events, which lead to amplified runoff rates. A low snow-covered fraction (SCF) restrains the potential for generating extreme floods during spring. With a high SCF, winter events entail a significant potential for pronounced runoff formation, but a combination of the key factors as mentioned above is less likely. However, a higher increase in air temperature could have resulted in approximately 25% more catchment rainfall for the investigated winter events. A scenario fulfilling most of the criteria for flooding potential would therefore start with a low SCF, followed by snowfall that forms a shallow homogeneous snow cover over large parts of the catchment, which is then followed by a storm involving warm air and extensive rain. Results show that the October 2011 event was exceptional in its combination of air temperature evolution, a high snow covered fraction, snow cover runoff synchronicity, and consequently high runoff excess intensities.

2 Modelling liquid water transport in snow under rain-on-snow conditions – considering preferential flow

Sebastian Würzer[a,b], Nander Wever[b,a], Roman Juras[a,c], Michael Lehning[a,b], Tobias Jonas[a]

[a]WSL Institute for Snow and Avalanche Research SLF, Davos, Switzerland
[b]École Polytechnique Fédérale de Lausanne (EPFL), School of Architecture, Civil and Environmental Engineering, Lausanne, Switzerland
[c]Faculty of Environmental Sciences, Czech University of Life Sciences Prague, Kamýcká 129, 165 21, Prague, Czech Republic

Summary

Rain on snow (ROS) has the potential to generate severe floods. Thus, precisely predicting the effect of an approaching ROS event on runoff formation is very important. Data analyses from past ROS events have shown that a snowpack experiencing ROS can either release runoff immediately or delay it considerably. This delay is a result of refreeze of liquid water and water transport, which in turn is dependent on snow grain properties but also on the presence of structures such as ice layers or capillary barriers. During sprinkling experiments, preferential flow was found to be a process that critically impacted the timing of snowpack runoff. However, current one-dimensional operational snowpack models are not capable of addressing this phenomenon. For this study, the detailed physics-based snowpack model SNOWPACK is extended with a water transport scheme accounting for preferential flow. The implemented Richards equation solver is modified using a dual-domain approach to simulate water transport under preferential flow conditions. To validate the presented approach, we used an extensive dataset of over 100 ROS events from several locations in the European Alps, comprising meteorological and snowpack measurements as well as snow lysimeter runoff data. The model was tested under a variety of initial snowpack conditions, including cold, ripe, stratified and homogeneous snow. Results show that the model accounting for

preferential flow demonstrated an improved overall performance, where in particular the onset of snowpack runoff was captured better. While the improvements were ambiguous for experiments on isothermal wet snow, they were pronounced for experiments on cold snowpacks, where field experiments found preferential flow to be especially prevalent.

2.1 Introduction

The flooding potential of rain-on-snow (ROS) events has been reported for many severe floods in the US (Kattelmann, 1997, Kroczynski, 2004, Leathers et al., 1998, Marks et al., 2001, McCabe et al., 2007), but also in Europe (Badoux et al., 2013, Freudiger et al., 2014, Rössler et al., 2014, Sui and Koehler, 2001, Wever et al., 2014a) where for example up to 55 % of peak flow events could be attributed to ROS events for some parts of Austria (Merz and Blöschl, 2003). With rising air temperature due to climate change, the frequency of ROS is likely to increase in high-elevation areas (Surfleet and Tullos, 2013) as well as in high latitudes (Ye et al., 2008). Besides spatial heterogeneity of the snowpack and uncertainties in meteorological forcing, deficits in process understanding make the consequences of extreme ROS events very difficult to forecast (Badoux et al., 2013, Rössler et al., 2014). For hydro-meteorological forecasters, it is particularly important to know a priori how much and when snowpack runoff is to be expected. Particularly, a correct temporal representation of snowpack processes is crucial to identify whether the presence of a snowpack will attenuate or amplify the generation of catchment-wide snowpack runoff. Most studies investigating ROS only consider the generation of snowpack runoff on a daily or multi-day timescale, where an exact description of water transport processes is less important than for sub-daily timescales (Wever et al., 2014b). Water transport processes are further usually described for snowmelt conditions, but not for ROS conditions, where high rain intensities may fall onto a cold snowpack below the freezing point. In this study however, we particularly focus on snowpack runoff generation at sub-daily scales with special attention to the timing of snowpack runoff which is influenced by preferential flow (PF).

Many studies have shown that flow fingering or PF is an important water transport mechanism in both laboratory experiments (Hirashima et al., 2014, Katsushima et al., 2013, Waldner et al., 2004) and under natural conditions, using dye tracer (Gerdel, 1954, Marsh and Woo, 1984, Schneebeli, 1995), temperature investigations (Conway and Benedict, 1994) or by measuring the spatial variability of snowpack runoff (Kattelmann, 1989, Marsh and Pomeroy, 1993, Marsh, 1999, Marsh and Woo, 1985). The variability of snowpack runoff is defined by the distribution and size of preferential flow paths (PFPs), which are dependent on the structure of the snowpack and weather conditions (Schneebeli, 1995). Beyond its importance for hydrological implications, PF may also be crucial for wet snow avalanche formation processes, where snow stability can be depending on the exact location of liquid water ponding (Wever et al., 2016a).

Most snow models describe the water flow in snow as a uniform wetting front, thereby implicitly only considering the matrix flow component. The history of quantitative modelling of water transport in snow starts with Colbeck (1972), who first described a gravity drainage

water transport model for isothermal, homogeneous snow. This was done by applying the general theory of Darcian flow of two-fluid phases flowing through porous media, neglecting capillary forces. Because water transport is not just occurring in isothermal conditions and snow can therefore not be treated as a classical porous medium, Illangasekare et al. (1990) were the first to introduce a 2-D model being able to describe water transport in subfreezing and layered snow. A detailed multi-layer physics-based snow model, where water transport was governed by the gravitational part of the Richards equation (RE) described in Colbeck (1972), was introduced by Jordan (1991). With the implementation of the full RE described by Wever et al. (2014b), the influence of capillary forces on the water flow was firstly represented in an operationally used snowpack model.

A model accounting for liquid water transport through multiple flow paths was developed by Marsh and Woo (1985), but was not able to explicitly account for structures like ice layers and capillary barriers. Recently, multi-dimensional water transport models have been developed, which allow for the explicit simulation of PFPs (Hirashima et al., 2014). These models are valuable for describing spatial heterogeneities and persistence of PFPs, but have not yet been shown to be suitable for hydrological or operational purposes. In general, multi-dimensional models are limited by the fact that they are computationally intensive, thus not thoroughly validated for seasonal snowpacks, and still lack the description of crucial processes such as snow metamorphism and snow settling.

In snowpack models which are used operationally, PFPs are not yet considered. The recently introduced RE solver for SNOWPACK led to a significant improvement of modelled sub-daily snowpack runoff rates. For this paper, we further modified the transport scheme for liquid water by implementing a dual-domain approach to represent PFPs. This new approach is validated against snow lysimeter measurements which were recorded during both natural and artificial ROS events.

This study aims to better describe snowpack runoff processes during ROS events within snowpack models that can be used for operational purposes such as avalanche warning and hydrological forecasting. This requires that the model results remain reliable, i.e. that improvements are not realized at the expense of a decreased model performance during periods without ROS, and that the model must not be too computationally expensive. This is the first study to test a water transport scheme accounting for PF which has been implemented in a snowpack model that meets the above requirements.

Our analysis of simulations of over 100 ROS events targets the following research questions:

- Is snowpack runoff during ROS in a 1-D model better reproduced with a dual-domain approach to account for PF than with traditional methods considering matrix flow only?

- Are there certain snowpack or meteorological conditions, for which the performance specifically benefits if PF is represented in the model?

This paper is structured as follows: Sect. 2.2 describes the snowpack model setup, the water transport models, input data and the event definition. Results of the simulations are shown in Sect. 2.3. This includes data of sprinkling experiments of ROS (2.3.1), natural ROS events (2.3.2) and the validation of the model on a long-term dataset from two alpine snow measurement sites (2.3.3). The results are discussed in Sect. 2.4, followed by the general conclusions found in Sect. 2.5.

2.2   Methods

All results in this study are derived from simulations with the one-dimensional physics-based snowpack model SNOWPACK (Bartelt and Lehning, 2002, Lehning et al., 2002b,a, Wever et al., 2014b) using three different water transport schemes, described in Sect. 2.2.2. The model was applied to four experimental sites that were set up for this study in the vicinity of Davos (Sect. 2.2.3). These sites were maintained over two winter seasons between 2014 and 2016 where data were recorded for several natural ROS events. At the same sites, we conducted a set of six sprinkling experiments to simulate ROS events for given rain intensities (Sect. 2.2.4). Furthermore, we conducted simulations for two extensive datasets from the European Alps: Weissfluhjoch (Switzerland, 46.83° N, 9.81° E, 2536 m a.s.l., WSL Institute for Snow and Avalanche Research SLF (2015), abbreviated as WFJ in the following) and Col de Porte (France, 45.30° N, 5.77° E, 1325 m a.s.l., Morin et al. (2012), abbreviated as CDP in the following). These datasets provide meteorological input data for running SNOWPACK as well as validation data, including snowpack runoff. Both datasets have already been used for simulations with SNOWPACK (Wever et al., 2014b) and provide data over more than 10 years each.

Below, the SNOWPACK model and the different water transport models are described first, followed by the description of the field sites for ROS observation in the vicinity of Davos. Then, we detail the setup of the artificial sprinkling experiments. After summarizing the WFJ and CDP dataset, we finally present the definition of ROS events that is used in this study. Most analyses were performed in R 3.3.0 (R Development Core Team, 2016) and figures were created with base graphics or ggplot2 (Wickham, 2009).

2.2.1   Snowpack model setup

The setup of the SNOWPACK model is similar to the setup used for simulations in Würzer et al. (2016). For all simulations, snow depth was constrained to observed values, which means that the model interprets an increase in observed snow depth at the stations as snowfall (Lehning et al., 1999, Wever et al., 2015). Because the study focuses on the event-scale and snowpack runoff is essentially dependent on the properties of the available snow, this approach was chosen such that we have the most accurate initial snow depth at the onset of the events to achieve the best comparability between the three water transport models. The temperature used to determine whether precipitation should be considered rain (measurements from rain

gauges) or snow (from the snow depth sensors) was set to achieve best results for reproducing measured snow height for precipitation driven simulations for the Davos field sites (between 0 and 1.0 °C). For WFJ and CDP, this threshold temperature was set to 1.2 °C, where mixed precipitation occurred proportionally between 0.7 and 1.7 °C. Turbulent surface heat fluxes are simulated using a Monin–Obukhov bulk formulation with stability correction functions of Stearns and Weidner (1993), as described in Michlmayr et al. (2008). At the Davos field sites (Sect. 2.2.3) incoming longwave radiative flux is simulated using the parameterization from Unsworth and Monteith (1975), coupled with a clear-sky emissivity following Dilley and O'Brien (1998), as described in Schmucki et al. (2014). For the roughness length z_0, a value of 0.002 m was used for all simulations at the Davos field sites and WFJ, whereas a value of 0.015 was used for CDP. The model was initialized with a soil depth of 1.4, 2.2 and 2.14 m (for WFJ, CDP and Davos field sites, respectively) divided into layers of varying thickness. For soil, typical values for coarse material were chosen to avoid ponding inside the snowpack due to soil saturation. The soil heat flux at the lower boundary is set to a constant value of 0.06 W m^{-2}, which is an approximation of the geothermal heat flux.

2.2.2 Water transport models

The two previously existing methods for simulating vertical liquid water movement within SNOWPACK are either a simple so-called bucket approach (BA) (Bartelt and Lehning, 2002) or solving the RE, a recently introduced method for SNOWPACK (Wever et al., 2014b,a).

The BA represents liquid water dynamics by an empirically determined irreducible water content θ_r which defines whether water stays in the corresponding layer or will be transferred to the layer below. This irreducible water content varies for each layer according to Coléou and Lesaffre (1998). The RE represents the movement of water in unsaturated porous media. Its implementation in SNOWPACK and a detailed description can be found in Wever et al. (2014b).

The PF model presented in this study is based on the RE model, but follows a dual-domain approach, dividing the pore space of the snowpack into a part representing matrix flow and a part representing PF. For both domains the RE is solved subsequently. The PF model is described by (i) a function for determining the size of the matrix and preferential flow domain, (ii) the initiation of PF (i.e., water movement from matrix flow to PF) and (iii) a return flow condition from PF to matrix flow.

The area of the preferential domain (F) is as a function of grain size (Eq. 2.1), which has been determined by results of laboratory experiments presented by Katsushima et al. (2013):

$$F = 0.0584 r_\text{g}^{-1.109}, \tag{2.1}$$

where r_g is grain radius (mm). F is limited between 1 and 90 % for reasons of numerical stability. The matrix domain is then accordingly defined as $(1 - F)$. Water is transferred from the matrix domain to the preferential domain if the water pressure head for a layer in the matrix domain is higher than the water entry pressure of the layer below, which can, according to Katsushima et al. (2013), also be expressed as a function of grain size. This condition is expected to be met if water is ponding on a microstructural transition (i.e. capillary barriers, ice lenses) inside the snowpack. Additionally, saturation was equalized between the matrix and the preferential domain, in case the saturation of the matrix domain exceeded the one in the preferential domain. To move water back into the matrix part, we apply a threshold in saturation of the PF domain and water will flow back to the matrix domain once this threshold is exceeded. This threshold is used as a tuning parameter in the model.

Refreezing of liquid water in the snowpack is crucial for modelling water transport in subfreezing snow and may also be important for modelling PF. The presented PF model has also been used to simulate ice layer formation under the presence of PF by Wever et al. (2016b). Therefore, a sensitivity study on the role of refreeze in the PF domain and the return flow condition from PF to matrix flow was conducted. It was found that neglecting refreeze led to the best results for reproducing ice layer formation, but did not significantly affect the performance in reproducing measured hourly snowpack runoff. Therefore, refreeze in the preferential domain is neglected in the presented study. The threshold in saturation for PF (return flow condition) was also determined by the sensitivity study described in Wever et al. (2016b). While they determined a threshold in saturation of 0.1 to reproduce ice-layer observations at WFJ best, a value of 0.06 was determined to reproduce observed seasonal runoff best. We therefore used the value of 0.06. In contrast to Wever et al. (2016b), we did not set the hydraulic conductivity in soil to 0, because this can lead to an inaccurate representation of observed lysimeter runoff due to modelled ponding on soil, which is not expected to happen on a snow lysimeter. Further details on the implementation of the PF model and its performance can be found in Wever et al. (2016b).

In summary, the PF model accelerates liquid water transport in the preferential domain by concentrating water mass in a smaller area, representing the area fraction of flow fingers in the snowpack. The saturation in the preferential domain is hence higher and unsaturated conductivity is larger. Further acceleration is achieved by disabling refreeze in the preferential domain.

2.2.3 Davos field sites

Four field sites have been installed within an elevational range of 950 to 1850 m a.s.l. in the vicinity of Davos, Switzerland, with one meteorological station and 3–4 snow lysimeters each (15 in total, 0.45 m diameter). The meteorological stations provided most data necessary for running the SNOWPACK model and missing parameters were estimated as described in Sect. 2.2.1. Lysimeters were installed at ground level with an approximate spacing of 10 m

horizontal distance. The lysimeters consisted of a funnel attached to a precipitation gauge buried in the ground, which monitored snowpack runoff with a tipping bucket. To block lateral inflow at the snow-soil interface, each lysimeter was equipped with a rim of 5 cm height around the inlet. The multiple snow lysimeter setups allowed analysing the spatial heterogeneity of snowpack runoff. Snowpack properties (SWE, LWC, HS, TS) were manually measured directly before each natural ROS event so that the initial conditions of the snowpack are known in detail. LWC was measured with the "Denoth meter", a device introduced by Denoth (1994). The onset of runoff was defined as the time when cumulative snowpack runoff (measured and simulated, respectively) has reached 1 mm.

2.2.4 Sprinkling experiment description

During winter 2014/15, a total of six artificial sprinkling experiments were performed on all four Davos field sites described above to be able to investigate snowpack runoff generation for different snowpack properties (Table 2.1). For each experiment, a sprinkling device was placed above a snow lysimeter, covered by an undisturbed natural snowpack, i.e. each lysimeter was only used for one experiment. The device used for sprinkling was a refined version of the portable sprinkling device described in Juras et al. (2013, 2016). The water used for sprinkling was mixed with the dye tracer Brilliant Blue FCF (concentration $0.4\,\mathrm{g\,L^{-1}}$) to be able to observe PFPs within the snowpack. Sprinkling was performed in four bursts of 30 min each, interrupted by 30 min breaks. Sprinkling was conducted over a $2 \times 2\,\mathrm{m}$ plot centred above the lysimeters, and with an intensity of $24.7\,\mathrm{mm\,h^{-1}}$, leading to a total of 49.4 mm artificial rain in each of the experiments. The intensities were determined by calibration experiments on lysimeters not covered by snow and are valid for a certain distance between the nozzle and the sprinkled surface and water pressure at the nozzle. Despite the fact that this value still represents a very intense ROS event, it is within range of natural ROS events and similar or much lower compared to previous studies ($19\,\mathrm{mm\,h^{-1}}$; Eiriksson et al. (2013); 48–$100\,\mathrm{mm\,h^{-1}}$; Singh et al. (1997)). For the sprinkling experiments, the exact timing of rain and intensities are known and the snowpack runoff measured at 1 min intervals allowed precise analysis of the performance of model simulations. Figure 2.1 shows a vertical cut of a snowpack after the sprinkling experiment and a top view of the lysimeter after the snowpack was removed for cold and wet conditions, respectively. The blue colour indicates where water transport took place and where sprinkled water was held by capillary forces or refrozen.

2.2.5 Extensive dataset for in situ validation

Two long-term datasets from two study sites in the European Alps providing snow lysimeter data and high-quality meteorological forcing data for running the energy balance model SNOWPACK were chosen to validate the different water transport models systematically. Datasets of both study sites used for the extensive in situ validation are publicly available. The CDP site, located in the Chartreuse range in southeastern France, has been described in Morin et al. (2012) and the Weissfluhjoch site (WFJ) in the Swiss Alps has been described in
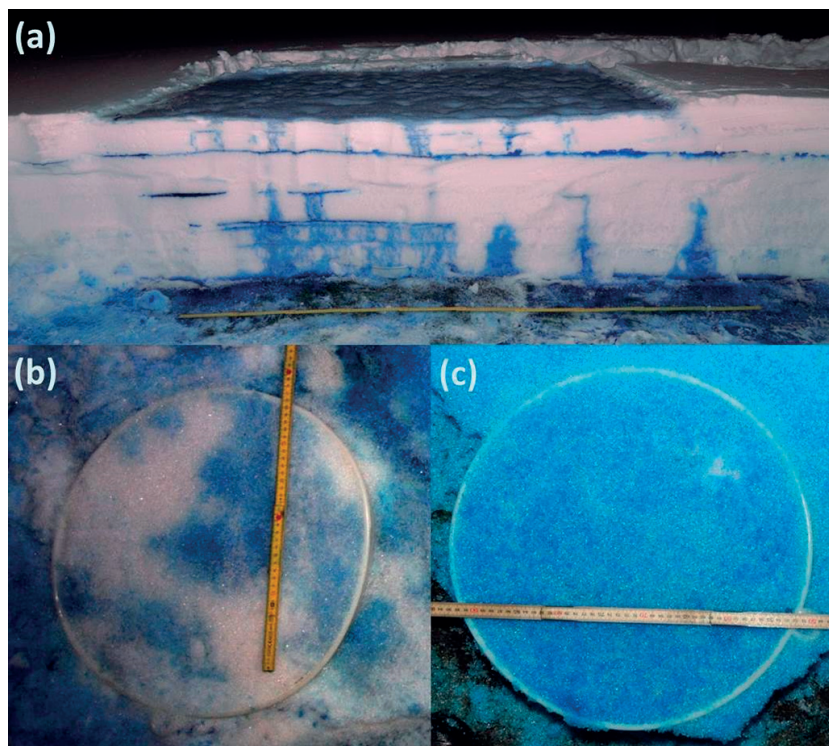
Figure 2.1 – **(a)** Vertical cut of a snowpack after the sprinkling experiment Sertig Ex3 (28 February 2015). Lateral flow and the presence of PFP were observed. PFP were generated at regions with rain water ponding at ice layers and layer boundaries with a change in grain size (creating capillary barriers). **(b)** Lysimeter area after sprinkling during winter conditions (Serneus Ex1, 26 February 2015): coloured areas indicate the area where water percolated due to PF. **(c)** Lysimeter area after sprinkling during spring conditions (Klosters Ex4, 26 March 2015): coloured area shows that water percolated uniformly, indicating dominating matrix flow.

Wever et al. (2015). WFJ (46.83° N, 9.81° E) is located at an elevation of 2536 m a.s.l. and CDP (45.30° N, 5.77° E) is located at 1325 m a.s.l. CDP experiences a warmer climate than WFJ and as a consequence the snowpack produces snowpack runoff more often throughout the entire snow season and ROS events are more frequent than at WFJ. A multi-week snowpack builds up every winter season at CDP, but is, in contrast to WFJ, interrupted by complete melt in some years. The WFJ site is equipped with a 5 m^2 snow lysimeter, which measures the liquid water runoff from the snowpack. It has a 60 cm high rim to reduce lateral flow effects near the soil–snow interface (Wever et al., 2014b). CDP is equipped with both a 5 and a 1 m^2 lysimeter. Here we use data from the 5 m^2 lysimeter, but include data from the 1 m^2 lysimeter to discuss the uncertainty associated with measurements of the snowpack runoff. The studied period for WFJ is from 1 October 1999 to 30 September 2013 (14 hydrological years). Because of possible errors in the lysimeter data in the winter seasons of 1999/00 and 2004/05 as described in Wever et al. (2014b), these data were excluded from the study. For CDP the studied period is from 1 October 1994 to 31 July 2011 (17 winter seasons) according to the data availability from the 5 m^2 lysimeter. The temporal resolution of lysimeter data is 1 h for CDP and 10 min for WFJ.
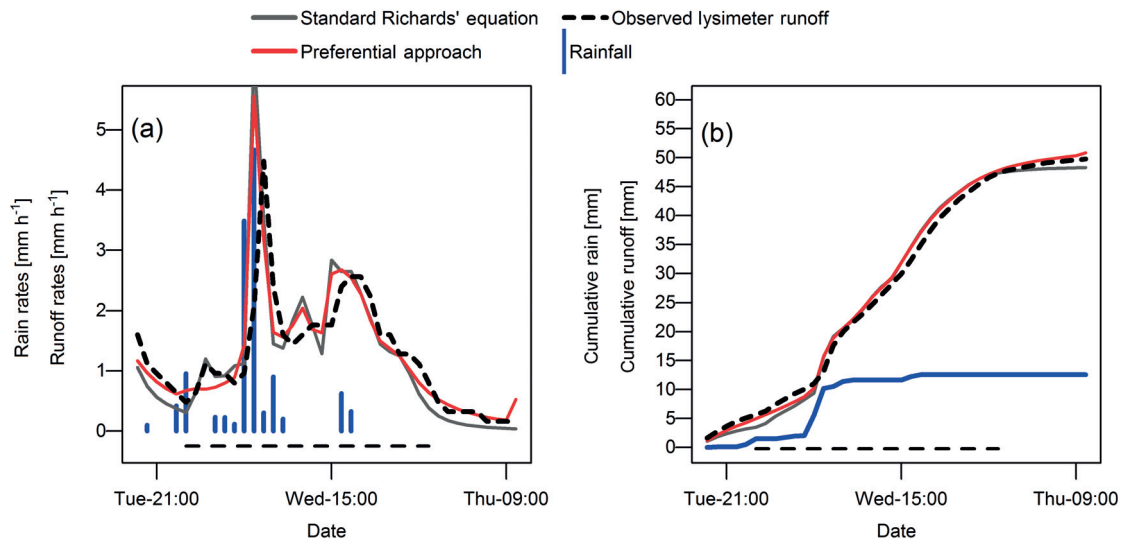
Figure 2.2 – **(a)** Example of a ROS event occurring at WFJ. The entire extent of the x axis refers to the evaluation period; the bar above the x axis refers to the event length. **(b)** Cumulative version of the plot.

Simulation results for CDP and WFJ as well as lysimeter data for WFJ were aggregated to an hourly timescale.

2.2.6 CDP + WFJ event definition

As the number and characteristics of ROS events are strongly dependent on the event definition, special care needs to be taken to determine beginning and end of a ROS event. Being interested in the temporal characteristics of snowpack runoff during ROS, we need to include the entire period from the onset of rain to the end of ROS-induced snowpack runoff. Here we use an event definition according to Würzer et al. (2016) with slightly decreased thresholds to identify ROS events. According to this definition, a ROS event requires a minimum amount of 10 mm rainfall to fall within 24 h on a snowpack with a height of at least 25 cm at the onset of rainfall. While the event is defined to begin once the first 1 mm of rain has fallen, the event ends once there is less than 3 mm of cumulative snowpack runoff recorded within the following 5 h. This definition resulted in a selection of 61 events at CDP and 40 events at WFJ. The model simulations were subsequently evaluated over a time window that extends the event length by 5 and 10 h at the beginning and end, respectively (Fig. 2.2). These extended evaluation periods allowed us to also investigate a possible temporal mismatch between modelled and observed snowpack runoff.

Table 2.1 – Snowpack pre-conditions and execution dates for the sprinkling experiments as well as R^2 values for the different model simulations. Measured values are snow height (HS), bulk liquid water content (LWC), bulk snow temperature (TS). No snowpack runoff measurements were available for Sertig (Ex3).

Experiment	Initial snowpack conditions				R^2 of hourly runoff of the simulations		
	HS [cm]	LWC [% vol]	TS [°C]	Date	RE	PF	BA
Serneus (Ex1)	48.5	0.1	−1.3	26-Feb-15	0.14	0.59	0.09
Davos (Ex2)	54.5	0.4	−2.5	27-Feb-15	0.24	0.62	0.08
Sertig (Ex3)	71.5	0	−1.6	28-Feb-15	–	–	–
Klosters (Ex4)	15.7	6.9	0	26-Mar-15	0.75	0.96	0.86
Klosters (Ex5)	7	4.9	0	8-Apr-15	0.70	0.84	0.88
Davos (Ex6)	39.3	0.9	−0.6	10-Apr-15	0.58	0.83	0.36

2.3 Results

2.3.1 Sprinkling experiments

During the winter period 2014/15, six sprinkling experiments (Ex1–Ex6) were conducted on four different sites to be able to investigate snowpack runoff generation for different snowpack properties. With distinct differences in snowpack properties but controlled rain intensities, these experiments were expected to reveal the influence of snow cover properties and differences between the water transport models best. For all experiments, initial snow height (HS), snowpack temperature (TS) and LWC profiles were measured (Table 2.1 and Fig. 2.3). According to these measurements, the snowpack conditions on which the sprinkling experiments were conducted can be separated into two cases: the first three experiments were conducted on dry and cold (i.e. below the freezing point) snow and will be called winter experiments. The snowpack of Ex4 and Ex5 was isothermal and in a wet state. At the onset of Ex6 however, part of the snowpack was below freezing and had just little LWC. Nevertheless, the snowpack already passed peak SWE and was in its ablation phase. Therefore the later three experiments (Ex4–Ex6) will be referred to as spring experiments in the following.

For all winter experiments (Figs. 2.4 and 2.5a, b, c), both modelled and observed total event runoff remained below the amount of sprinkling water. Energy input estimated by the SNOW-PACK simulations suggests that snowmelt was insignificant for the winter experiments, but refreeze led to significant retention of liquid water. Additionally some sprinkled rain was retained as LWC at the end of the experiments. During Ex3 no snowpack runoff was observed, visual inspection afterwards revealed an impermeable ice layer covering both the lysimeter and the adjacent ground. During spring conditions, on the other hand, snowmelt (5.1, 8.4 and 27.4 mm respectively) led to snowpack runoff exceeding total sprinkling input, except for measured snowpack runoff in Ex6 (Figs. 2.4 and 2.5d, e, f).
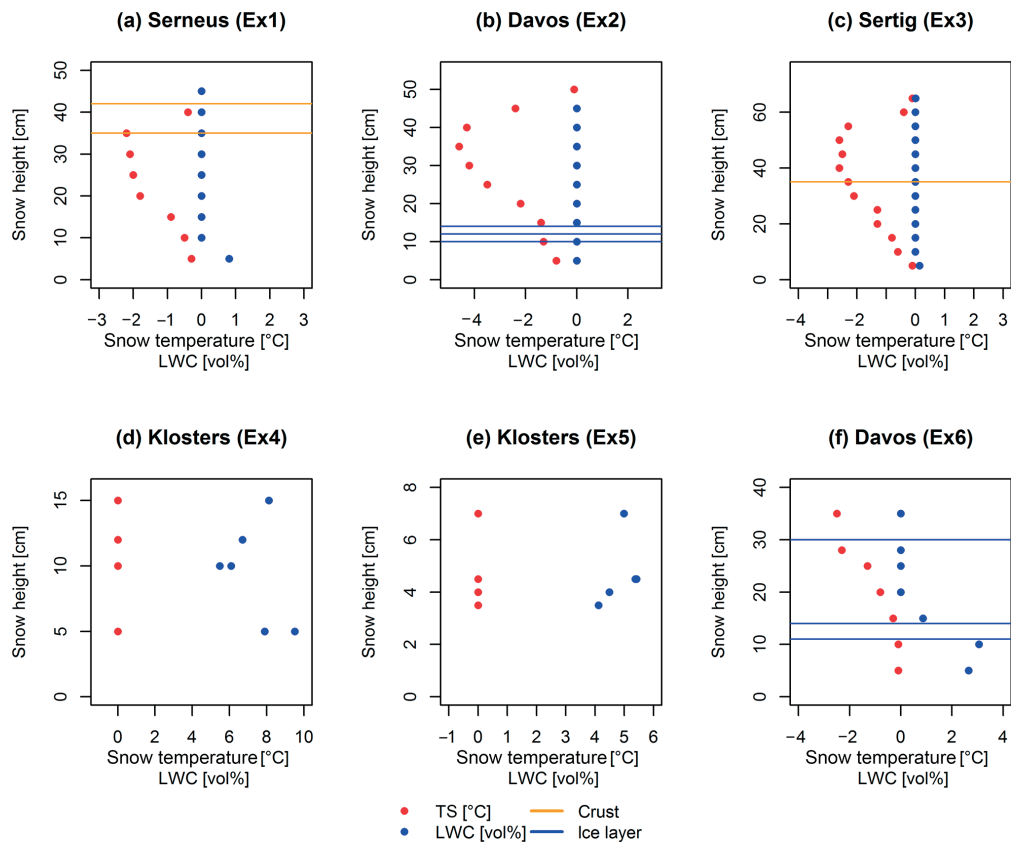
Figure 2.3 – Snow temperature and LWC profiles measured directly before the sprinkling experiment started. The lines represent observed ice layers (blue) and crusts (orange).

Additionally, Fig. 2.5 shows that only the PF model was able to reproduce all four peaks of observed snowpack runoff for winter conditions (Ex1 + 2), and even the magnitude of the first peak of Ex1 was captured well. For spring conditions however, all three models managed to represent four peaks corresponding to the four sprinkling bursts, but the PF model showed best correspondence with observed snowpack runoff (Figs. 2.4 and 2.5d, e, f; Table 2.1). Regarding the onset of snowpack runoff, the PF model especially led to faster snowpack runoff for the first two winter experiments, where the RE and BA models showed delayed snowpack runoff onset. For spring conditions the faster snowpack runoff response of the PF model led to a slightly early snowpack runoff. Maximal snowpack runoff rates for dry and cold conditions were generally overestimated by all models, whereas wetter conditions led to a minor underestimation (except for Ex3, where no snowpack was measured).

Regarding the overall correlation between measured and simulated snowpack runoff, PF outperformed the other models (Table 2.1), in particular during winter conditions. Summarizing, this initial assessment suggests that the PF approach has potential advantages in particular (a) as to the timing of snowpack runoff and (b) for cold snowpacks which are not yet entirely ripened.
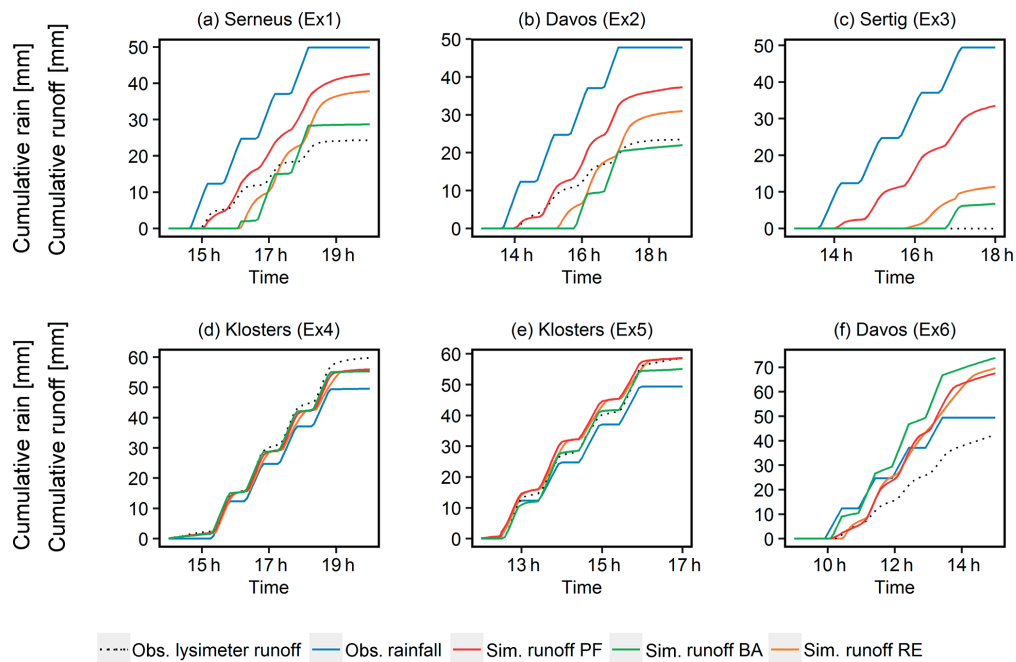
Figure 2.4 – Cumulative rain and snowpack runoff displayed for the six sprinkling events. Ex1 **(a)**–Ex3 **(c)** were conducted during winter conditions, Ex4 **(d)**–Ex6 **(f)** were conducted during spring conditions.
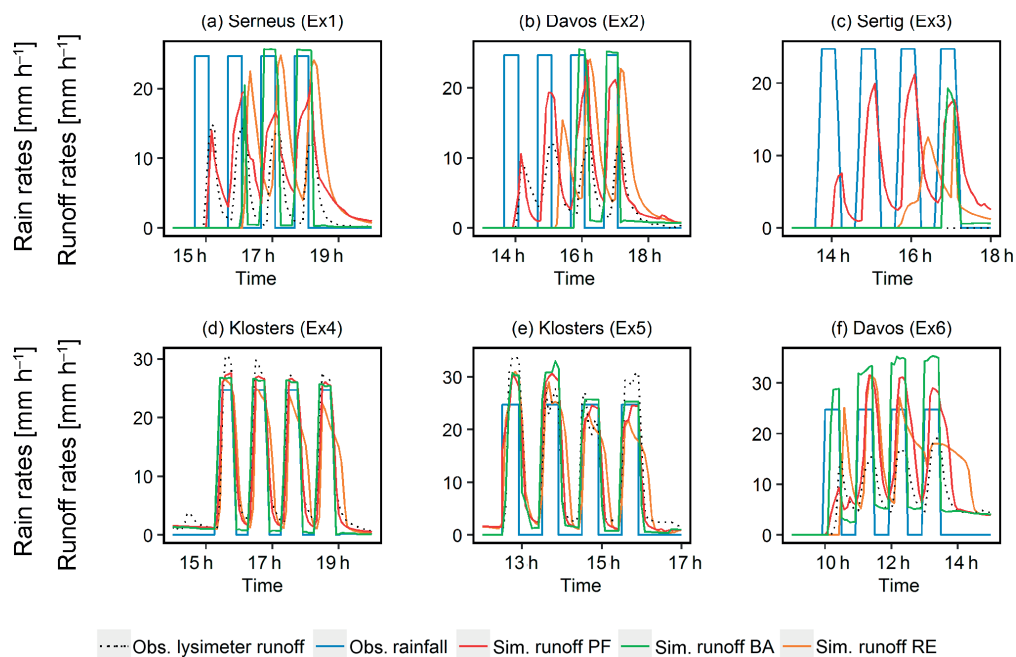
Figure 2.5 – Rain and snowpack runoff displayed as hydrographs for the six sprinkling events. Ex1 **(a)**–Ex3 **(c)** were conducted during winter conditions, Ex4 **(d)**–Ex6 **(f)** were conducted during spring conditions.

2.3.2 Natural occurring ROS events

In January 2015, two ROS events occurred in the vicinity of Davos. They were observed over an elevational range of 950 to 1560 m a.s.l. on the same sites on which also the sprinkling experiments were conducted. Figure 2.6 shows the course of cumulative rainfall and snowpack runoff for both dates and all sites. Pre-event conditions (HS, LWC, TS) were measured shortly before the onset of rain for both events and are shown together with coefficients of determination (R^2) for hourly snowpack runoff of the different models Table 2.2.
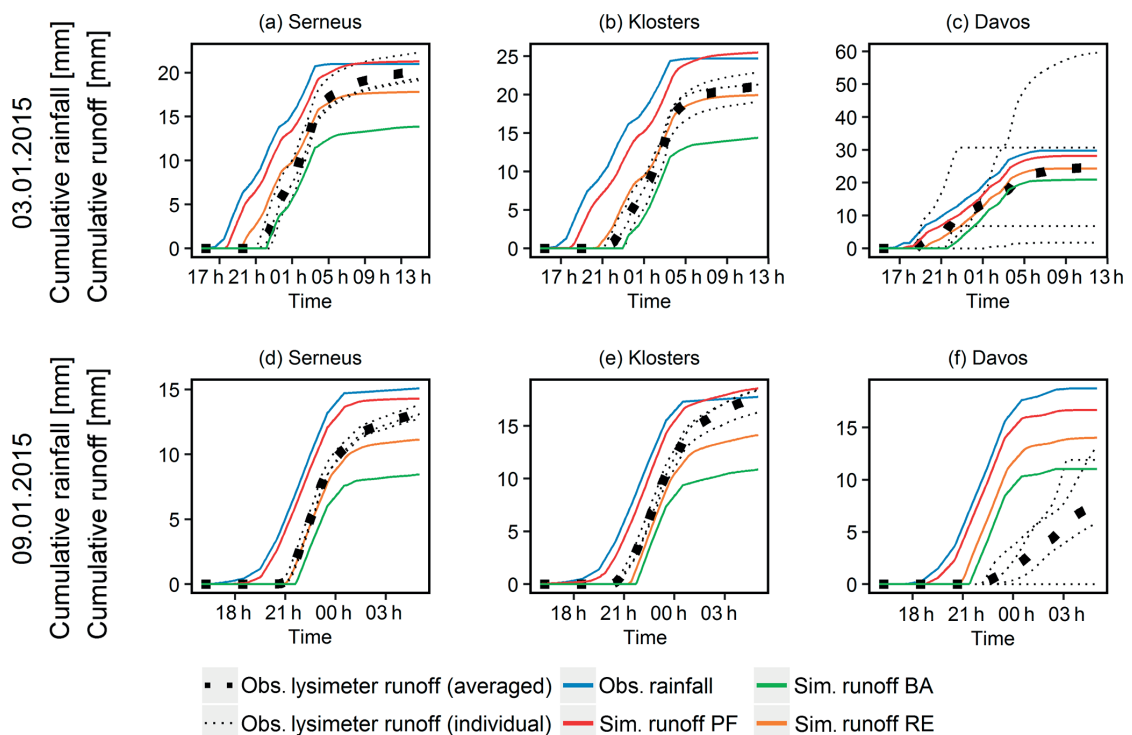
Figure 2.6 – Natural ROS events on 3 and 9 January 2015 in **(a, d)** Serneus, **(b, e)** Klosters and **(c, f)** Davos.

For the event of 3 January 2015 (Fig. 2.6, upper row) the lower sites Serneus and Klosters (950 and 1200 m a.s.l.) showed a similar snowpack runoff dynamics regarding the delayed onset and the total amount (cumulative sum averaged over the three corresponding lysimeters: 20.3 and 21.1 mm, respectively). Also, the heterogeneity between data from the individual lysimeters was relatively low (Range of 3.1 and 3.9 mm, respectively). For the highest located site (Davos), however, the snowpack runoff measured by all four lysimeters showed a greater variability (Fig. 2.6c) in the delayed onset of snowpack runoff (0 to 7 h) and the total amount of snowpack runoff (mean 24.7 mm; range of 57.9 mm). The snow cover mostly built up within 1 week before the event. Cold temperatures led to a light melt refreeze crust at the top, but no distinct ice layers were observed. For the lower sites (Serneus and Klosters), the PF and RE models generated snowpack runoff too early (PF: approx. 3 h; RE: 0.2 to 1.4 h). The BA model generated snowpack runoff rather too late (1.3 to 2 h), but still within range of the variability of observed

Table 2.2 – Snowpack pre-conditions and R^2 for hourly snowpack runoff for natural events on
3 and 9 January.

	Site	Pre-event snowpack conditions			R^2 for hourly snowpack runoff		
		HS (cm)	LWC (% vol)	TS (°C)	RE	PF	BA
03-Jan-2015	Serneus	19	0	0	0.63	0.35	0.83
	Klosters	24	0	−0.1	0.72	0.39	0.78
	Davos	20	0	−0.4	0.27	0.33	0.17
09-Jan-2015	Serneus	14.5	0.1	−0.2	0.94	0.57	0.79
	Klosters	18	0.1	−0.2	0.84	0.73	0.73
	Davos	19.5	0.1	−0.6	0.00	0.04	0.00

snowpack runoff for Serneus. However, the cumulative lysimeter snowpack runoff showed
good accordance with modelled PF and RE snowpack runoff at Serneus, whereas PF led to an
overestimation at Klosters and BA to an underestimation of cumulative snowpack runoff at all
sites. At the higher-elevation site Davos, the RE model led to a better representation of mean
observed snowpack runoff amount, when compared with BA and PF. The mean observed
snowpack runoff onset however was represented best by the PF model (0.3 h early) when
compared to the BA (3.4 h delay) and RE (1.1 h delay).

For the event of 9 January 2015 (Fig. 2.6, bottom row) the lower sites showed again little
temporal and spatial heterogeneity in lysimeter runoff (range of 1 and 2.2 mm, respectively),
whereas this was more the case for Davos again (range of 13.3 mm) probably owing to ice layers
that were formed after the event on 3 January. Observed mean event snowpack runoff was
more diverse for all elevations, where Klosters had the highest cumulative snowpack runoff
(Serneus 13.3 mm; Klosters 17.7 mm; Davos 7.8 mm). If compared to observed total snowpack
runoff, the PF model overestimated snowpack runoff for Serneus and Klosters, whereas the RE
and especially the BA model underestimate event snowpack runoff for both sites. For Davos,
all models were overestimating event snowpack runoff and led to early snowpack runoff. Apart
from the RE model, which represented onset of snowpack runoff correctly for Serneus, none
of the models were able to model snowpack runoff onset correctly for any of the sites.

Table 2.3 – R^2 and mean absolute errors for hourly snowpack runoff for 17 and 14 years, for
CDP and WFJ, respectively.

	R^2 hourly snowpack runoff			RMSE of snowpack runoff (mm h^{-1})		
	BA	RE	PF	BA	RE	PF
CDP	0.33	0.50	0.52	0.56	0.44	0.40
WFJ	0.48	0.77	0.78	0.51	0.30	0.28
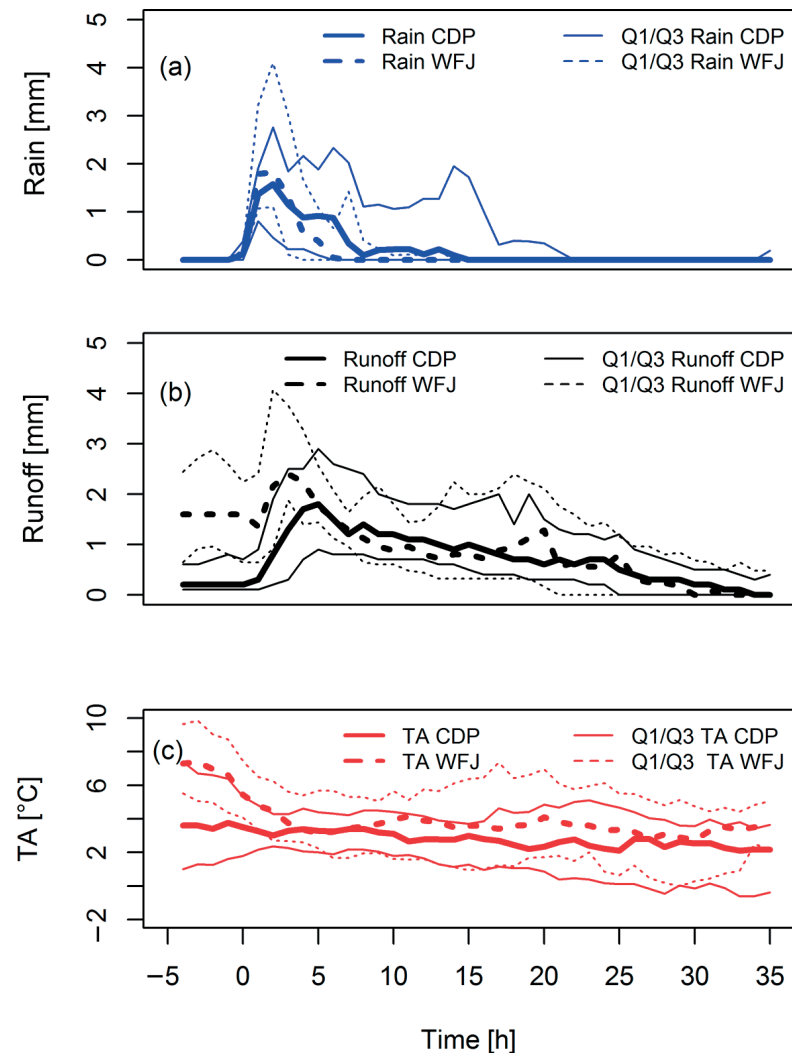
Figure 2.7 – Temporal course of median rain **(a)**, measured snowpack runoff **(b)** and air temperature **(c)** for WFJ (dotted) and CDP (solid) aggregated over all 40 and 61 events respectively. The thinner lines represent the lower and upper quartiles, respectively. The displayed period is extended by 5 h prior to event commencement according to the event definition (0 h).

2.3.3 Validation on a long-term dataset

Modelled and observed snowpack runoff for the whole dataset

Given the partly contradictory findings on the performance of the three model variants based on the above assessment for artificial ROS simulations under controlled conditions (Sect. 2.3.1), as well as natural ROS events (Sect. 2.3.2), further more systematic model tests were needed. Therefore we validate the different models based on extensive datasets from the two sites WFJ and CDP, as described in Sect. 2.2.5.

Before we focus on the specific performance of the PF model for a large number of individual

Chapter 2. Modelling liquid water transport in snow under rain-on-snow conditions – considering preferential flow

ROS events, we first analysed the overall model performance throughout the whole study period, i.e. over entire winter seasons. For this, we analysed observed and modelled hourly snowpack runoff provided snow heights exceeded 10 cm to ensure that lysimeter runoff was caused by snowpack runoff and not rainfall. For both sites, R^2 values for PF were slightly higher than for RE (Table 2.3), which both clearly outperformed the BA. The root mean squared errors (RMSEs) of the PF model were also lower compared to RE and BA. We can therefore conclude that the implementation of the PF approach slightly improves water transport over entire winter seasons.

ROS event characteristics of the extensive dataset

Median characteristics of the individual ROS events at CDP and WFJ are summarized in Fig. 2.7. The temporal course of median rain and snowpack runoff rates of all events at WFJ (40 individual events) and CDP (61 individual events) are shown in Fig. 2.7a, b. ROS events at WFJ showed generally higher maximum rain intensities than at CDP, leading to higher median snowpack runoff intensities at the beginning of the events. Whereas at WFJ, ROS events tended to be short and intense, at CDP the event rainfall extended over a longer period of time. Interestingly, we observed relatively high initial snowpack runoff rates before the actual beginning of the ROS event, especially for WFJ, which suggests that many ROS events at this site occurred during the snowmelt period. Median snowpack runoff reached a peak after 1 and 3 h after the onset of rain for WFJ and CDP, respectively. At WFJ snowpack runoff and rain rates at the beginning of the events were generally higher than at CDP. The course of the median air temperature during ROS events at both sites is shown in Fig. 2.7c. Especially for WFJ, median air temperature (TA) dropped with the onset of rain and median TA was higher than at CDP. The mean initial ROS event snow height (HS) for WFJ was 95 cm, which is approximately the average snow height during mid-June (for 70 years of measurements). The mean initial HS for CDP is 67 cm. With a SD of 42 cm, the variability of initial HS for WFJ was higher than for CDP (29 cm).

Modelled and observed snowpack runoff at the event scale

Below we investigate the performance of the three water transport schemes at the event scale. Modelled snowpack runoff was assessed against observations by the coefficient of determination (R^2) and the RMSEs. To further analyse the representation of snowpack runoff timing, we defined an absolute time lag error (TLE) as the difference between the onsets of modelled and observed snowpack runoff in hours. The onset of snowpack runoff is defined as the time when cumulative snowpack runoff has reached 10 % of total event-snowpack runoff.

Figure 2.8 shows box plots of R^2 (a, d), RMSE (b, e) and absolute TLE (c, f) for all 40 ROS events at WFJ (a, b, c) and 61 events at CDP (d, e, f), respectively. For both sites, R^2 values show that the BA model performance was inferior to the RE model which was in turn slightly outperformed by the PF model. The interquartile range of R^2 values for CDP was generally
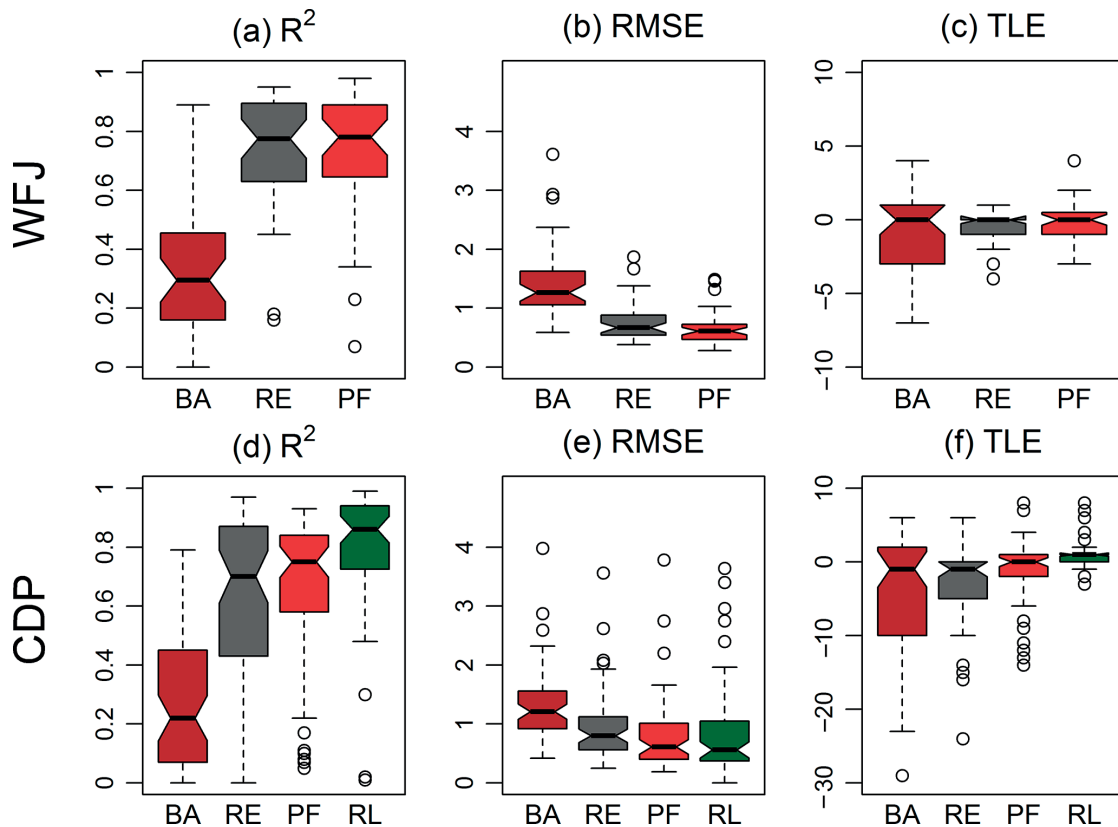
Figure 2.8 – RMSE, R^2 and TLE for simulations of 61 ROS events at the CDP site and of 40 ROS events at the WFJ site for all models (BA, RE, PF) and the reference lysimeter (RL) available only for CDP.

higher than for WFJ and increased from BA to RE, whereas it was decreasing for PF. The PF also led to a reduction in RMSE by approximately 50 % if compared to the BA, but less (9 % for WFJ and 25 % for CDP) if compared to the RE model. Whereas the median of TLEs for all models at WFJ was 0 and therefore all models reproduced the onset of snowpack runoff very well, the interquartile range decreased from BA to the RE and PF models. The same behaviour in interquartile range decrease could be observed for CDP, where the magnitude of TLE was higher than for WFJ and mostly negative. The median TLE was again 0 for the PF and −1 h in the case of BA and RE, indicating that for these models, snowpack runoff was on average a bit delayed compared to the observations. For WFJ, TLE for BA was more often positive (early modelled snowpack runoff), which led to a very good median for BA, but also a larger interquartile range. Hence, the PF model showed the most consistent results, especially if regarding the interquartile range. For CDP we added the comparison between the 1 and 5 m^2 lysimeters installed at CDP (Sect. 2.2.5) as a reference to Fig. 2.8, referred to as RL. This comparison can be seen as a benchmark performance, as it represents the measurement uncertainty of the validation dataset. As expected, RL shows the highest overall performance measures, but while the results for both PF and RE were reasonably close to those of RL, the BA model performed considerably worse.
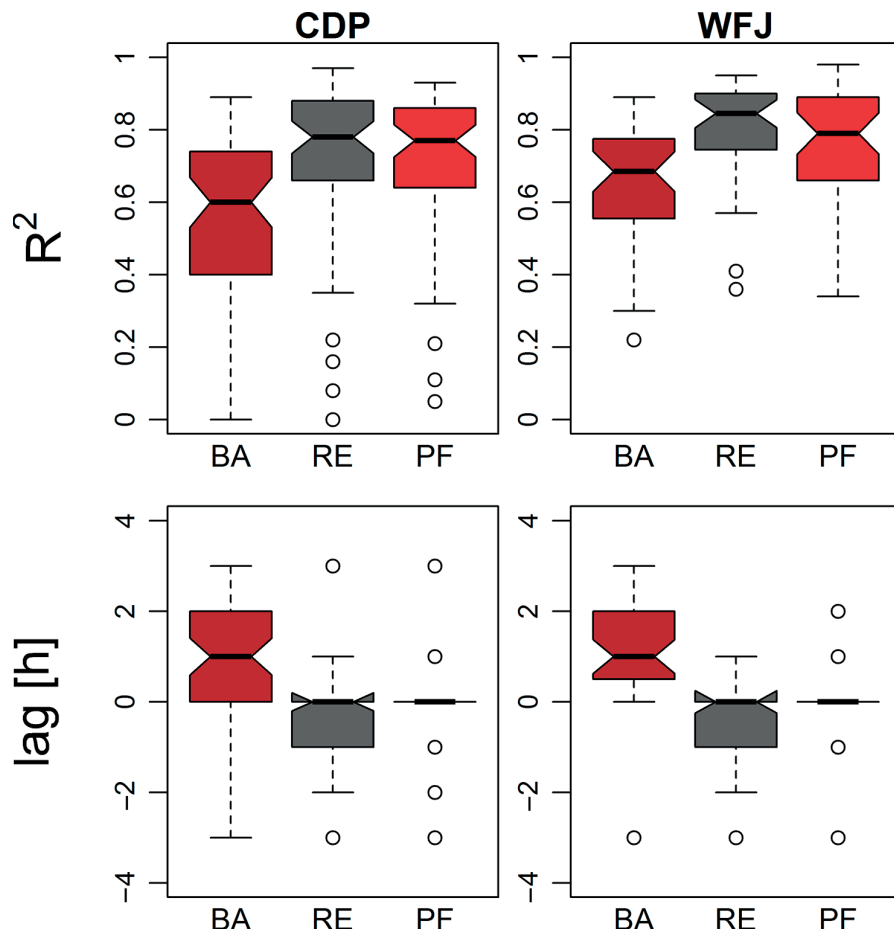
Figure 2.9 – Best R^2 values and corresponding lags using a cross-correlation function allowing a time shift (lag) of max $\pm 3\,\text{h}$.

The results shown in Fig. 2.8 may be influenced by both a time lag as well as the degree of reproduction of temporal dynamics. To separate both effects, we conducted a cross-correlation analysis, allowing a shift of up to 3 h to find the best R^2 value. Figure 2.9 shows both the time lag, as well as the best R^2 value achieved. Interestingly, the BA model showed best correlations if the modelled snowpack runoff was shifted by 1 or 2 h (consistently too early compared to observations). The RE model, on the other hand, showed best correlations for a shift in the other direction (consistently too late compared to observations). Neither was the case for PF with lags centred around 0.

The R^2 of the cross-correlation analysis gives some indication of how well the temporal dynamics of the observed snowpack runoff can be reproduced, neglecting a possible time lag. The results in Fig. 2.9 show an improvement in R^2 values for both sites and all models if a time lag is applied. Greatest improvements were observed for the BA model for both sites. The good timing with the PF model is confirmed by almost no lag for WFJ and only a small lag for CDP needed to maximize R^2. For CDP, both RE and PF had maximized R^2 values in range of

the lysimeter comparison (RL).

2.4 Discussion

Even though PF of liquid water through snow is a phenomenon that has been known and investigated for a long time, it has not yet been accounted for in 1-D snow models that are in use for operational applications. The results of this study show that including this process into the water transport scheme can improve the prediction of snowpack runoff dynamics for individual ROS events as well as for the snowpack runoff of entire snow seasons. Moreover, the representation of the onset of snowpack runoff is improved. This is particularly important at the catchment scale, where a delay of snowpack runoff relative to the start of rain may affect the catchment runoff generation, especially if the time lag varies across a given catchment.

During the sprinkling experiments, sprinkling intensities were higher than average rain intensities during ROS but still within range of peak rain intensities during naturally occurring ROS events in the Swiss Alps (Rössler et al., 2014, Würzer et al., 2016) and the Sierra Nevada, California (Osterhuber, 1999). The use of the PF model clearly led to a better representation of the runoff dynamics for all experiments, including shallow and ripe snowpacks during spring conditions as well as cold and dry snowpacks representing winter conditions. The improvements were strongest for winter conditions, suggesting that under these conditions accounting for PF is most relevant. This is supported by observations of PFPs during winter conditions (Fig. 2.1a), which were not visible after the spring experiments. During winter conditions just a fraction of the lysimeter area was coloured with tracer, indicating PF of the sprinkled water (Fig. 2.1b), whereas spring conditions left the whole cross-section of the lysimeter coloured (Fig. 2.1c). While a fast runoff response can be expected for wet and shallow snowpack and may be easier to handle for all models tested, it is the cold snowpacks that both RE and BA models did not manage to represent well: runoff from these models was more than 1 h delayed (Ex1 and Ex2), and missed approx. 10 mm of snowpack runoff within the first hour of observed runoff. This can partly be explained by the fact that BA and RE need to heat up the subfreezing snowpack before they can generate snowpack runoff, whereas refreezing is neglected in the preferential domain of the PF model and runoff can occur even in a not yet isothermal snowpack. Adjusting parameters like the irreducible water content θ_r for the BA model could probably lead to earlier runoff under these conditions, but thereby lead to earlier runoff, for example for WFJ events, where TLE already is positive for several events.

Despite the improved representation of the temporal runoff dynamics of the PF model (Table 2.1), the total event runoff of both RE and PF models is very similar for most conditions. Notably, the total event runoff for dry snowpacks is mostly overestimated by all models, suggesting an underestimation of water held in the capillarities. In cold snowpacks, dendricity of snow grains may still be high, such that water retention curves developed for rounded grains underestimate the suction. Additionally, high lateral flow was observed during the experiment for those conditions (Fig. 2.1a). This leads to an effective loss of sprinkling water per surface

33

area of the lysimeter, which of course cannot be reproduced by the models. Therefore, observed snowpack runoff likely underestimates the snowpack runoff that would have resulted from an equivalent natural ROS event and we assume that the performance of the PF and RE models to capture the event runoff is probably better than reported in Table 2.1. Note that neglecting refreeze in the PF model should not be accountable for differences in the total event runoff between the RE and PF model, if we assume that the cold content is depleted by the end of the event.

Interestingly, despite having the coldest snowpack, time lag for the first natural ROS event at Davos was shorter than for the other two sites. This relationship where a cold and non-ripe snowpack with low bulk density led to smaller lag times was also found during sprinkling experiments conducted by Juras et al. (2017). We assume that this is an indication for the presence of pronounced PFPs under those conditions, which is also supported by the high spatial variability of snowpack runoff. Glass et al. (1989) state that the fraction of PF per area is decreasing with increasing permeability, which itself was found to be increasing with porosity (Calonne et al., 2012). Therefore, with a decreasing PF area due to lower densities, the cold content of a snowpack loses importance, but saturated hydraulic conductivity is reached faster within the PFPs. The combination of those effects then is suspected to lead to earlier runoff. This behaviour should be ideally reproduced by the PF model and indeed the onset of runoff is caught well for this event. Here, our multi-lysimeter setup raises the awareness that the observed processes can show considerably spatial heterogeneity as documented, for example, in Fig. 2.6. The formation of ice layers also underlies spatial heterogeneity. Moreover, the creation of PFPs is strongly dependent on structural features like grain size transitions leading to capillary barriers. Unfortunately, no detailed information about grain size is available in the observations to verify this.

The PF model led to improvements in reproducing hourly runoff rates at CDP and WFJ for a dataset comprising several years of runoff measurements. This is an important finding, demonstrating that the new water transport scheme aimed at a better representation of PF during ROS events, did not negatively impact on the overall robustness of the model. To the contrary, the overall performance over entire seasons could even be improved. All three models represent the overall seasonal runoff better for WFJ than for CDP (Table 2.3), which was also found on the event scale (Fig. 2.8). Moreover, the CDP simulations exhibit a larger interquartile range in R^2 values and are therefore generally less reliable. The observed differences in model performance between both sites may either be caused by differences in snowpack or meteorological conditions or by issues with the observational data. Moreover, SNOWPACK developments have in the past often been tested with WFJ data, which could lead to an unintended calibration favouring model applications at this site. Despite an obvious contrast in the elevation of both sites, the average conditions during ROS events seem to vary. Figure 2.7 suggests that at WFJ short and rather intense rain events dominate. The higher maximum rain intensities at WFJ, compared to CDP, are probably due to the later occurrence of ROS at this site (May–June), where air temperatures and therefore rain intensities are usually higher than earlier in the season (Molnar et al., 2015). Regarding mean intensities over the

Table 2.4 – Pearson correlation coefficients between event-R^2 and stratigraphic features at WFJ and CDP. Stratigraphic features are marked grain size changes (bigger than 0.5 mm) and density changes (bigger than 100 kg m^{-3}) in two adjacent simulated layers as well as the wet layer ratio (percentage of layers exceeding 1 % vol over layers below 1 % vol) and the percentage of melt forms.

		Pearson correlation coefficient between event R^2 and the following:			
		no. of grain size changes	no. of density changes	ratio of melt forms	wetting ratio
WFJ	PF	−0.44	−0.45	−0.16	−0.20
	RE	−0.54	−0.47	0.17	0.13
	BA	−0.56	0.16	−0.11	−0.09
CDP	PF	−0.14	0.07	0.37	0.39
	RE	−0.19	0.12	0.57	0.66
	BA	−0.11	−0.26	0.15	0.14

event scale, data shown in Fig. 2.7 further imply that short and intense ROS events typically attenuate the rain input (ratio runoff to rain < 1), whereas long ROS events rather lead to additional runoff from snowmelt, which is in line with results presented in Würzer et al. (2016).

Snow height is generally higher at WFJ where the average initial snow height for the ROS events analysed was approximately 30 cm higher than at CDP. Ideally, the performance of the water transport scheme in the snowpack should not be affected by the snow depth. At both sites, the snowpack undergoing a ROS event is mostly isothermal with a mean initial LWC of 1.8 % vol (CDP) and 3.0 % vol (WFJ). The initial snowpack densities at both sites were quite different. At WFJ, densities for all ROS events are around 450–500 kg m^{-3}, whereas for CDP densities are spread from around 200 kg m^{-3} up to 500 kg m^{-3}. This suggests that the variable performance of all models at CDP (Fig. 2.8d) may be associated with early season ROS events. At CDP, a linear regression fit suggests a positive, albeit weak correlation between snowpack bulk densities and event-R^2 for the RE (R^2 of 0.2), but no correlation for both the PF and the BA model. It seems that the RE model had some difficulties with low-density snow, which was not the case for the PF model (Fig. 2.10). This may explain why PF outperformed RE at CDP, but not for WFJ.

Remaining inaccuracies in the representation of runoff for low densities for both models applying the RE may be explained by the fact that the water retention curve have been derived by laboratory measurements with high-density snow samples (Yamaguchi et al., 2012b). The parameters defining the PF area (F) have also been developed from snow samples with a density mostly above 380 kg m^{-3} (Katsushima et al., 2013).

We further analysed snowpack stratigraphy derived from the SNOWPACK simulations, such as marked grain size changes (bigger than 0.5 mm) and density changes (bigger than 100 kg m^{-3}) in two adjacent simulated layers as well as the wet layer ratio (percentage of layers exceed-
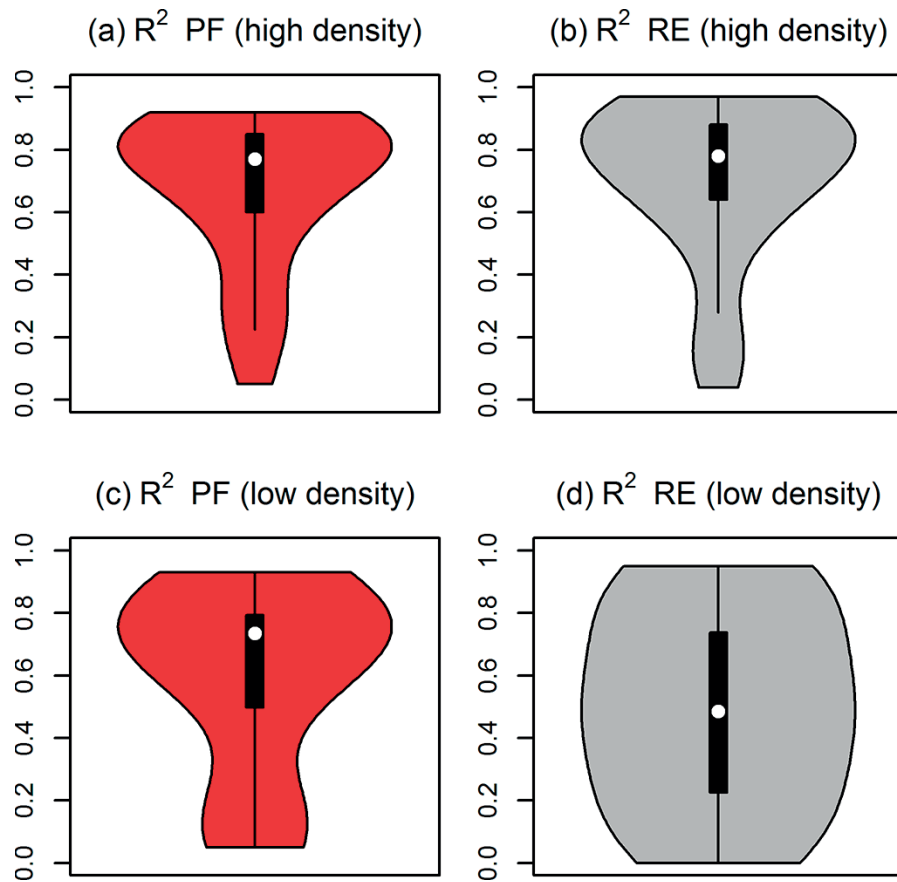
Figure 2.10 – Distribution of event-R^2 for CDP events for the PF **(a, c)** and RE **(b, d)** model. The sample is split into initial bulk snow densities above $350\,\mathrm{kg\,m^{-3}}$ **(a, b)** and below $350\,\mathrm{kg\,m^{-3}}$ **(c, d)**.

ing 1 % vol over layers below 1 % vol) and the percentage of melt forms (Table 2.4). These stratigraphy measures represent possible capillary barriers having implications on the single event-R^2 and might help understanding the advantages and disadvantages of the different models. Any considerable correlation between the abundance of stratigraphy features and event-R^2 would be indicative of potential errors in the respective model. Negative albeit small correlations could be found between the number of grain size changes and the event-R^2 for WFJ. Similar correlations were noted with regards to the number of changes in density between layers for the RE and PF model. In both cases correlations were less negative for the PF model indicating a more balanced and ultimately less degraded performance with increasing number of potential capillary barriers. While at WFJ most events occurred with ripe snow this was not the case for CDP. There, positive correlations were found between the ratio of melt forms and the wet layer ratio with event-R^2 for the RE model (Pearson's R of 0.57 and 0.66) and for the PF model (Pearson's R of 0.37 and 0.39). In this case the PF model also showed more balanced results that were less influenced by the initial LWC, which is in line with our findings of the sprinkling experiments.

System input rates (sum of melt rates and rain rates) are known to significantly affect water transport processes. For example, the area of PF (Eq. 2.1) is likely to depend on the water supply rate. Data using sandy soils from Glass et al. (1989), shown in DiCarlo (2013), suggest that with increasing system input rates the finger width of PF is increasing. Even though we have used the lowest influx rates from Katsushima et al. (2013), these rates still exceeded what seems representative of natural ROS events. We therefore analysed the effect of system input rates on the performance of our water transport models. Positive, albeit weak correlations (R^2 of 0.07 to 0.21) could be observed between event-R^2 and system input rates for all models, suggesting that they generally performed (slightly) better for higher influx rates. For the PF model this could probably be explained by the PF parameters depending on laboratory measurements with high influx rates.

In combination with the hydraulic properties for lower-density snow samples, additional laboratory experiments might be able to determine the number and size of PFPs for lower input intensities and snow densities. Especially the calibrated parameters threshold for saturation (Θ_{th}) and the number of PFPs for refreeze (N) could benefit from such experimental studies. Even though CDP and WFJ provide long-term measurements on an adequate temporal resolution, these data give little information about spatial variability of snowpack runoff limiting further validation opportunities. Large area multi-compartment lysimeter setups might help to improve estimating size, amount and spatial heterogeneity of flow fingers. Sprinkling experiments with preferably low sprinkling intensities on such a device could fill a knowledge gap about water transport in snow under naturally occurring conditions.

2.5 Conclusions

A new water transport model is presented that accounts for PF of liquid water within a snow-pack. The model deploys a dual-domain approach based on solving the Richards equation for each domain separately (matrix and preferential flow). It has been implemented as part of the physics-based snowpack model SNOWPACK which enables us for the first time to account for PFPs within a model framework that is used operationally for avalanche warning purposes and snow melt forecasting.

The new model was tested for sprinkling experiments over a natural snowpack, dedicated measurements during natural ROS events, and an extensive evaluation over 101 historic ROS events recorded at two different alpine long-term research sites. This assessment led to the following main conclusions.

Compared to alternative approaches, the model accounting for preferential flow (PF) demonstrated an improved overall performance, particularly for lower densities and initially dry snow conditions. This led to smallest interquartile ranges for R^2 values and considerably decreased RMSEs for a set of more than 100 ROS events. When evaluated over entire winter seasons, the performance statistics were superior to those of a single domain approach (RE), even if the differences were small. Both PF and RE models, however, outperformed the model using a

bucket approach (BA) by a large margin (increasing median R^2 by 0.49 and 0.48 for WFJ and 0.53 and 0.48 for CDP). In sprinkling experiments with 30 min bursts of rain at high intensity, the PF model showed a substantially improved temporal correspondence to the observed snowpack runoff, in direct comparison to the RE and BA models. While the improvements were small for experiments on isothermal wet snow, they were pronounced for experiments on cold snowpacks.

Model assessments for over 100 ROS events recorded at two long-term research sites in the European Alps revealed rather variable performance measures on an event-by-event basis between the three models tested. The BA model tended to predict too early onset of snowpack runoff for wet snowpacks and a delayed onset of runoff for cold snowpacks, whereas RE was generally too late, especially for CDP. Combined with results from a separate cross-correlation analysis, results suggested the PF model to provide the best performance concerning the timing of the predicted runoff.

While there is certainly room for improvements of our approach to account for PF of liquid water through a snowpack, this study provides a first implementation within a model framework that is used for operational applications. Adding complexity to the water transport module did not negatively impact on the overall performance and could be done without compromising the robustness of the model results.

Improving the capabilities of a snowmelt model to accurately predict the onset of snowpack runoff during a ROS event is particularly relevant in the context of flood forecasting. In mountainous watersheds with variable snowpack conditions, it may be decisive if snowpack runoff occurs synchronously across the entire catchment, or if the delay between onset of rain and snowpack runoff is spatially variable, e.g. with elevation. In this regard, accounting for PF is a necessary step to improve snowmelt models, as shown in this study.

Data availability

Meteorological driving data for the SNOWPACK model as well as the lysimeter data are accessible via doi: 10.16904/1 (WSL Institute for Snow and Avalanche Research SLF, 2015) for WFJ and under doi: 10.5194/essd-4-13-2012 (Morin et al., 2012) for CDP. All other meteorological and lysimeter data are available on request. The SNOWPACK model is available under a LGPLv3 licence at http://models.slf.ch. The version used in this study corresponds to revision 1249 of /branches/dev.

Acknowledgements

3 Influence of Initial Snowpack Properties on Runoff Formation during Rain-on-Snow Events

Sebastian Würzer[a,b], Tobias Jonas[a], Nander Wever[a,b], Michael Lehning[a,b]

[a]WSL Institute for Snow and Avalanche Research SLF, Davos, Switzerland
[b]École Polytechnique Fédérale de Lausanne (EPFL), School of Architecture, Civil and Environmental Engineering, Lausanne, Switzerland

Summary

Rain-on-snow (ROS) events have caused severe floods in mountainous areas in the recent past. Due to the complex interactions of physical processes, it is still difficult to accurately predict the effect of snow cover on runoff formation for an upcoming ROS event. In this study, a detailed physics-based energy balance snow cover model (SNOWPACK) was used to assess snow cover processes during more than 1000 historical ROS events at 116 locations in the Swiss Alps. The simulations of the mass- and energy balance, liquid water flow and the temporal evolution of structural properties of the snowpack were used to analyze runoff formation characteristics during ROS. Initial liquid water content and snow depth at the onset of rainfall were found to influence the temporal dynamics, intensities and cumulative amount of runoff. The meteorological forcing is modulated by processes within the snowpack, leading to an attenuation of runoff intensities for intense and short rain events, and an amplifying effect for longer rain events. The timing of runoff generation relative to the rainfall seems to be strongly dependent on initial liquid water content, snow depth, and rainfall intensities. As these snowpack and meteorological conditions usually exhibit a strong seasonality, cumulative runoff generation during ROS also varies seasonally. ROS events with intensified snowpack runoff were found to be most common during late snowmelt season, with several such events also occurred in late autumn. These results demonstrate the strong influence of initial snowpack

properties on runoff formation during ROS events in the Swiss Alps.

3.1   Introduction

Rain-on-snow (ROS) events have often been associated with floods all over the world. Many of the largest floods in the US could be linked to ROS events (Kattelmann, 1997, Marks et al., 2001, Kroczynski, 2004, McCabe et al., 2007, Leathers et al., 1998). In Europe, several studies showed ROS to be responsible for flood generation, where 21% and 70% of the peak flows were identified to be associated with ROS in some parts of Bavaria (Sui and Koehler, 2001) and Austria (Merz and Blöschl, 2003), respectively. Moreover, frequencies and magnitudes of ROS events were found to be dependent on elevation, where upland basins were identified as most influenced by ROS events with flooding potential (Freudiger et al., 2014). It has been predicted that the frequency of ROS is likely to increase in high elevation areas (Surfleet and Tullos, 2013) as well as in high latitudes (Ye et al., 2008) due to climate change. Additionally, future changes in hydro-meteorological regimes may increase ROS frequencies in Switzerland (Köplin et al., 2014).

Spatial heterogeneity of the snow cover, uncertainties in meteorological input variables and deficits in process understanding make extreme events very difficult to forecast (Rössler et al., 2014, Badoux et al., 2013). However, most ROS events do not lead to floods. As has been shown in previous studies, even similar rainfall events can produce very different snowpack runoff responses, depending on many factors such as initial snow depth and liquid water content (LWC) (Kroczynski, 2004, Badoux et al., 2013). Therefore, for hydrometeorologists concerned with operational runoff forecasting, it is particularly important to know a priori if an upcoming ROS event will lead to more or less intense runoff generation. Snowpack processes like snow melt, water percolation, refreezing of infiltrating water and snowpack settling transform the rain input into snowpack runoff that may differ in cumulative amount, in temporal dynamics, and in its intensities (Wever et al., 2014a). To estimate the streamflow response, information on the timing of snow cover runoff from contributing areas is essential. The timing of snow cover runoff was found to be dependent on snow cover properties like ripeness (Colbeck, 1975, Singh et al., 1997) and depth (Kohl et al., 2001, Wever et al., 2014a). Accordingly, Garvelmann et al. (2015) discussed the importance of the spatial distribution of total retention of liquid water on temporal dynamics of the meltwater release within a catchment during ROS. These findings demonstrate how important it is to consider physical snow cover processes in detail when assessing runoff formation during ROS events.

Also, meteorological conditions causing snowmelt can differ in space and time. Radiation is known to be an important driver of snowmelt in many regions worldwide (e.g. Cline, 1997, Marks and Dozier, 1992). However, during ROS, the presence of a cloud cover leads to a reduced incoming shortwave radiative flux, whereas an increase in incoming longwave radiative flux may lead to a small positive net longwave radiative flux, where energy fluxes directed to the snow cover surface are defined to be positive in this study. While it is known

that heat advected by rain provides little direct energy for snow melt (Prowse and Owens, 1982, Moore and Owens, 1984) the turbulent fluxes of sensible and latent heat (collectively referred to as turbulent heat fluxes) have been shown to account for high snow melt intensities during ROS conditions (Dyer and Mote, 2002, Dadic et al., 2013). Consistently, various studies found that flooding associated with ROS events featured high wind speeds (Harr, 1981, Berris and Harr, 1987). The dominating character of turbulent heat fluxes during ROS has been reported in several studies, accounting for 60-90% of energy available for snowmelt on open field sites (Garvelmann et al., 2014, Marks et al., 1998, 2001). Hence, process-oriented snow cover models that account for energy balance terms individually and resolve water retention and transport processes within the snowpack are the preferred choice when analyzing runoff formation during ROS events.

In this study we take the perspective of a forecaster by attempting to estimate the effects of an existing snow cover on runoff formation based on information about snow cover and meteorological conditions typically available prior to an ROS event. This is why, unlike many previous studies, we include a large range of initial snowpack conditions and precipitation scenarios that actually occurred at 116 measuring stations and over the past 16 years; without excluding events that did not result in snowpack runoff. In order to allow reliable snowpack model runs, we selected stations that could provide all meteorological variables required as model input as well as snow data to validate model results. Such data were available for 116 stations across the Swiss Alps, spreading over an elevational range from 1560-2972 m above sea level (ASL). With this wide-range approach we enhance the potential to single out a few important parameters which can be used to forecast the effect of snow on runoff formation for upcoming rain events of different magnitudes. Note that no snow lysimeter network exists in the Alps, which is why observational data alone would not allow for such a study.

This is the first study to analyze detailed snow cover processes for more than 1000 naturally occurring ROS events with a detailed physical snowpack model. Moreover, we assess those processes from the perspective of a forecaster and discuss both critical and non-critical events without prior restriction to extreme conditions. In this context, critical refers to events during which snowpack processes lead to increased runoff generation relative to conditions without snow cover. The analysis of the simulations aims to answer the following research questions:

- What are the main contributing energy balance terms for different magnitudes of rain-on-snow events?

- Under what meteorological conditions does the state of the snow cover have an amplifying, damping and/or delaying effect on runoff generation?

- What is the influence of the initial snowpack conditions on the evolution of snow cover runoff generation?

This paper is structured as follows: Input data, the snow cover model, the model setup and the event definition are described in section 3.2. Results of the simulations are shown
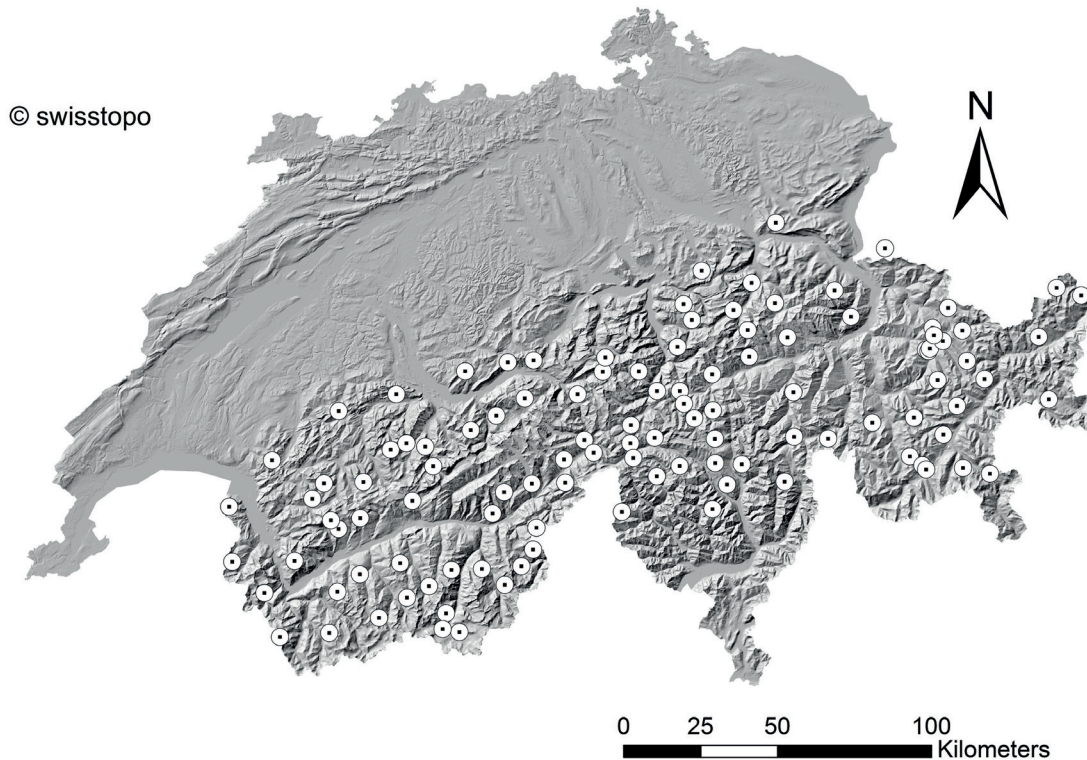
Figure 3.1 – Map of Switzerland with locations of the stations used for the analysis. Reproduced by permission of the Swiss Federal Office of Topography (swisstopo; JA100118)

and discussed in section 3.3. This includes a general description of ROS, including spatial and temporal occurrence (section 3.3.1), driving energy terms (section 3.3.2), the processes concerning runoff generation during ROS (section 3.3.3) and the ability to predict temporal occurrence of runoff (section 3.3.4). General conclusions are found in section 3.4.

3.2 Methods

All results in this study are derived from simulations with the one-dimensional physical SNOWPACK model using measurement data from 116 automated weather stations operating within the Interkantonales Mess- und Informationssystem (IMIS) network in the Swiss alpine region (Figure 3.1). A comparable model setup was already used to analyze one major ROS event in October 2011 in the Swiss Alps (Wever et al., 2014a, Badoux et al., 2013). In this section, the input data for the simulations are discussed first, followed by the description of the model and the used model setup. Then, we come up with an approximation of the available retention capacity (ARC) for further discussion on how to transfer results from detailed snowpack simulations into simpler forecasting models. Finally, the definition of ROS events used in this study is introduced.

3.2.1 Input data

The IMIS network stations measure several meteorological values and snow cover conditions such as wind speed and direction, temperature, relative humidity, surface temperature, soil temperature, reflected shortwave radiation and snow depth. The temporal resolution of all input quantities used here is 1h. The station network is operationally used with the SNOWPACK model for avalanche warning purposes (Lehning et al., 1999). The station sites are generally located in locally flat terrain ranging in elevation from 1560 to 2972 m ASL. This elevation band represents approximately 35% of the area of Switzerland and is both high enough to accommodate seasonal snow over several months and low enough to allow for concurrent liquid precipitation.

Unfortunately, the rain gauges of IMIS stations are unheated due to limited power supply and therefore provide no reliable measurements in case of snowfall and mixed-phase precipitation, which is often observed during ROS. This is why we used a gridded precipitation data set provided by MeteoSwiss (RhiresD; MeteoSwiss, 2013), assembled from data of the automated station network SwissMetNet and of a dense network of totalizer rain gauges. This product is the most elaborate product for Switzerland available today. Daily precipitation sum of the RhiresD data set were disaggregated into hourly sums by using the relative hourly amounts of precipitation registered at the three SwissMetNet stations which showed highest correlation with the grid cell closest to the respective IMIS station.

3.2.2 Model description

The physics-based snowpack model SNOWPACK simulates the evolution of the snow cover as a 1D column. A detailed model description is provided in Bartelt and Lehning (2002) and Lehning et al. (1999, 2002b,a). Bartelt and Lehning (2002) describe the one-dimensional equations governing heat transfer, water transport and mechanical deformation. The model snow microstructure and metamorphism routines are described in Lehning et al. (2002b). Finally, the characterization of meteorological forcing and thin layer formation as well as a complete evaluation for the entire model is found in Lehning et al. (2002a).

Snow melt occurs in SNOWPACK, when the temperature of a specific simulated layer is $0\,°\text{C}$ and additional energy is provided. Additional energy is added by either heat conduction in the snow matrix or by the shortwave radiative flux penetrating the snow. The net shortwave radiative flux is presented as a source term in the top layers of the snowpack to account for the penetration of shortwave radiation in the snowpack as described by Lehning et al. (2002b). Observed reflected shortwave radiation and a parameterized albedo (Schmucki et al., 2014) are used to approximate the net shortwave radiative flux. The heat flux at the top of the snow cover, consisting of the sum of net longwave radiative flux (Wm^{-2}), sensible heat flux (Wm^{-2}), latent heat flux (Wm^{-2}) and heat advection flux by liquid precipitation (Wm^{-2}), is prescribed as a Neumann boundary condition when the snow surface is melting (Bartelt and Lehning, 2002). For sub-freezing snowpack conditions, measured snow surface temperature is prescribed as a

Dirichlet boundary condition to get an accurate estimate of the snow cover temperature at the onset of events (Bartelt and Lehning, 2002). The turbulent surface heat fluxes are simulated using a Monin-Obukhov bulk formulation for surface exchange. Stability correction functions of Stearns and Weidner (1993), as described in Michlmayr et al. (2008) are used to consider stable conditions. If no measurements of the incoming longwave radiative flux are available, it is parameterized (see Section 3.2.1).

The vertical liquid water movement within the snow cover is either simulated by a simple so called bucket scheme (Bartelt and Lehning, 2002) or solving the Richards' equation, a recently introduced method for SNOWPACK (Wever et al., 2014b,a). Wever et al. (2014b) also describe some recent developments of the model.

3.2.3 Model setup

The SNOWPACK model (Version 3.2.1 Revision 746) was used to simulate the snow cover development during full hydrological years, starting on October 1st. Simulated snow depth was constrained to observed values, which means that the model interprets increase in observed snow depth at the IMIS stations as snowfall (Lehning et al., 1999, Wever et al., 2015). A temperature threshold ranging from $0.7\,°C$ to $1.7\,°C$ was used to determine whether precipitation should be considered rain (from RhiresD) or snow (from the snow depth sensors) or in form of mixed precipitation (proportionally between 0.7 and $1.7\,°C$). 90% of all measured temperatures during ROS events in the data set are above $1.2\,°C$. Because snowfall is determined by the snow depth measurements, no compensation for solid precipitation undercatch had to be performed.

For simulating the percolation of meltwater and rainwater, the Richards' equation approach was chosen because it was found to improve the representation of runoff timing from the snowpack, especially for sub-daily timescales (Wever et al., 2014b,a) as well as several aspects of the representation of the internal snowpack structure due to liquid water flow processes (Wever et al., 2015). The model was initialized with a soil depth of 3.3 m, with a grid spacing between 5 cm in the upper layers and 20 cm in the lower layers in order to be able to accurately describe the heat and water flux between the soil and the snowpack. Soil heat flux at the lower boundary is set to a constant value of $0.06\,\mathrm{W\,m^{-2}}$, which is an approximation of the geothermal heat flux (Pollack et al., 1993, Davies and Davies, 2010). For soil, typical values for very coarse material were chosen, such that there was no ponding inside the snowpack due to soil saturation. A free drainage boundary condition was taken as the lower boundary condition for liquid water flow in the soil. A threshold value of $-3\,°C$ was used to determine whether a Dirichlet or Neuman boundary condition should be used. For the roughness length z_0, a value of 0.002 m was used. Incoming longwave radiative flux was simulated using the parameterization from Unsworth and Monteith (1975), coupled with a clear sky emissivity following Dilley and O'Brien (1998), as described in Schmucki et al. (2014).

3.2.4 Available retention capacity

A simple estimation of the amount of liquid water that could be stored in the existing snow cover may enable predicting the start of snowpack runoff without the necessity of running a complex snowpack model. The Available Retention Capacity (ARC) was determined by the liquid water refreezing capacity inside the snow cover, the capillary holding capacity (HC) and the liquid water already present in the snow cover (LWC$_{init}$). Many studies found the HC to be within a range of 0-10% of volume of the snow cover (Kattelmann, 1987b, Coléou and Lesaffre, 1998). Here, we assumed the HC to be 3.5% of volume of the snow cover, expressed in mm water equivalent (mm w.e.) as:

$$HC = C_H H_S \rho_W,$$ (3.1)

where $C_H = 0.035$ is the holding capacity as volume fraction, ρ_W is the density of water (kg m^{-3}) and H_S the snow cover depth (m). The liquid water refreezing capacity is directly related to the cold content (CC) of the snowpack. The CC represents the energy needed to warm the snow cover to an isothermal 0 °C, usually described as the amount of liquid water from melt or rainfall that must be frozen in a subfreezing snowpack to release that energy (DeWalle and Rango, 2008). It was calculated according to Eq. (3.2), proposed by Wever et al. (2015):

$$CC = \frac{c_I}{c_F} \rho_S H_S (T_M - T_S),$$ (3.2)

where c_I is the specific heat of ice (J kg^{-1} K^{-1}), c_F the latent heat of fusion (J kg^{-1}), ρ_S the density of snow (kg m^{-3}), CC the cold content in mm w.e. and $(T_M\text{-}T_S)$ the average temperature deficit (K) as difference between T_M, the temperature where snow melts (K), and T_S, the temperature of the snow cover (K). Therefore the *ARC* is described in terms of mm w.e. as follows:

$$ARC = HC + CC - LWC_{init},$$ (3.3)

Note that all variables required to calculate ARC according to Eq. (3.3) are usually available in relatively simple conceptual snowmelt models that are often used in operational hydrological models.

3.2.5 Event-Definition and dependent variables

The definition of what constitutes a ROS event has an essential effect on the number and spatiotemporal characteristics of such events and is usually set depending on the purpose of

the study. Certainly a study that focusses on extreme ROS events only will lead to results that differ from studies on a broader range of ROS events. For single case studies, the temporal limits of the event are often arbitrarily chosen. Other studies analyzing larger numbers of ROS events often define ROS to be a day or 24 hours with specific rainfall amounts (Mazurkiewicz et al., 2008) or, additionally, a minimum decrease in snow cover depth (McCabe et al., 2007). Here, we attempt to investigate ROS events from the perspective of a forecaster knowing about the presence of a snow cover and predicted rainfall, but not about the expected amount of snow melt. Therefore, selection criteria were chosen such that there had to be substantial rainfall on a substantial snow cover without the need for melt or a decrease in snow cover depth. Because of potential refreezing inside the snowpack, snow melt may not occur, and in the case of mixed precipitation or a transition from rain to snow, snow cover can even increase during ROS. Therefore, in this study a ROS event was considered to be when at least 20 mm rain fell within 24 hours on a snow cover of at least 25 cm at the onset of rain. The start of an event was set after the first 3 mm of cumulative rainfall; end conditions were fulfilled if less than 3 mm of cumulative rain as well as less than 6 mm of cumulative runoff occurred within 10 and 5 hours, respectively. Defining the end of a ROS event based on both rain and snowpack runoff made sense from the perspective of flood forecasting, but led to a few events with extended length due to continued snowmelt after the rain had stopped.

To ensure accurate model simulations as input for the analysis, we excluded all event simulations with a root mean square error (RMSE) between simulated and observed snow depth during an event exceeding 20 cm. This criterion reduced the number of considered ROS events from 1336 to 1063 with an average RMSE of 6.2 cm. Excluded simulations were possibly affected by inadequate meteorological forcing data, in particular the precipitation input.

The term rainfall duration denotes the sum of hours with rainfall occurring during an event. Rainfall intensity is the quotient of rainfall amount divided by rainfall duration. This means that periods without rainfall are neglected when calculating rainfall intensities. Maximum rainfall intensity refers to the highest hourly rainfall value during an event. Initial observed and simulated snow depths refer to the initial values at the beginning of an event.

3.3 Results and Discussion

3.3.1 Spatiotemporal occurrence and general characteristics of ROS events

Before discussing meteorological and snowpack conditions and their effect on runoff generation during ROS, we first analyzed the temporal and spatial occurrence of ROS. The event definition given above led to a total of 1063 individual station events (IE), or single ROS events occurring at a single station. Synchronous events (SE) are a set of IE that occur simultaneously at multiple locations. Over the entire 16-year period considered in this study (October 1998 till September 2014) 163 SE were identified, accounting for 939 or approximately 90% of IE. This corresponds to approx. 10 SE per year with an average of 5.8 locations involved. Figure 3.2
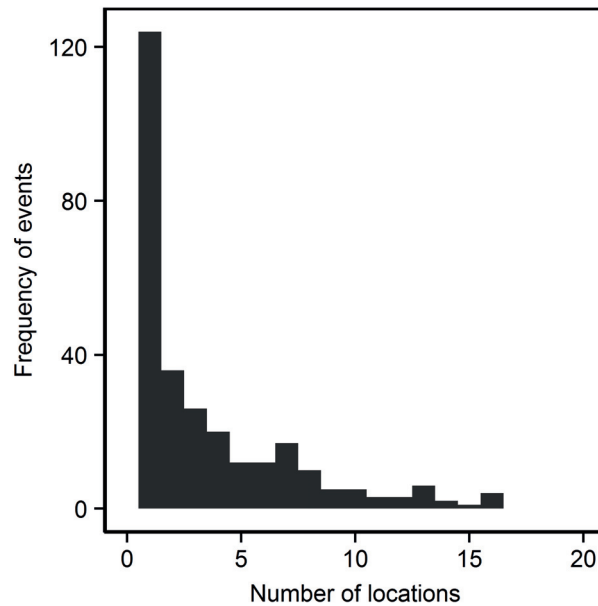
Figure 3.2 – Number of locations involved in synchronous ROS events

presents a distribution of the number of IE per event. Events with 1 location being involved have the highest frequency. In contrast, events with many locations being involved are rather rare. For example, synchronous events involving more than 15 locations occurred approximately once a year. Note that these numbers represent the spatial extent of ROS events that match the event definition used here at the given distribution of IMIS locations in Switzerland. However, they may not be representative of ROS events at elevations below 1500 and above 3000 m ASL. (which are not covered by the IMIS station network, Figure 3.3).

Figure 3.3 presents the occurrence of ROS events by date of year and elevation. The color indicates the runoff excess, which corresponds to the cumulative difference between snow cover runoff and rain input per IE. Negative excess values indicate that at least some fraction of rain water is retained in the snow cover, whereas positive values indicate additional snowpack runoff from snow melt and from the destruction of the snow cover matrix, which in turn decreases the retention capacity (Wever et al., 2014a). At elevations between 1560 and 2972 m ASL, as expected, most ROS events occurred during the months of May and June. At this time of the year a significant snow cover is still present when temperatures become high enough for precipitation to occur as rain. Further ROS events occurred between October and April, mostly below 2300 m ASL. Interestingly, many autumn events could be associated with larger scale ROS events and occur simultaneously at many locations (not shown). In fact a ROS event in October 2011 (Wever et al., 2014a) caused regional floods and was among those ROS events with the highest overall snowpack runoff. High positive runoff excess was mostly generated by events in late spring and early summer, whereas autumn events typically featured a neutral runoff balance, with exceptions as mentioned above. Events during winter and early spring, on the other hand, normally retained runoff.
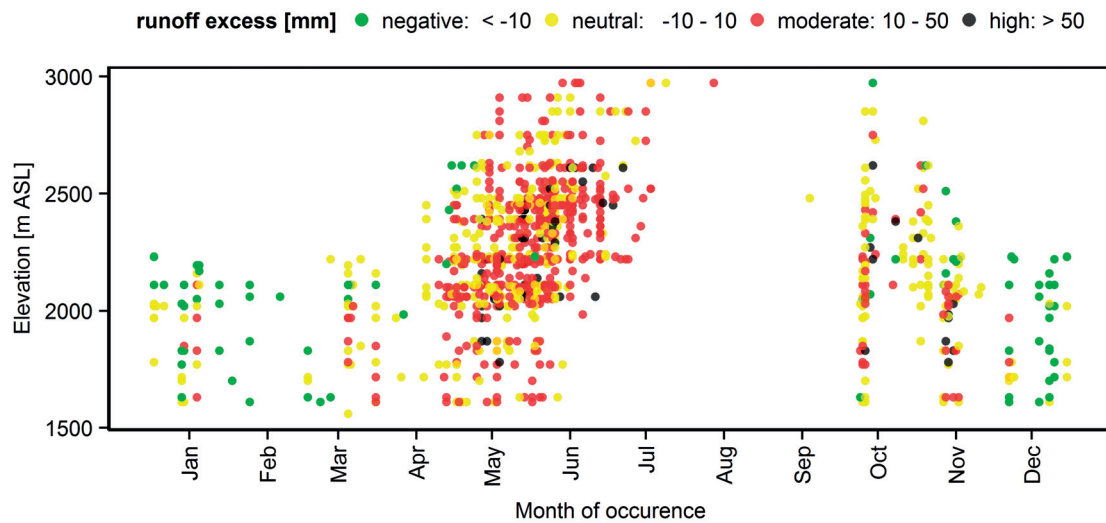
Figure 3.3 – Occurrence of ROS events by elevation and month. The colors denote the event-specific runoff excess, which is the cumulative runoff minus cumulative rainfall.

In contrast to other studies (e.g. Freudiger et al., 2014, Surfleet and Tullos, 2013), we did not exclude ROS events that did not generate snowpack runoff, or ROS events with only marginal snowmelt contribution. This led to three typical patterns of the cumulative runoff to rain ratio, which could be identified from the simulations of all IE events (Figure 3.4). The first pattern (a) describes events for which cumulative runoff never exceeds the cumulative rainfall, usually accompanied by a delayed initiation of snowpack runoff. The second pattern (b) is representative of events for which cumulative snowpack runoff exceeds the rain input from the very beginning. This pattern of event requires melting or at least saturated initial snowpack conditions. Finally, under the third pattern (c) fall ROS events that start as in the first pattern but persist long enough to allow cumulative snowpack runoff to exceed rainfall in the course of the event. These 3 event patterns show that the presence of a snow cover can have a dampening, amplifying or delaying effect on the rainfall - snowpack runoff relationship. The relative occurrence of these patterns over all 1063 IE analyzed is pattern (a): 17%, pattern (b): 14%, pattern (c): 69%. During 4% of all events no runoff was generated.

The average length of the studied ROS events was 23 hours, with less than 5% being longer than 48 hours. The rainfall statistics for all analyzed IE events are shown in Table 3.1. According to the event definition, the minimal amount of rainfall is 20 mm, whereas the highest amount recorded was 613 mm. The mean rainfall duration was 18 hours, ranging from 3 to 96 hours. With rainfall intensities reaching from 0.8 to 10.9 mm h^{-1} and a mean intensity of 2.4 mm h^{-1}, values exceeded those recorded for ROS events in Sierra Nevada, California (Osterhuber, 1999). Regarding initial snow depths, minimal values were just above 25 cm, again due to the threshold of the event definition. The highest initial snow depth recorded was 430 cm.
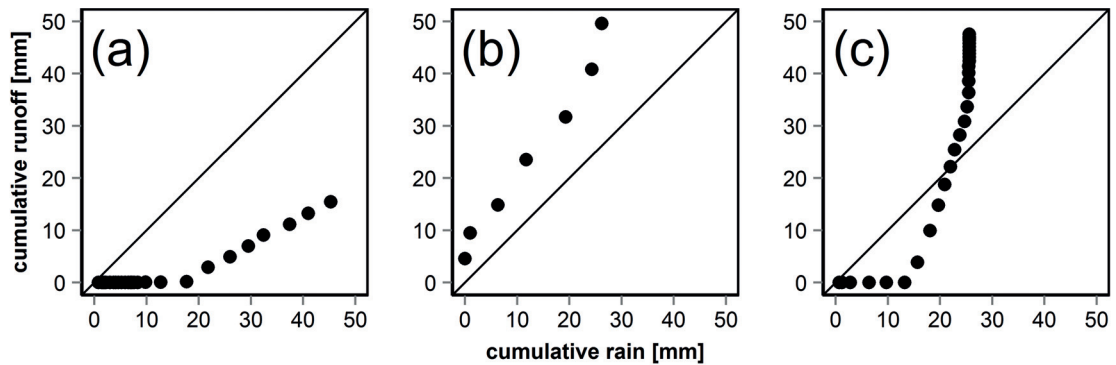
Figure 3.4 – Temporal trajectory of the ratio between cumulative snowpack runoff and cumulative rain input at hourly time steps for three ROS event patterns.

Table 3.1 – Rainfall and snow cover statistics for all ROS events.

	Mean	Min	Max	Std dev
Rainfall amount (mm)	42	20	613	36
Rainfall duration (h)	18.0	3.0	96	10.5
Rainfall intensity ($mm\,h^{-1}$)	2.4	0.8	10.9	1.3
Max rainfall intensity ($mm\,h^{-1}$)	6.7	1.5	51.7	4.1
Initial snow depth observed (cm)	116	26	433	74
Initial snow depth simulated (cm)	115	25	429	73
RMSE snow depth simulated 2 observed (cm)	6.2	0.5	20.0[a]	5.0

[a] Events with an RMSE higher than 20.0 cm were excluded from the analysis.

3.3.2 Energy balance terms during ROS

Excess snowpack runoff, generated during 83% of all events (pattern b + c), typically requires snow melting during a ROS event. Figure 3.5 illustrates single energy terms and their contribution to the overall energy input to the snow cover, both in mm melt equivalent (mm m.e.), where mm melt equivalent is referring to the energy required to conduct the phase change of ice to liquid water.

The overall radiation balance strongly depends on the time of day at which an event occurs (Garvelmann et al., 2014). Often net longwave radiative flux (LWR) is negative, but can become positive during warm and moist ROS events. During daytime, net shortwave radiative flux (SWR) can compensate negative LWR. However, both LWR and SWR typically remain small terms and for 97% of all IE, the sum did not contribute more than an equivalent of 20 mm (in total) or $0.6\,mm\,h^{-1}$ snowmelt. Earlier, latent and sensible heat fluxes were shown to be the main melt energy input for individual events (Marks et al., 1998, Wever et al., 2014b, Garvelmann et al., 2014). Our analysis confirms that those energy terms also show high correlations with the total energy input for a large range of ROS events in the Swiss Alps. In
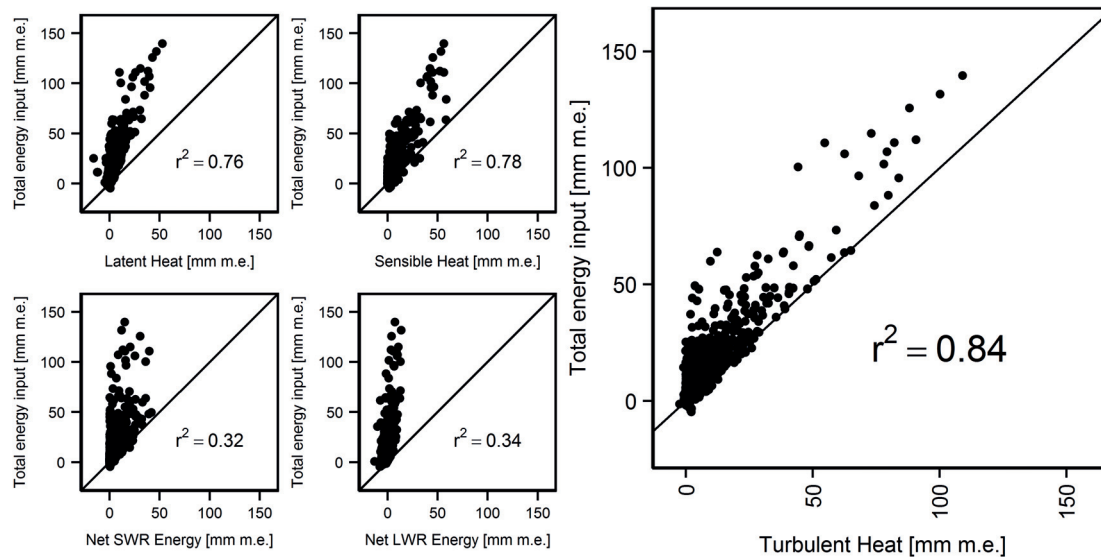
Figure 3.5 – Contribution of single energy balance terms to the total energy input to the snowpack during all ROS events analyzed: latent heat, sensible heat, net shortwave radiation, net longwave radiation, and turbulent (sensible plus latent) heat flux (mm m.e.). Ground heat flux and heat advected by rain are not shown.

contrast, radiative fluxes are both poorly correlated with total energy input. If added up (Figure 3.5 right panel), turbulent heat fluxes provide most of the energy input, particularly for those events that feature a snowmelt-contribution exceeding 50 mm m.e. Providing less than 1% of total energy input on average, ground heat flux was found to be of minor importance (data not shown). Advected heat by rain provided on average 13% of total energy input. It is therefore a non-negligible source for melt energy, but can be rather easily estimated in advance of an event, if estimates of expected precipitation amount and air temperature are available.

From a mass balance perspective, snow melt was on average responsible for 27% of total runoff, whereas rain contributed 73% to total runoff. Other studies found snowmelt contributions ranging from 22% to 70% on the catchment scale (Garvelmann et al., 2015, Sui and Koehler, 2007, Rössler et al., 2014).

3.3.3 Runoff characteristics of simulated ROS events

From the perspective of hydrological forecasting, both magnitude and timing of snowpack runoff are relevant. A delay of snowpack runoff relative to the start of rain may affect the runoff generation at the catchment scale, in particular if this time lag varies across a given catchment. As a demonstrative example of this, Garvelmann et al. (2015) analyzed two subsequent ROS events. For one of the events, river runoff rates were considerably higher as the whole catchment generated snowpack runoff simultaneously (within 1h). In contrast, for the other event, snowpack runoff generation was delayed up to 12 h at higher elevations, leading to less pronounced river runoff rates and significantly smaller peak flows. In the following we analyze
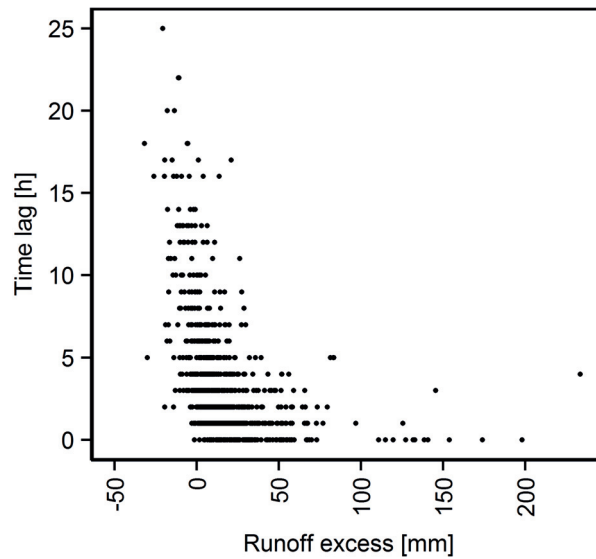
Figure 3.6 – Time lag between the start of rainfall and the start of snowpack runoff as it relates to runoff excess. Events without runoff are excluded from the figure (no time lag).

time lag as a function of initial snowpack conditions.

As a first observation, the simulations of all ROS events show a correlation between time lag (time between event start and cumulative runoff exceeding 3mm) and runoff excess (Figure 3.6). Events with high excess runoff are associated with short time lags between the beginning of rain and the beginning of snowpack runoff. Such events typically occur in late spring or early summer and feature a high initial LWC. On the other hand, events that exhibit a time lag above 5 hours do not provide significant excess runoff if at all. The highest time lags can be found for events with a net retention of rainwater (i.e., negative runoff excess) in the snow cover at the end of the event.

The time lag in terms of the initial snow depth was further analyzed by separating data into three categories of initial LWC (Figure 3.7). The overall correlation of time lag to the initial snow depth is rather poor ($r = 0.13$). For low and high initial LWC values, the time lag was correlated to the initial snow depth at $r = 0.49$ and $r = 0.45$, respectively. With intermediate initial LWC this correlation is less pronounced ($r = 0.27$). The results for dry snow conditions are consistent with those shown in Wever et al. (2014a), who analyzed a specific ROS event under fresh and dry snow conditions based on data from 14 stations. Additionally, in experimental studies under constrained conditions, the effect of snow depth on time lag has been shown (e.g. Kohl et al., 2001). However, when looking at dependencies in data from a range of different naturally-occurring ROS events, Berg et al. (1991) came to the conclusion that there is little correlation between time lag and initial snow depth, although snow depth became important for time lag to peak outflow in its interaction with melt potential. Therefore, snow depth can be considered to be an important measure for runoff timing, but only if considering similar

53
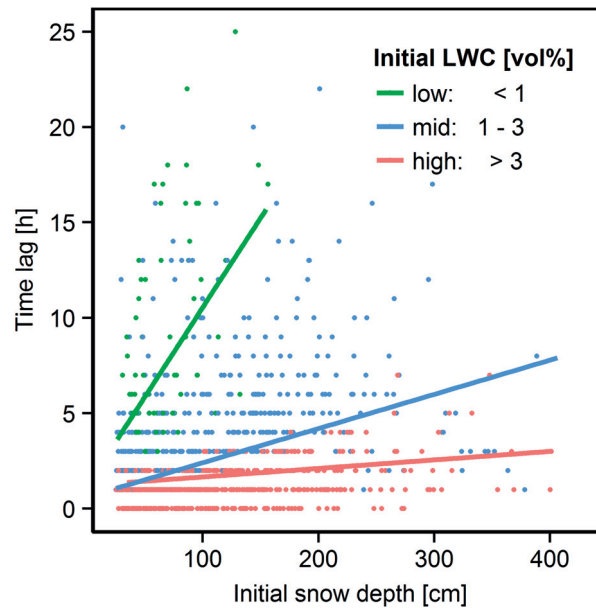
Figure 3.7 – Time lag as a function of initial snow depth for events with different initial LWCs, indicated by different colors. The solid lines denote a linear regression fit for the respective initial LWC class.

initial snow cover conditions, in particular LWC.

Transferring the above findings to a catchment that features a variable distribution of snow depth (usually governed by an elevational gradient), the following two scenarios arise under the assumption of spatially constant rain input. In the case of low initial LWC, time lag is correlated with snow depth. Hence snowpack runoff will not occur synchronously throughout the catchment. Moreover, areas with higher snow depth (and thus higher time lags) are associated with limited excess runoff (Figure 3.6). Both mechanisms may reduce the associated flood risk, in particular if the duration of the rain is shorter than the involved time lags. By contrast, high initial LWC will typically lead to short time lags, resulting in temporally synchronous snowpack runoff throughout the catchment with only a marginal effect of the spatial variability in snow depth. Moreover high excess runoff has only been observed in the case of events with a short time lag. These considerations demonstrate that the initial LWC might be a valuable indicator to assess the flood risk associated with an upcoming ROS event.

As shown above, initial snow cover properties can provide useful information about the course of an event. However, the rain-runoff behavior of a ROS event is not just determined by initial snow cover properties, but also by the rain water input signal itself. To approximate a corresponding signal propagation velocity, the initial snow depth was divided by the time lag for IE. For low initial LWC, the above defined velocities can be regarded as the velocity at which the wetting front propagates through the snowpack. This analysis was constrained to IE with a time lag >= 2h, to avoid including data from IE with immediate runoff release that represent the displacement of initial liquid water content rather than the propagation of rain input. In Figure
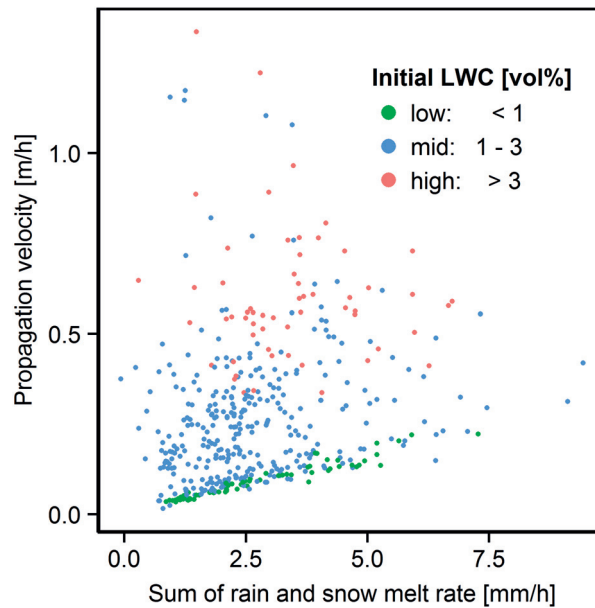
Figure 3.8 – Initial snow depth divided by the time lag (propagation velocity) over the rate at which liquid water is added to the snowpack (rain plus snowmelt) for different initial LWCs.

3.8 this velocity is displayed against the liquid water input generated by melt and rain, both dependent on meteorological variables. Contrary to Figure 3.7, levels of correlations differ much more for different initial LWC values. At low initial LWC the velocity is well correlated with the rate at which new liquid water is added to the snowpack (r=0.9). For higher LWC values however, the correlation is much weaker and velocities are hard to predict (r_{mid} = 0.03, r_{high} = 0.01). The positive relationship between liquid water input and meltwater front propagation has been found earlier and the modelled velocities are comparable with experimental results by Jordan (1983) and experimental results shown in Colbeck (1972), which are both studies representing spring melt conditions. Wetting front propagation velocities may differ strongly, as results from artificial rain experiments and naturally occurring ROS events show: Most values found in literature show values ranging from $0.04\,\mathrm{m\,h}^{-1}$ to $1.8\,\mathrm{m\,h}^{-1}$ (Gerdel, 1954, Conway and Benedict, 1994, Jordan, 1983). In the concept of Richards' equation, the hydraulic conductivity is a function of the liquid water content of the snow (Wever et al., 2014b). Only in case of low initial LWC, typical rainfall intensities are sufficient to rapidly change the already present LWC values, directly impacting the hydraulic conductivity and thereby the propagation velocity. This offers an explanation for why there is a positive relationship between water input rate and propagation velocity. Note that the propagation velocity is limited by refreezing inside the snowpack and low hydraulic conductivity in lower parts of the snowpack. Therefore, the propagation velocity varies only moderately on rainfall intensities and snow depth and is shown to be a good predictor for time lag, as illustrated in Figure 3.7. For moderate or high initial LWC, the hydraulic conductivity is already increased, and the impact of rainfall or additional snow melt is comparatively small. The propagation velocity is more dependent on the initial state of the snow cover, in particular the vertical distribution of liquid water inside

the snowpack.

However, indications also exist that this conceptual picture may change with further increasing precipitation intensities. E.g. Singh et al. (1997) found a velocity of $6\,\mathrm{m\,h^{-1}}$ for high precipitation intensities (48-100 $\mathrm{mm\,h^{-1}}$) during an artificial sprinkling experiment. These precipitation intensities are outside the range found in natural conditions in this study in the Swiss Alps, but also for ROS events in other regions, e.g. the western US (Osterhuber, 1999). We argue that preferential flow paths get increasingly important, as it was shown that they appear to carry more water down efficiently with increasing water input intensities (Katsushima et al., 2013, Hirashima et al., 2014). When snow gets closer to saturation, as may happen in those flow channels, flow velocities may increase significantly. Walter et al. (2013) found noticeably higher values for liquid water movement velocities, reaching up to $36\,\mathrm{m\,h^{-1}}$ on average in experimental studies with saturated snow samples. Note, however, that this comparison is not trivial since individual water "particles" as measured by these authors may move much faster than the "bulk" signal propagation velocity considered here.

Experimental studies on artificial ROS events often represent specific rainfall scenarios, whereas results from this study are based on the full natural variability of more than 1000 rainfall events on snow. For example, the events studied here do not only involve homogeneous snowpacks, which are weakly layered, but also strongly layered or deep snow covers in which water flow is influenced by the presence of capillary barriers and ice layers leading to ponding of liquid water inside the snow cover. For the large range of snowpack and meteorological conditions considered in this study, Figure 3.8 displays the importance of rain input intensities for the temporal runoff response.

During a ROS event, snowpack processes transform the rain input into snowpack runoff that may differ in cumulative amount, in temporal dynamics, and in its intensities. While we have looked at aspects regarding amounts and timing of snowpack runoff, we will now analyze the snowpack runoff intensities.

Figure 3.9 displays snowpack runoff intensities relative to rain intensities, where both quantities were averaged over the period in which runoff and rainfall occurred, respectively. Our results show distinct dependencies. First, for intense and short rain events (> $4\,\mathrm{mm\,h^{-1}}$ and < 10 hour duration), snow cover processes attenuated rain intensities. On the other hand longer rain events (> 10 hours) typically entailed an amplifying effect with only a few exceptions. Only short low intensity rainfalls (< $4\,\mathrm{mm\,h^{-1}}$ and < 10 hour duration) may lead to either effect.

Furthermore, snow cover properties had an influence on runoff-intensities. Figure 3.10 displays event-averaged snowpack runoff intensities in terms of the initial snow depth. The results show that the highest runoff intensities are associated with shallow snow covers. Conversely, runoff intensities are rather low for the deepest snow covers and therefore increased snow depth tended to moderate snowpack runoff intensities.
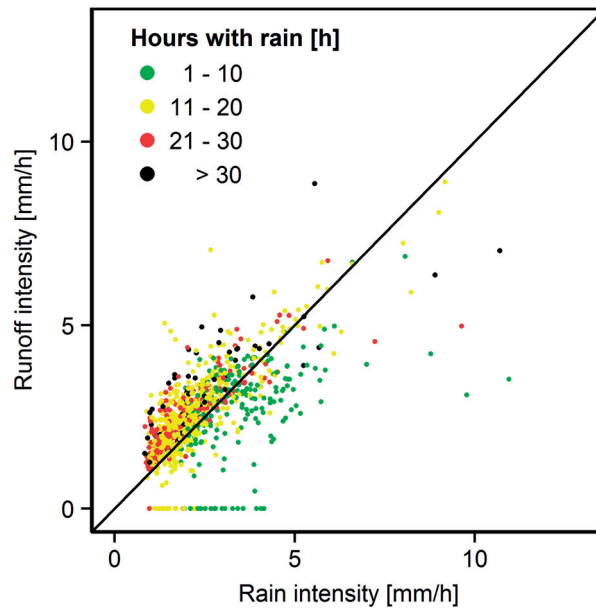
Figure 3.9 – Runoff intensities (averaged over the duration of runoff) vs. rainfall intensities (averaged over the duration of rainfall) for rainfall events of different length.
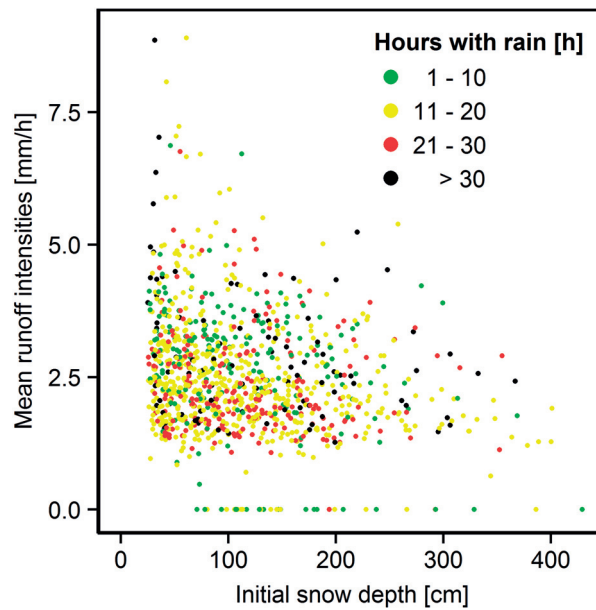
Figure 3.10 – Runoff intensities in terms of the initial snow depth for rainfall events of different lengths.

Note that our findings represent a general albeit weak trend with a large scatter of data between snow depth and runoff intensities when looking at a large range of ROS events. The observed scatter is attributable to the additional dependence of runoff intensities on other variables, e.g., rain intensities (Figure 3.9) or other snow cover properties. Colbeck and Davidson (1973)
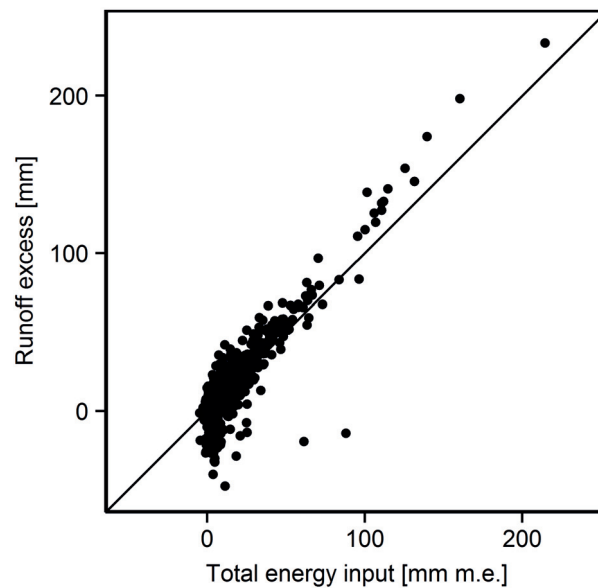
Figure 3.11 – Runoff excess (runoff minus rain) in terms of total energy input.

found the maximum flow rate to decrease with snow depth; however they only investigated rain events on ripe snow. In contrast, Berg et al. (1991) reported a low positive correlation of flow intensities with snow depth during ROS. Also, for a set of ROS events under similar meteorological forcing, the dependencies might be different from our findings. Wever et al. (2014a) noted that during an intensive ROS event (October 2011, European Alps) runoff intensities were slightly higher for deeper snow covers. The authors explained this behavior by the additional liquid water release that comes with settling and the destruction of the snow matrix inside the snow cover during intensive rain, which was found to be more pronounced in deep snow covers.

In an attempt to quantify the influence of this effect as well as that of snow melt on snowpack runoff in our simulations of more than 1000 ROS events, we compared the total energy input to the runoff excess, which is snowpack runoff minus rain input (Figure 3.11). It seems that for ROS with large runoff excess, there is always slightly more liquid water released than what can be explained from rain input plus snowmelt. In those cases the destruction of the snow matrix and the affiliated reduction in the liquid water holding capacity could contribute roughly up to 20% additional snowpack runoff (relative to the snowmelt contribution).

3.3.4 Available retention capacity of snow covers experiencing ROS

The available liquid water holding capacity may provide a key for forecasting the timing of snowpack runoff for an upcoming ROS event. While the liquid water holding capacity could be directly derived from the state variables of SNOWPACK (e.g. grain size, snow density), here we opted for a derivation that is also accessible if using less complex, conceptual snowmelt
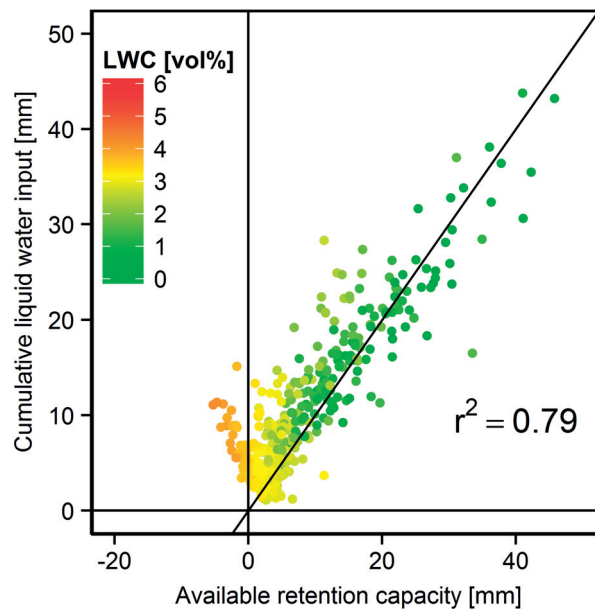
Figure 3.12 – Cumulative liquid water input (rain plus snowmelt) from the beginning of the ROS event until first snowpack runoff is released as a function of the available LWC retention capacity.

models to ensure a wider applicability. The LWC holding capacity used here was calculated as described in the methods section (Eq. 3.3).

Neglecting preferential flow, the ARC has to be filled before the snow cover will release runoff. To test the utility of the ARC we have compared ARC with cumulative rain input plus total snow melt over the period from the start of the ROS event to the moment at which snowpack runoff started (Figure 3.12). The data shown in Figure 3.12 are limited to events with an initial snow water equivalent of less than 500 mm and a time lag between water input and snowpack runoff > 0. Generally the ARC provides reasonably good predictive capabilities of the liquid water input that the snowpack can take before snowpack runoff commences (r^2 = 0.79 / RMSE = 4.5mm). However, further testing of this concept using snow lysimeter data would provide additional insights.

3.4   Conclusions

Based on measured meteorological and snowpack data from 116 locations and for 16 years, 1063 historical ROS events in the Swiss Alps could be identified and evaluated. To assess the relevant snow cover processes in detail, all events were analyzed using the physically-based snow cover model SNOWPACK. This is the first study to investigate snowpack state and meteorological conditions and their effect on runoff generation for such a vast number and range of ROS events. Contrary to many other studies, we also considered smaller events leading to little or no snowpack runoff to generalize findings about processes during ROS.

Chapter 3. Influence of Initial Snowpack Properties on Runoff Formation during Rain-on-Snow Events

From these results we can make the following main conclusions: Latent and sensible heat provided the main energy source for individual events and showed the highest correlations with the total energy input. Typical patterns, describing a damping, amplifying or delaying effect on the rainfall-snowpack runoff relationship were found to be dependent on meteorological and snow cover conditions. ROS events with high initial liquid water content events were associated with high runoff excess (difference between cumulative snow cover runoff and rain input) and short time lags (time between event start and occurrence of runoff as defined). Those conditions were found to be typical for ROS events in late spring and early summer. In contrast, if initial snowpack conditions did not permit immediate snowpack runoff excess, then runoff was typically limited and average time lags were found to be considerably larger. These characteristics were typical for mid-winter events, where initial snow cover conditions were mostly cold and dry. During autumn, ROS events were less frequent compared to late spring and early summer, but those events were often larger scale events that occurred simultaneously at many locations with moderate to high runoff excess values.

From the perspective of hydrological forecasting, findings of this study are useful because they show the effects of the existing snow cover on runoff formation for upcoming ROS events. Relevant factors to consider include wind velocities, initial snow depth and liquid water content. As an example, we showed that under certain conditions the time lag between the start of rain and the onset of snowpack runoff was correlated to snow depth. Under these circumstances, the variability of snow depths within a given catchment should have a considerable influence on the peak streamflow, where uniform conditions entail a greater risk of high peak flows. For an easier transfer of the results, we were able to demonstrate the utility of a rather simple estimation of the available retention capacity, which can be derived from basic snow cover properties available in many hydrological models, dealing with snow cover by empirical relationships, e.g. a simple degree-day approach. The available retention capacity could be used to calculate the expected onset of snowpack runoff in response to rainfall in good agreement with the results of the complex snowpack model used in this study. Despite using an enormous amount of measured data to run and validate the SNOWPACK runs analyzed above, this study relies on an accurate simulation of the liquid water transport inside the snow cover. Using lysimeter data, Wever et al. (2014b) have shown that the model is capable of accurately representing liquid water dynamics for both a high alpine site (Weissfluhjoch, Switzerland) and a low alpine site (Col de Porte, France). Therefore, we assume that the model is also applicable to other comparable sites at similar elevations but acknowledge that a direct validation of the simulated results is not possible given the currently available data (i.e. the lack of snow lysimeter data at other sites in the Alps as the two mentioned above). In general, we expect applicability of the results for regions outside the European Alps, which act as a boundary between Mediterranean-type, Atlantic, and continental climates (Beniston, 2005). Because a physics-based snow cover model was chosen, results are expected to be transferrable to any other region and elevation, if they feature similar meteorological and snow cover conditions. A classification system for seasonal snow covers is described in Sturm et al. (1995) and can be used as a first estimation on expected snow covers in different

regions. The snowpacks investigated in this study could predominantly be described as a transition between alpine and maritime snow cover. Finally, results of this study might differ from previous case studies of singular extreme events, because a) the relevance of individual processes during ROS is varying between events and b) case studies generally represent only a limited range of boundary conditions.

To improve the utility of studies like this, it would be desirable to extend this study to lower mountain and subalpine ranges, which were found to play an important role in runoff formation (Sui and Koehler, 2001, Freudiger et al., 2014). Further, our results represent snow cover processes at flat alpine field sites. Incorporating terrain as well as landuse effects will require attention in future research.

Concluding, the main findings can be summarized as:

- Latent and sensible heat provided the main energy source for individual ROS events

- The snowpack runoff was found to be dependent on duration and intensity of rain as well as on initial snowpack conditions.

- ROS events with high initial liquid water content were associated with high runoff excess and short time lags.

- Relevant factors to consider for hydrological forecast include wind velocities, initial snow depth and liquid water content.

Acknowledgements

4 Spatio-temporal aspects of snowpack runoff formation during rain-on-snow

Sebastian Würzer[a,b] , Tobias Jonas[a]

[a]:WSL Institute for Snow and Avalanche Research SLF, Davos, Switzerland
[b]:École Polytechnique Fédérale de Lausanne (EPFL), School of Architecture, Civil and Environmental Engineering, Lausanne, Switzerland

Summary

Rain-on-snow (ROS) is a complex phenomenon leading to repeated flooding in many regions with a seasonal snow cover. The potential to generate floods during ROS depends not only on the magnitude of rainfall, but also on the areal extent of the antecedent snow cover and the spatio-temporal arrangement of meteorologic and snowpack properties. The complex interaction of these factors makes it difficult to accurately predict the effect of snow cover on runoff formation for an upcoming ROS event. In this study, the detailed physics-based snow cover model SNOWPACK was used to assess the influence of snow cover properties on translating rain input to available snowpack runoff during 191 ROS events for 58 catchments in the Swiss Alps. Conditions identified by the simulations that led to excessive snowpack runoff were a large snow covered fraction, spatially homogeneous snowpack properties, prolonged rainfall events and a strong rise in air temperature over the course of the event. These factors entail a higher probability of snowpack runoff occurring synchronously within the catchment, which in turn favors higher overall runoff rates. The findings suggest that during autumn and late spring, flooding due to ROS is more likely to happen, whereas during winter a coincidence of the above conditions is quite rare. For example, an autumn event which occurred in October 2011 resulted from a combination of spatially-homogeneous snowpack conditions following a recent snowfall and high, but not exceptional rainfall, and led to major flooding. The results of this study provide key factors to assess in advance of an incoming ROS event and emphasize the importance of detailed snow monitoring for flood forecasting in snow-affected watersheds.

4.1   Introduction

Many mountainous regions of the world experience rain on snow (ROS) situations on a regular basis. Il Jeong and Sushama (2017) report that 80% of the annual January to May maximum daily runoff for large parts of Northern America is associated with ROS events. Additionally, for some parts of Austria, Merz and Blöschl (2003) determined 55% of the annual peak flows to stem from ROS. While common, ROS situations do not necessarily lead to flooding. However, the biggest floods in those regions, involving severe damage and loss of lives, are often associated with ROS (e.g. Pomeroy et al., 2016, Wayand et al., 2015, McCabe et al., 2007, Kroczynski, 2004). The importance and unpredictability of those floods is reflected by the number of case studies dealing with their causative factors (e.g. Wever et al., 2014a, Rössler et al., 2014, Pomeroy et al., 2016, Liu et al., 2016, Garvelmann et al., 2015, Kroczynski, 2004).

Even though rainfall input usually dominates snow cover runoff for most ROS events, snowmelt can increase snow cover runoff by a factor of two during events with moderate rainfall totals (Würzer et al., 2016, Wayand et al., 2015). The transient storage of rain water in the snowpack can conceptually be regarded as a part of the runoff routing processes of precipitation input to the catchment outlet (Blöschl, 2013) and therefore the snow cover can enhance or delay runoff formation processes and determine the timing of snowmelt (Lundquist et al., 2005). While on the point scale complex snow cover processes and the unknown temporal evolution of meteorological forcing make it difficult to accurately predict snowpack runoff, assessing ROS on the catchment scale additionally comprises dealing with the spatial heterogeneity of snow cover properties and spatially variable meteorological inputs that influence both snowmelt and hydrological processes (Westrick and Mass, 2001). For example, high antecedent soil moisture is often observed during spring snowmelt conditions (Kampf et al., 2015, Fang and Pomeroy, 2016, Webb et al., 2015, Wever et al., 2017) and can augment catchment runoff significantly. Preferential flow of liquid water through snow can have a distinct impact on timing and amount of snowpack runoff and has been examined using dye tracers (Schneebeli, 1995, Würzer et al., 2017, Williams et al., 2010), radar measurements (Albert et al., 1999), temperature investigations (Conway and Benedict, 1994) and by measuring the spatial variability of snowpack runoff (Kattelmann, 1989, Marsh and Pomeroy, 1993, Marsh, 1999, Marsh and Woo, 1985).

Frozen soils which coincide with the presence of snow and basal ice layers, often formed during preceding ROS events (Würzer et al., 2017), can locally decrease the infiltration capacity of the soil. Under such circumstances, high snowpack runoff intensities can cause lateral overland flow, increasing the magnitude of runoff transported to the streams considerably (Teufel et al., 2017, Bayard et al., 2005, Stähli et al., 2001).

A delay of snowpack runoff after the start of rain may affect the runoff generation at the catchment scale, in particular if this time lag varies across the catchment. Further, air temperatures and snow cover extent usually do not support snowmelt in the whole catchment

synchronously. Biggs and Whitaker (2012) found most snowmelt during spring to originate from critical elevation zones which only comprised a limited area of the catchment. White et al. (2002) found a strong relationship between the peak flow rate and the area contributing to melt depending on the catchment hypsometric curve. However, stream peak flows are higher when whole catchments generate runoff synchronously for both spring snowmelt (Lundquist et al., 2004) and during ROS (Garvelmann et al., 2015). Jones and Perkins (2010) concluded that prolonged precipitation and synchronized snowmelt from all areas of a catchment produce rapid and synchronized discharge responses and are the dominant controls on generation of extreme floods during ROS. Also Pomeroy et al. (2016) mentioned the remarkable synchrony of flooding in all tributaries to the Bow River during Canada's most costly flood in June 2013. Whitfield and Pomeroy (2016) reported that particularly large flood events are the result of widespread ROS, suggesting that a large area affected by ROS probably has a bigger impact than high local snowmelt intensities. Physiographic controls like elevation influence depth, persistence, and properties of a snowpack and co-determine the location of the rain-snow-transition zone. For long lasting events which involve a substantial amount of snowmelt, higher elevations with persistent snowpacks become the primary source of catchment runoff (Garvelmann et al., 2015).

The basic requirements for ROS to happen are the presence of a snowpack and air temperatures that allow precipitation to fall as rain. With rising air temperatures, future climate will likely involve more precipitation falling as rain rather than snow. Therefore, ROS frequency, area, and runoff amount attributed to ROS is expected to rise in high-latitude (Ye et al., 2008, Putkonen and Roe, 2003, Il Jeong and Sushama, 2017) and mountainous regions (Köplin et al., 2014, Il Jeong and Sushama, 2017),where snow cover is still present during winter. However, ROS frequencies might decrease due to reduced snowfall and consequently less days with snow cover on the ground in mid-latitude regions or lower elevations (McCabe et al., 2007). Similar consideration also applies to a Swiss catchment, where increasing ROS frequencies are expected with rising air temperatures until further warming counteracts the initial effect (Beniston and Stoffel, 2016).

Large ROS-attributed floods have been studied with special regards to the coincidence in flood peak timing between small tributaries (Jones and Perkins, 2010) and the hydrological processes involved (Rössler et al., 2014). Yet there is little understanding of the role of snow cover properties and their spatial heterogeneity in supporting the synchronous generation of runoff within the catchment during ROS other than snow height. These factors and the limited process representation in subsequent hydrological modeling (Rössler et al., 2014) make the runoff resulting from ROS events difficult to predict. Quite similar meteorological conditions were shown to lead to significantly different consequences for different ROS events, dependent on antecedent snow cover conditions like liquid water content (LWC) (Kroczynski, 2004).

In this study we use the SNOWPACK model to assess the influence of initial snow cover properties in translating rain input to snowpack runoff for 191 ROS events within 58 catchments in the Swiss Alps. This enables investigation of following research questions:

- How do meteorology, initial snowpack properties, and catchment characteristics jointly control runoff formation during ROS events?

- Are there particular combinations of storm, snowpack, and catchment characteristics that entail an increased risk of excessive runoff and subsequent flooding?

This paper is structured as follows: Section 4.2 describes the SNOWPACK model, input data and the definition of a ROS event. Results of the simulations, as well as their implications on flood generation are presented and discussed in Section 4.3, followed by the conclusions in Section 4.4.

4.2 Methods

All results in this study are derived from simulations with the one-dimensional physics-based snow cover model SNOWPACK, which is described in Section 4.2.3. The model was applied to virtual stations that were spatially distributed over 58 catchments in the Swiss Alps (See Section 4.2.2) to simulate a total of 191 ROS events. The virtual stations were generated to form a gridded representation of each catchment at 2 km horizontal spacing. The pre-processing library MeteoIO (Bavay and Egger, 2014) was used to extrapolate meteorological data from the IMIS station network (Lehning et al., 1999), as described in Section 4.2.2. IMIS data have already been used for simulating ROS events with SNOWPACK in previous studies (Wever et al., 2014b, Badoux et al., 2013, Würzer et al., 2016).

4.2.1 Event Definition and Data Selection

The definition of a ROS event determines the number and spatio-temporal characteristics of events in a given record of meteorological data. To take the perspective of flood forecasting, our event definition is primarily based on precipitation in combination with an existing snow cover, as opposed to runoff-based definitions. However, we excluded spatially limited events which mostly occurred during summer months due to local convective precipitation events. The event selection was further limited to 15 winter (October to March) and 6 spring (April to May) events, where at least 5 of the IMIS stations experienced ROS at the same day. In the following, the term "event" refers to the above selection of 21 events which occurred simultaneously at multiple catchments. These events result in 191 individual records for a single catchment and event, hereafter referred to as a catchment event (CE). To classify as a CE, they had to fulfill the event definition used by Würzer et al. (2016): A ROS event is identified if a minimum of 20 mm of rainfall falls within 24 hours on a snowpack of at least 25 cm in depth at the onset of rainfall. The onset of an event was set to occur when 3 mm of cumulative rain fell in the catchment. The end criterion was reached after less than 3 mm rain and runoff was simulated within 5 consecutive hours, respectively. Note that these definitions were slightly adapted from the original start and end criteria given in Würzer et al. (2016) as these were developed for a single location, not entire catchments as analyzed in this study.

4.2.2 Data
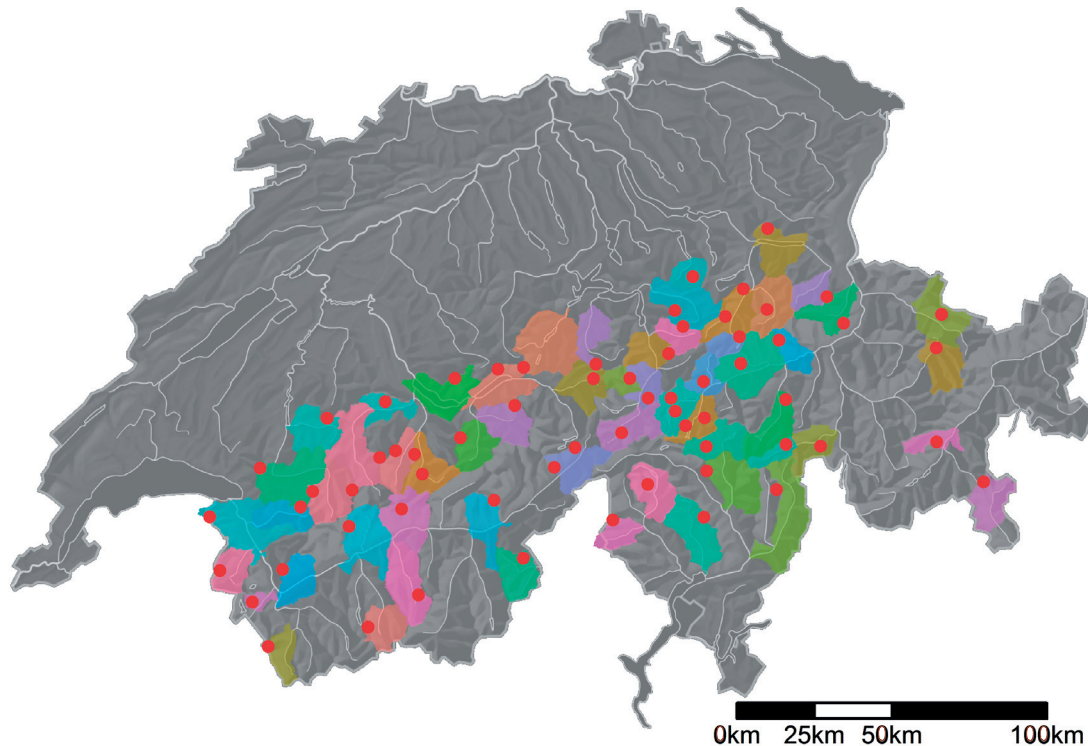
Figure 4.1 – Map of Switzerland with locations of the catchments and IMIS stations used for the analysis.

The boundaries of the catchments used in this study are defined according to the swiss catchment classification scheme for, on average, domains of 150 km^2 (FOEN, 2015). Catchments were selected for this study if at least one IMIS station where a CE occurred was situated within its boundaries. This leads to a total of 58 catchments (Figure 4.1) ranging in size between 44 and 336 km^2.

The IMIS monitoring network was initially set up to serve the national avalanche forecast in Switzerland. It comprises automatic stations to measure both meteorological and snow parameters such as: wind speed and direction, air temperature, relative humidity, surface temperature, soil temperature, reflected shortwave radiation, and snow depth. Data is recorded at 30 minute intervals and further aggregated to arrive at a 1h model input dataset.

The following settings were used for MeteoIO to project available station data to the 2 km grid of virtual stations: A constant lapse rate of 6.5 °C was considered for air temperature (TA). Relative humidity was distributed by the method described in Liston and Elder (2006). Wind speed measured at IMIS stations within the catchment (average wind speed, if more than one station) was uniformly distributed over the catchment. For incoming short wave radiation, a solar radiation interpolation scheme with terrain shading as described in Bavay and Egger (2014) was used. Incoming longwave radiative flux at each virtual station was simulated using

the parameterization from Unsworth and Monteith (1975), coupled with a clear sky emissivity following Dilley and O'Brien (1998), as described in Schmucki et al. (2014). The rain gauges of IMIS stations are unheated and therefore provide no reliable measurements in case of snowfall and mixed-phase precipitation, which is often observed during ROS. We therefore used a gridded 2 km precipitation dataset provided by MeteoSwiss (RhiresD, MeteoSwiss, 2013), as used in previous studies to derive precipitation input for the SNOWPACK model (Würzer et al., 2016). The presence of canopy strongly affects the accumulation of snow and the energy balance and was found to significantly control snowmelt during ROS (Marks et al., 1998). A forest classification was derived from the Swiss land use statistics (FSO, 2017), which separates 15 classes of land use. For the current study, we distinguished between three land use classes: forest, shrubland, and open. Forest canopy parameters used in the canopy module are described in Section 4.2.3.

4.2.3 Model Description & Setup

The physics-based snow cover model SNOWPACK represents the evolution of the snow cover in a 1-dimensional profile, which is comprised of a multitude of individual layers. A detailed description can be found in Bartelt and Lehning (2002), Lehning et al. (2002b,a, 1999) and Wever et al. (2014b). The model is driven by hourly meteorological data as described in section (4.2.2). Snowmelt occurs if the temperature of a layer exceeds 0°C and additional energy is provided. The energy input to the snow cover during melting conditions is calculated from radiative fluxes, turbulent heat fluxes, soil heat flux and advective energy provided by rain. The turbulent surface heat fluxes were simulated using a Monin–Obukhov bulk formulation for surface exchange. Stability correction functions of Stearns and Weidner (1993), as described in Michlmayr et al. (2008) were used to consider stable conditions. A dual domain approach based on the Richards' equation, which can account for the generation of preferential flowpaths, was chosen to model the transport of liquid water within the snowpack (Wever et al., 2016b, Würzer et al., 2017). The model was initialized with a soil depth of 3 m to be able to accurately describe the heat and water flux between the soil and the snowpack. Soil heat flux at the lower boundary is set to a constant value of $0.06\,\mathrm{W\,m^{-2}}$, which is an approximation of the geothermal heat flux. In the absence of measured soil data, typical values for coarse soils were chosen to avoid ponding inside the snowpack due to saturated soil. A free drainage boundary condition was taken to prescribe the lower boundary condition for liquid water flow in the soil. In SNOWPACK, the canopy is represented by a 2-layer canopy module as described in Gouttevin et al. (2015), requiring information on canopy height, canopy closure and basal area. Canopy height is approximated to be 25 and 2 m for forest and shrubland, respectively. Canopy closure (85 % for forest and 70 % for shrubland) and leaf area index (3 for forest and 2 for shrubland) was set according to Moeser et al. (2014). The basal area was set to be $40\,\mathrm{m^2\,ha^{-1}}$.

4.3 Results and Discussion

4.3.1 Runoff formation at point versus catchment scale
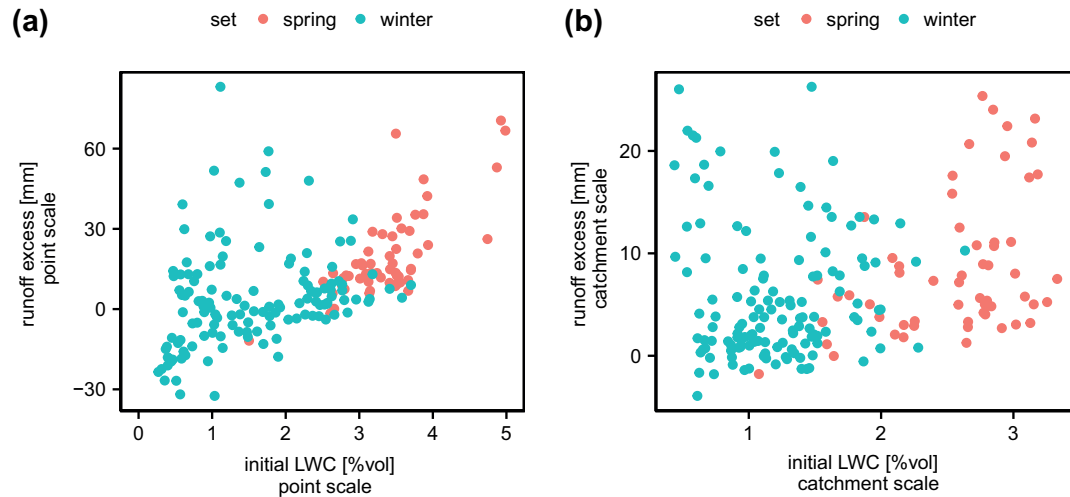
Figure 4.2 – Correlation of runoff excess and initial LWC for (a) point and (b) catchment scales. For better visibility, we omitted a point-simulation with initial LWC of 11 %vol and 58 mm runoff excess in (a).

Compared to runoff formation processes for an individual point or site, assessing processes for entire catchments additionally involves addressing the spatial dimension. We shall therefore contrast some considerations derived separately for these two scales. Similar to the approach chosen in this study, Würzer et al. (2016) simulated snow cover processes for ROS events using the SNOWPACK model and IMIS data, but only looked at locations of monitoring stations without considering between-station aspects. This enabled a direct comparison between results derived for both point locations and catchment areas (represented by the average value of all virtual stations from the equivalent simulation on a grid). Note that in this comparison there is typically one IMIS station (point scale) per watershed (catchment scale), see Figure 4.1.

The cumulative differences between snow cover runoff and rain input per event, henceforth referred to as runoff excess, is an important value when assessing a ROS event, since it summarizes if the presence of a snow cover leads to additional runoff or if it retains water. Figure 4.2 shows the correlation between runoff excess and initial LWC for point simulations (Figure 4.2a) and catchment scale simulations (Figure 4.2b). For winter CEs which usually feature a rather low LWC, correlations are weak to non-existent for both scales. However, at the point scale there is a certain correlation between high initial LWC values and runoff excess (R^2=0.55), which is not the case for the catchment scale (R^2=0.16). This demonstrated that results derived for individual locations may not necessarily transfer into catchment-level findings. In this case, spatially heterogeneous snowpack properties dilute, cancel out, or even reverse effects

that hold true for individual locations. Particularly, partial snow cover and asynchronous timing of runoff from different parts of a catchment does not typically allow high runoff excess volumes as recorded for individual locations (Figure 4.2).
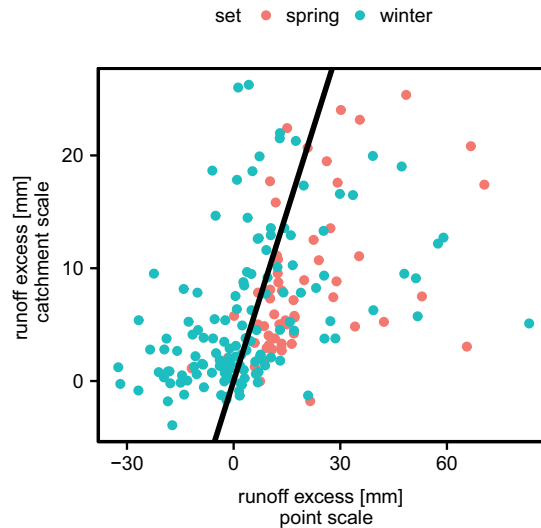
Figure 4.3 – Correlation between runoff excess on the catchment and point scale. The black line denotes to the 1:1 line.

To further elaborate on this matter, we have tested a direct comparison of catchment and point scale runoff excess by associating results for individual IMIS stations with respective results for the catchments in which they reside. Figure 4.3 shows a rather weak correlation between both datasets (R^2 of 0.18 and 0.22 for winter and spring CEs, respectively). It can further be noted that relatively few simulations show overall retention of runoff (negative excess) on the catchment scale, which is not the case for point-scale simulations and suggests that normally the area creating additional melt is larger than the area where rainwater is retained. In fact, only approximately 20% of the CEs entail a retention area exceeding the area generating additional runoff excess. For events where both data sets show positive runoff excess, most of the catchment scale simulations result in runoff excess below the 1:1 line, which implies that snow-free areas, areas only experiencing snowfall, and areas with partial retention have led to lower excess values on the catchment scale. However, since some simulation pairs are also above the 1:1 line, point scale simulations can obviously not be used as an approximate limit for runoff excess values that are normally not exceeded at the catchment scale.

To further investigate the influence of the snow cover fraction (SCF) on runoff excess, we have included SCF in a multiple regression analysis of runoff excess at the catchment scale versus both runoff excess at the point scale and SCF. When we included SCF, the explained variance increased from 0.22 to 0.46, but only in the case of spring CEs. This suggests that SCF is a limiting factor for additional snowmelt during spring CEs. The above considerations are hampered by the fact that IMIS stations only represent a random location within each of the catchments considered here. We have therefore replaced the point simulations for the IMIS

station locations with respective simulations for a point at the catchment's medium altitude and redone the regression analysis. With a R^2 of 0.47 for winter and 0.64 for spring CEs, the correlations were considerably improved. Highest and lowest values in Figure 4.3 are observed for point simulations, which suggests that an averaging behavior of processes is taking place on the catchment scale. This behavior can be attributed to spatially heterogeneous properties of the snow cover as well as storm properties resulting, e.g., from an elevational gradient. Zero-values for runoff excess from snow free areas and areas with snowfall are included in the mean runoff excess totals of the CEs.

The rather weak correlations for CE and point scale runoff excess show the limited applicability of point-scale observations for assessing ROS on the catchment scale. We therefore think it is necessary to analyze runoff generation behavior for ROS situations with a spatially distributed approach.

4.3.2 Snowmelt and retention zones during ROS
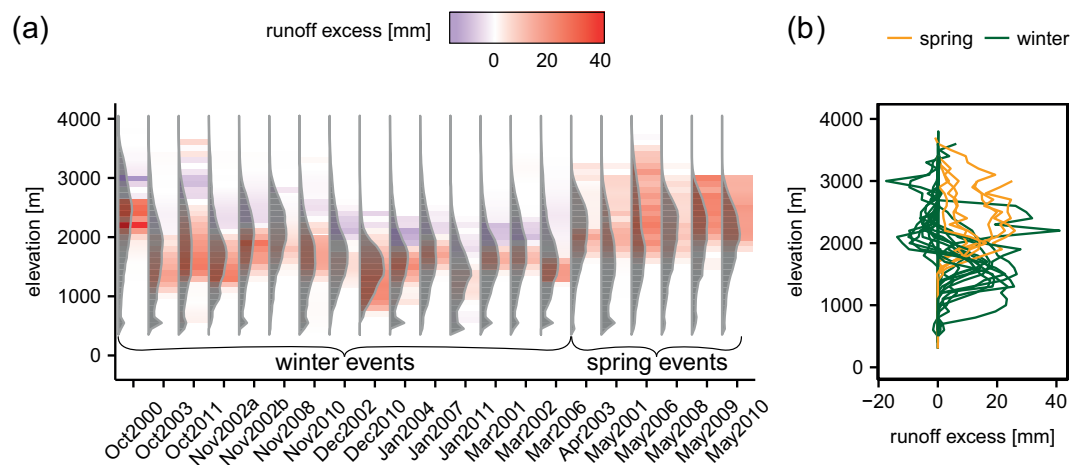
Figure 4.4 – Mean runoff excess as a function of elevation for all 21 events, where results for all CEs associated with the same rain event where evaluated together.

Before discussing the spatio-temporal course of the ROS events and the effects of meteorological and snowpack conditions on the catchment runoff generation, we shall first look at the elevational characteristics of the events investigated. Figure 4.4 (a) presents the mean cumulative runoff excess generation for each of the 21 events in 100 m elevation zones. The respective hypsometric curves are shown as profiles (in gray). Relative to the terrain, runoff excess (negative or positive) is only noted for a limited altitude range. Below the snowline, runoff excess is zero as rain input equals water available at the ground surface. Above the snowfall limit, there is no rain input and it is mostly too cold to melt so that consequently there is no runoff excess either. During winter events all simulations incorporate both areas

71

that contribute additional runoff from snowmelt and areas that retain at least some rain water. Spring events, on the other hand, do not usually incorporate rainwater retention at any elevation. Areas leading to positive runoff excess are found generally at lower elevations for winter than for spring events, which is most apparent from Figure 4.4 (b). A similar seasonality in runoff excess has already been observed by Würzer et al. (2016).

Well-defined elevation zones which generate the majority of runoff excess can be regarded as the critical elevation zones during ROS. Similar to Biggs and Whitaker (2012), who analyzed runoff formation during spring snowmelt conditions, we identified such critical zones for the events analyzed here. Specifically we assessed which fraction of the catchment (represented by the fraction of grid cells) is at least needed to generate 75% of the catchment runoff excess. This analysis revealed that in fact only 25% and 40% of the area was needed to generate 75% of the runoff excess for winter and spring CEs, respectively. These percentages are equivalent of 300 and 500 m range in altitude. Rain water retention in at least some areas is one factor to explain why only a relatively small fraction of the catchment is involved in the generation of runoff excess in winter. During spring events, however, runoff excess is produced within a considerably larger fraction of the catchment area that is approximately equal to the SCF. This implies that the potential for snowmelt is often exhausted during spring CEs. For the winter events, however, this is not the case and substantially more snowmelt could be generated if supported by current snowpack conditions and the energy balance. These findings illustrate that the potential for flood generation is indeed dependent on initial snowpack and meteorological conditions, since both factors determine the area that contributes snowmelt runoff. If we further include physiographic aspects, then snowmelt as well as runoff excess is normally restricted to a certain range in elevation. Whether or not this range coincides with a considerable portion of the catchment area is critically important for the effect of snow cover on runoff generation during ROS (Figure 4.4).

4.3.3   Spatio-temporal course of a ROS event

During ROS, rain intensities, air temperatures, and snow cover conditions can change rapidly over the course of the event. Therefore it is necessary to examine the spatio-temporal dynamics of the above factors. Figure 4.5 (a) shows the temporal course of runoff excess generation for a catchment during the October 2011 ROS event. Rain and snow cover runoff are displayed in Figure 4.5 (b) for the same observation period and catchment. In the beginning of the CE, rain was retained in the snow cover at nearly all elevations, leading to an overall negative runoff excess for the whole catchment. However, after some hours all elevations above the snowline started to contribute snowmelt, leading to an overall positive runoff excess for the whole catchment. In this case, synchronous timing of snowmelt between all snow-covered areas within the catchment not only increased the overall runoff, but also the maximum runoff intensity (by 20% relative to the maximum rain intensity). Since high runoff intensities were found to produce fast overland flow (Bayard et al., 2005), synchronous timing of meltwater release over large fractions of the watershed may entail a greater risk of critical runoff rates
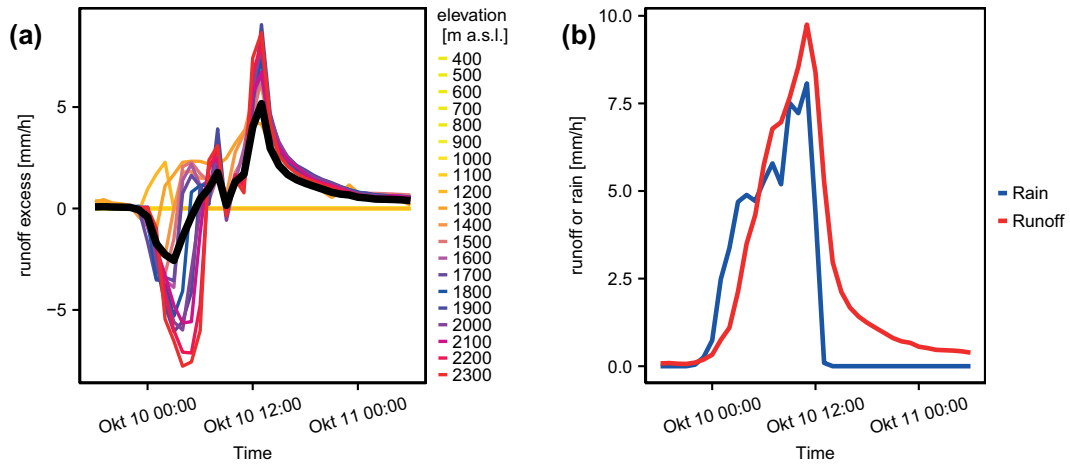
Figure 4.5 – (a) Example of the temporal course of runoff excess in different elevations of a catchment during a ROS event in October 2011. Rain and snowpack runoff catchment averages are displayed in (b). We see that runoff excess is negative in the beginning of an event, leading to a delayed increase in runoff. During the course of an event, runoff increase is higher and finally exceeds catchment rain.

and floods (Jones and Perkins, 2010).

4.3.4 Factors promoting the synchronized generation of runoff excess

A delay of snowpack runoff relative to the start of rain may affect the runoff behavior at the catchment scale, in particular if this time lag varies across a given catchment. Earlier studies have found short time lags being associated with high LWC and shallow snow covers (Würzer et al., 2016), suggesting that high catchment LWCs lead to spatially synchronous generation of runoff within the catchment. For our further analysis, we define lag time as the time period between the onset of rain (catchment-mean) and the onset of either runoff or rain (at an individual location). Rain and runoff lag times can therefore vary spatially across a given catchment. Figure 4.6 shows the correlation between the standard deviation of lag times and mean CE air temperature, where colors denote the initial LWC. The standard deviation of the runoff lag times is used as a proxy to measure synchronicity of the onset of runoff within a catchment, where low values denote high synchronicity and vice versa. The results show that this synchronicity is increasing with both air temperature and initial LWC. The data further imply that the effect of snow height on lag time can only be of a limited nature if the initial LWC is high.

A multiple regression analysis was conducted to explain the variance in runoff synchronicity in terms of LWC, air temperature, and rain synchronicity. The above predictors explained 90% of the variation in runoff synchronicity. While this is a good correlation, it is important to note that temperature and rain synchronicity are not independent from one another as
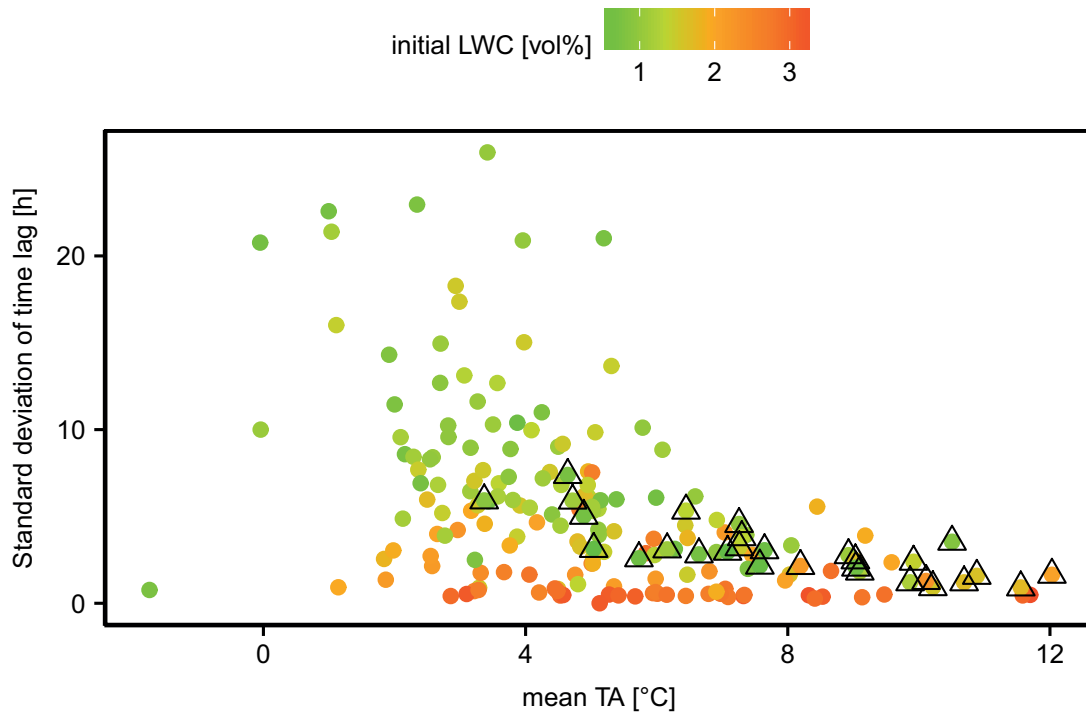
Figure 4.6 – Correlation of standard deviation of the lag time and mean air temperature, where lag time is defined as the time period between onset of rain and onset of runoff. CEs of the October 2011 ROS event are marked with triangles.

temperatures determine the phase of precipitation. High enough temperatures therefore promote increased synchronicity in both rain input and snowmelt output.

At the point scale, snowpack runoff intensities were shown to be dependent on rain intensities as well as the event length (Würzer et al., 2016). Figure 4.7 shows a repetition of the analysis for the catchment scale (a) in comparison to the original results (b). The color differentiates between rain events lasting below and above 20 hours. For both spatial scales, snow cover processes attenuated rain intensities for most of the intense and short rain events (i.e. > 4 $mm\,h^{-1}$ and < 20 h). Longer rain events, on the other hand, typically entailed an amplifying effect with only a few exceptions for the point scale and a fairly accurate match between rain and runoff intensities at the catchment scale. Also in this example catchment scale averaging processes seem to take place, which is why the ratio of runoff intensity to rain intensity is generally lower as compared to equivalent results from point scale simulations. In particular snow free areas equilibrate the overall ratio between rain and runoff as excess runoff is zero for these areas per definition.

Spatial compensating mechanisms between catchment processes mostly evolve due to the heterogeneous distribution of snow cover within the catchment. We therefore assessed the coefficient of variation (CV) of initial snow height to characterize the heterogeneity. Respective
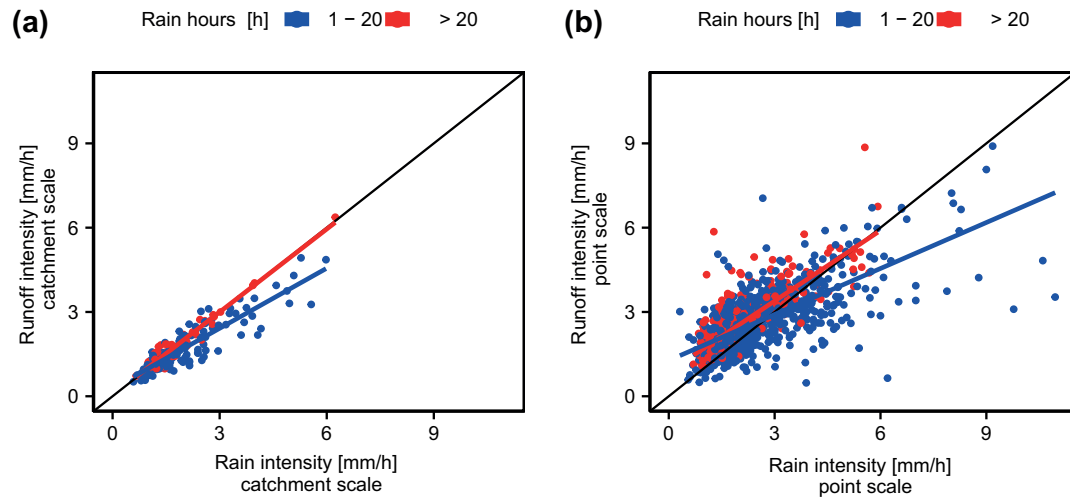
Figure 4.7 – Runoff intensities (averaged over the duration of runoff) vs. rainfall intensities (averaged over the duration of rainfall) for rainfall events of different length for (a) catchment simulations and (b) point simulations of Wuerzer et al. (2016).

CV values are shown against the maximum runoff excess intensity in Figure 4.8a, where colors denote the initial SCF. The data show that a low CV of initial snow height is not necessarily indicative of high maximum runoff excess intensities, even though a tendency is present and high max. runoff excess intensities are only found for comparably low CV values. With increasing variability of snow cover, on the other hand, maximum catchment runoff intensities are considerably limited by the presence of a snow cover. For the SCF, the effect is the opposite: With a high SCF, a wide range of runoff excess intensities is possible, whereas low SCFs are necessarily associated with low maximum runoff excess intensities.

Figure 4.8b describes the relationship between mean runoff excess intensities and snow height for point and catchment simulations (mean initial catchment snow height). The highest runoff intensities are associated with shallow snow covers and deep snow covers are associated with low runoff intensities. Both data sets show a similar pattern, suggesting that high snow depths tend to moderate snowpack runoff intensities at both spatial scales. However, mean catchment values normally fall below values derived from point simulations, due to areas either retaining rain water or having snowfall instead of rainfall.

Results shown in Figure 4.8 support previous findings that a catchment which is widely covered by a homogeneous (Figure 4.8b) and shallow (Figure 4.8a) snow cover has the potential to generate high runoff excess intensities during ROS.
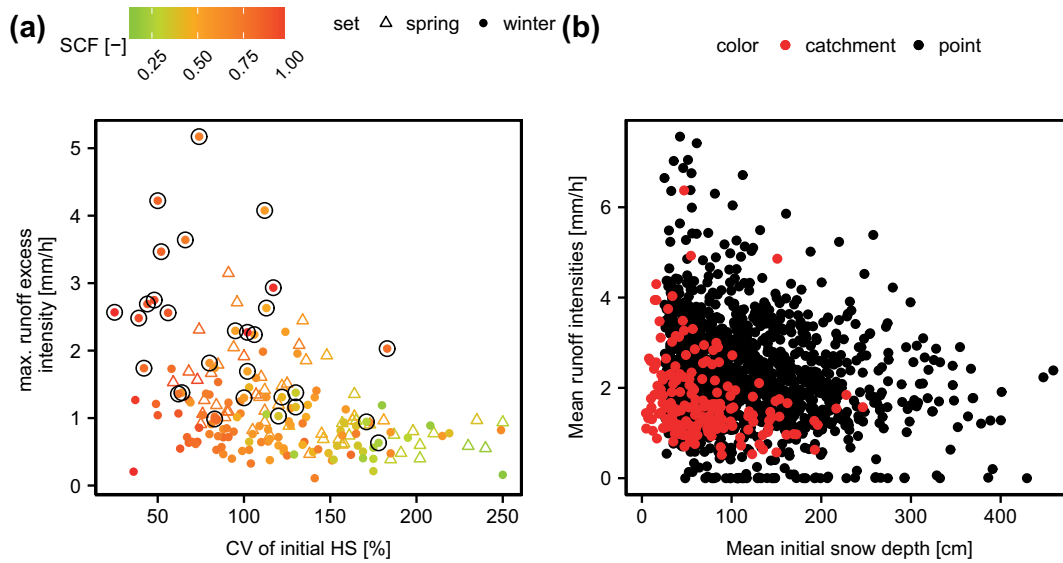
Figure 4.8 – (a) Runoff intensities in terms of the initial snow height for events. Point scale simulations are in black color, the catchment simulations are in red. (b) Maximum simulated runoff excess vs. coefficient of variation for initial snow height. Colors show the initial SCF.

4.3.5   Implications for forecasting runoff generation and flooding potential

Of all 21 events, the October 2011 event was by far the biggest of the analyzed events particularly in terms of the spatial extent (i.e. number of involved stations). The resulting damages and the inability of the operational forecast to predict the extreme nature of this particular event was motivation for several studies on ROS (Badoux et al., 2013, Rössler et al., 2014, Wever et al., 2014a). For this event, the return periods of rainfall were around several years, but resulting stream peak flows were in range of return periods of 50 to 300 years, which raised the question of what mechanisms snow cover or other meteorological conditions led to extreme runoff rates (Badoux et al., 2013). Figure 4.9 may provide a clue; it displays the correlation between maximum runoff excess intensity and the change in air temperature over the duration of the event. Colors denote the increase in SCF over the 3 days before the start of rain and triangles mark CEs of the October 2011 event. The synopsis demonstrates that the October 2011 event was exceptional in combining a large increase of SCF and a strong rise in air temperatures, which all together led to the highest runoff excess intensities of all 191 CEs. A recent snowfall down to low elevations in the days before the event led to large areas covered by fresh snow, providing a shallow homogeneous snow cover at a large SCF. We have seen above that these very conditions were both associated with high runoff intensities (Figure 4.8). A strong rise in air temperature over the course of the event further promoted a high synchronicity in the timing of runoff across the involved catchments (Figure 4.6).

In summary, the October 2011 event fulfilled four key criteria that have been identified in this
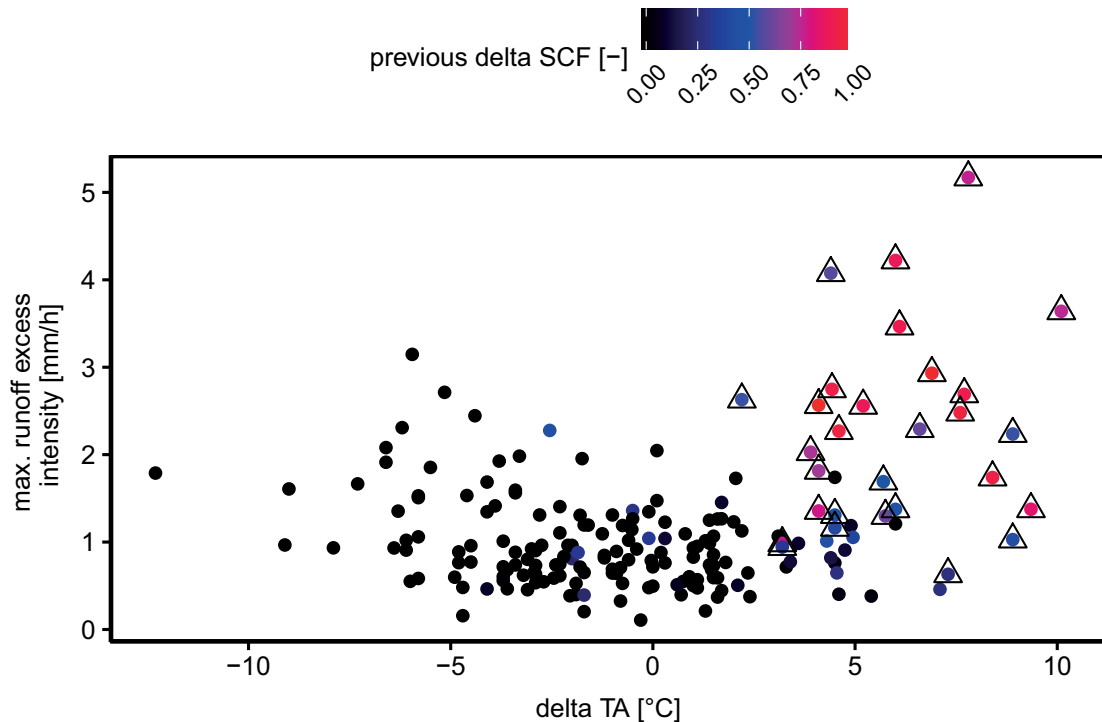
Figure 4.9 – Correlation of maximum runoff excess intensity and the temperature change (delta TA) over the course of the event for all CEs. The color denotes the increase in SCF within the 3 days before the event. Triangles mark CEs of the October 2011 event.

study as indicative of high runoff excess and intensities (Figures 4.6, 4.8 and 4.9). In particular the above snow cover conditions seem most likely to occur in an autumn scenario, when a cold front results in the first significant snowfall for the season forming a shallow homogeneous snow cover over large parts of the catchment. Further into the winter season elevational snow distribution gradients usually build up, which prevent conditions similar to those recorded for the October 2011 event. Only towards the end of the snowmelt season a late snowfall down to low elevations might potentially entail comparable circumstances. But normally, SCF is a limiting factor in spring to prevent excessive runoff over extended areas.

The multitude of interacting factors influencing synchronized and widespread snowmelt illustrate the challenge of accurately predicting runoff for an incoming ROS event. Many of theses factors are difficult to assess, such as the spatial distribution of snowpack properties that are relevant but rarely measured anywhere (e.g. the LWC). Furthermore, there are always uncertainties in meteorological forecasts, which impact our ability to predict the amount, timing, and spatial distribution of precipitation and snowmelt. The effect of snow cover on runoff excess and its synchronicity may be predicted most precisely for spring events: Since the snow cover usually has a high LWC and therefore its retention capacity is limited, short time lags and little retention can be expected. However, snowmelt during spring ROS is normally limited by the SCF. With high initial SCF, winter events usually exhibit a much higher

potential for generating additional runoff. But these situations require a detailed knowledge of the spatial distribution of snowpack properties, its retention potential, and its thermal state, an assessment of which will remain challenging. Fortunately, as argued above, ROS events causing excessive runoff during winter seems the least likely scenario if compared to autumn and spring situations. However, warmer winter temperatures in future climate could increase the occurrence of mid-winter rain events.

As a contrasting example to the October 2011 event, the October 2000 event had less pronounced snow cover extent and the rain-snow transition zone during the event was lower due to declining air temperature over the course of the event. Consequently, rainfall and snowmelt were limited to lower elevations and relatively little catchment runoff excess for the CEs was reported. Nevertheless, because of extreme rainfall intensities at lower elevations, this event also led to localized floodings and debris flows, but, compared to the 2011 event, over a much reduced spatial extent. With higher air temperatures the consequences of this event could have been more devastating. The October 2011 event was limited by comparatively moderate rainfall amounts and the October 2000 event was limited by SCF and low air temperatures, yet despite these limitations, both events caused considerable damages and economic losses, but still had the potential to generate even more runoff. It is therefore imperative to continuously monitor snow cover properties and other factors that allow for the accurate prediction of excessive runoff for a upcoming ROS event, to be able to prepare mitigation efforts where needed well in advance.

4.3.6 Outlook

To improve the utility of studies like this, it would be desirable to further investigate the implications of ROS on the formation of fast runoff processes like lateral surface flow. Webb et al. (2017) stated that the spatial heterogeneity of soil moisture below the snowpack is less investigated than the state of the overlaying snow cover. Results from Kampf et al. (2015) show that longer snow persistence and wetter than average soil moisture conditions on a slope enable the development of saturation overland flow. Additionally, within the snowpack, certain processes remain difficult to assess. Würzer et al. (2017) and Juras et al. (2017) showed that preferential vertical flow of liquid water within a snowpack considerably influences rain water retention. Eiriksson et al. (2013) further revealed the importance of preferential lateral flow in sloped terrain for runoff formation in complex topography. In this study, we found that the snow cover processes considerably moderated the synchronicity of catchment runoff formation during ROS. However, any subsequent hydrological modeling critically depends on an accurate representation of runoff formation processes to be able to translate the water input at the soil surface to runoff at the catchment outlet in a realistic manner.

4.4   Conclusions

In this study we analyzed the effect of snow cover characteristics, meteorology and topography on translating rain input to snowpack runoff for 21 large-scale ROS events that occurred in 58 catchments in Switzerland between 2000 and 2011. The use of a physics-based snow cover model particularly assessing the role of the spatial variability of snow cover processes during ROS. The simulation results were used to identify controls and conditions that entailed increased runoff volumes and high runoff intensities.

Our analysis revealed that the following factors support extensive runoff:

   A) spatially homogeneous snow cover conditions (Fig 4.8a)

   B) shallow snow covers (Fig 4.8b)

   C) high snow cover fraction (Fig 4.8a)

   D) high / increasing air temperatures over the course of the ROS event (Fig 4.6 and Fig 4.9)

   E) high initial LWC (Fig 4.6)

   F) long lasting ROS events (Fig 4.7)

The above factors are all, directly or indirectly, connected to the likelihood of runoff being generated synchronously from the entire catchment, which in turn promotes high mean runoff intensities.

These findings show that ROS events leading to flooding are most likely to occur in autumn or towards the end of spring. A particular scenario could involve starting with a low SCF, then a cold front results in a snowfall forming a shallow homogeneous snow cover over large parts of the catchment, which is then followed by a considerable temperature rise and leads to extensive rain. Such a scenario automatically fulfills most of of the above mentioned criteria. Under different meteorological conditions, ROS events are either limited by a low initial SCF in autumn and spring, or cannot support synchronous runoff generation due to pronounced spatial differences in snow cover properties in winter.

While the simulations complement meteorological and snow data for a large number of ROS events in Switzerland, the findings should apply to any region with similar meteorological and snow cover conditions.

Data Availability

Meteorological driving data for the SNOWPACK model will be made available on a data repository. The SNOWPACK model is available under a LGPLv3 license at http://models.slf.ch. The version used in this study corresponds to revision 1249 of /branches/dev.

Acknowledgments

5 Further contributions

Two further publications, Wever et al. (2016b), and Juras et al. (2017) were conducted in close collaboration in the setting of this dissertation project and both represent an important contribution to understanding water transport processes during ROS. A third, non peer-reviewed publication (Würzer and Jonas, 2017) constitutes a summary article of the studies presented in Chapter 3 and 4, published in German language. The abstracts of these publications, in case of Würzer and Jonas (2017) a translation, can be found below.

5.1 Simulating ice layer formation under the presence of preferential flow in layered snowpacks

Nander Wever[a,b], Sebastian Würzer[a,b], Charles Fierz[b], Michael Lehning[b,a]

[a]:École Polytechnique Fédérale de Lausanne (EPFL), School of Architecture, Civil and Environmental Engineering, Lausanne, Switzerland
[b]:WSL Institute for Snow and Avalanche Research SLF, Davos, Switzerland

For physics-based snow cover models, simulating the formation of dense ice layers inside the snowpack has been a long-time challenge. Their formation is considered to be tightly coupled to the presence of preferential flow, which is assumed to happen through flow fingering. Recent laboratory experiments and modelling techniques of liquid water flow in snow have advanced the understanding of conditions under which preferential flow paths or flow fingers form. We propose a modelling approach in the one-dimensional, multilayer snow cover model SNOWPACK for preferential flow that is based on a dual domain approach. The pore space is divided into a part that represents matrix flow and a part that represents preferential

flow. Richards' equation is then solved for both domains and only water in matrix flow is subjected to phase changes. We found that preferential flow paths arriving at a layer transition in the snowpack may lead to ponding conditions, which we used to trigger a water flow from the preferential flow domain to the matrix domain. Subsequent refreezing then can form dense layers in the snowpack that regularly exceed $700\,\mathrm{kg\,m^{-3}}$. A comparison of simulated density profiles with biweekly snow profiles made at the Weissfluhjoch measurement site at 2536 m altitude in the Eastern Swiss Alps for 16 snow seasons showed that several ice layers that were observed in the field could be reproduced. However, many profiles remain challenging to simulate. The prediction of the early snowpack runoff also improved under the consideration of preferential flow. Our study suggests that a dual domain approach is able to describe the net effect of preferential flow on ice layer formation and liquid water flow in snow in one-dimensional, detailed, physics-based snowpack models, without the need for a full multidimensional model.

5.2   Rainwater propagation through snowpack during rain-on-snow sprinkling experiments under different snow conditions

Roman Juras[a,b], Sebastian Würzer[b,d], Jirka Pavlásek[a], Tomáš Vitvar[a,c], and Tobias Jonas[b]

[a]:Faculty of Environmental Sciences, Czech University of Life Sciences Prague, Kamýcká 129, 165 21, Prague, Czech Republic
[b]:WSL Institute for Snow and Avalanche Research SLF, Davos, Switzerland
[c]:Faculty of Civil Engineering, Czech Technical University in Prague, Thákurova 7, 166 29 Prague 6, Czech Republic
[d]:École Polytechnique Fédérale de Lausanne (EPFL), School of Architecture, Civil and Environmental Engineering, Lausanne, Switzerland

The mechanisms of rainwater propagation and runoff generation during rain-on-snow (ROS) are still insufficiently known. Understanding storage and transport of liquid water in natural snowpacks is crucial especially for forecasting of natural hazards such as floods and wet snow avalanches. In this study, propagation of rainwater through snow was investigated by sprinkling experiments with deuterium enriched water and applying an alternative hydrograph separation technique on samples collected from the snowpack runoff. This allowed quantifying the contribution of rainwater, snowmelt and initial liquid water released from the snowpack. Four field experiments were carried out during winter 2015 in the vicinity of Davos, Switzerland. Blocks of natural snow were isolated from the surrounding snowpack to inhibit lateral exchange of water and were exposed to artificial rainfall using deuterium-enriched

water. The experiments were composed of four 30 minutes periods of sprinkling, separated by three 30 minutes breaks. The snowpack runoff was continuously gauged and sampled periodically for the deuterium signature. At the onset of each experiment antecedent liquid water was first pushed out by the sprinkling water. Hydrographs showed four pronounced peaks corresponding to the four sprinkling bursts. The contribution of rainwater to snowpack runoff consistently increased over the course of the experiment but never exceeded 86 paths that allowed rainwater to efficiently propagate through the snowpack limiting the time for mass exchange processes to take effect. On the contrary, experiments conducted on ripe isothermal snowpack showed a slower response behaviour and resulted in a total runoff volume which consisted of less than 50 % of the rain input.

Keywords: hydrograph separation, stable isotopes, sprinkling experiment, preferential flow, flood forecasting

5.3   The influence of snow cover properties on runoff formation during rain-on-snow events

Sebastian Würzer[a] and Tobias Jonas[a]

[a]:WSL Institute for Snow and Avalanche Research SLF, Davos, Switzerland

Rain-on-snow (ROS) events were causing major flood events in alpine and sub-alpine regions in the past. In October 2011, such an event led to severe regional flooding in Switzerland. It still presents a great challenge to predict the impact of the snow cover on the runoff generation for an upcoming ROS event. Processes are complex and spatio-temporally variable; moreover, accurate data in order to be able to assess these processes in detail are missing. In this study, the physics-based snow cover model SNOWPACK was used to model snow cover processes during more than 1000 historical ROS events at station locations and 191 events across whole catchments in Switzerland. The resulting simulations of mass and energy balance as well as liquid water transport were used to investigate runoff formation during ROS events. In most cases, rain is dominating snowpack runoff generation, however, in some cases snowmelt can contribute up to 70% to the snowpack runoff. The main source of such high melt contributions are turbulent heat fluxes. Events with excessive snowpack runoff were most frequently observed during the late ablation phase in early summer and partly in autumn. Using systematic analyses, the study results exhibit several meteorological factors as well as snowpack properties, which promote increased runoff formation during ROS events.

6 Discussion and Outlook

The presented thesis investigated how initial snow cover properties and certain storm characteristics influence snowpack runoff generation during rain-on-snow (ROS). This chapter discusses the significance and implications of the study results presented in Chapters 2-4, as well as limitations of the thesis research and recommendations for follow-up research. The three studies forming this thesis each address a particular set of snowpack and/or meteorological processes that represent snowpack runoff generation at different spatial scales. This research shows that the governing processes change as the scale changes, from snow microstructure to an entire catchment snow cover. As an example, results presented in Chapter 3 suggest that the initial liquid water content (LWC) of a snowpack and the length of the rain event dominate runoff formation at the point scale. However, results presented in Chapter 4 suggest that rising air temperatures and a large area covered by homogeneous snow prevail over processes found to be dominant at smaller scales.

For the simulations presented in Chapter 4, the preferential flow (PF) model presented in Chapter 2 was already available. This has to be considered if comparing results from Chapter 4 with the ones in Chapter 3, based on simulations using the original Richards' Equation (RE) model. As an example, findings from Chapter 2 and Juras et al. (2017) indicate, that accounting for the presence of PF would lead to higher propagation velocities for individual events with low initial LWCs presented in Chapter 3 (Figure 3.8). Similarly, highest time lags in Figure 3.7 should be expected to be lower, if considering PF. Therefore, the statement that snowpack runoff will not occur synchronously throughout the catchment in case of low LWC and variable distribution of snow depth is put into perspective by findings of Chapter 2. Results in Chapter 4 suggest that synchronous snowmelt runoff can occur for low initial LWC, however, these events usually entail homogeneous catchment snow cover conditions. However, for all individual events with high initial LWC, these values are not expected to change significantly by accounting for PF (See Chapter 2).

The overall retention of rain water, expressed as negative runoff excess, is probably slightly overestimated by neglecting PF in simulations of Chapter 3. However, lateral flow in the sprinkling events conducted in Chapter 2 (Figure 2.4) hinders to assess the performance of the PF

simulations relative to the RE simulations for rainwater retention. Moreover, Figure 2.6 shows an ambiguous picture about the two models representing rain water retention accurately, where only the bucket approach (BA) can be considered to overestimate retention. The available retention capacity (ARC; Chapter 3) was defined in order to achieve an easier transfer of the results to hydrological models using a retention capacity. However, the findings in Chapter 2 clearly suggest a limited applicably for this concept for dry, cold and low density snowpack. This limitation is further discussed in Section 6.1.1. Nonetheless, results in Chapter 4 show that also for simulations accounting for PF, liquid water retention still plays an important role in higher elevations. Further, the modulating effect of snow cover on snowpack runoff for rain events of different length was shown for both point and catchment simulations. This also accounts for the rather negative correlation of snow depth with snowpack runoff rates (Figure 3.10 and 4.8b).

Current process understanding makes it difficult to up-scale and assess processes which were found to be essential at smaller scales. Therefore, some issues will be discussed in more detail. Section 6.1 discusses the limitations in assessing preferential flowpaths (PFPs) with observations and models. Additionally, an outlook is provided on the implications of lateral flow processes for catchment runoff formation. Section 6.2 discusses how such processes could be incorporated in hydrological models and an outlook detailing how the findings of the presented study could improve hydrological modelling is presented.

6.1 The relevance and limitations of modelling preferential flow

Modelling hourly point-scale snowpack runoff crucially depends on a correct representation of water transport (Wever et al., 2014a, and Chapter 2). Catchment runoff formation processes, however, additionally depend on a variety of catchment properties like prevailing geology and soils. Therefore, one might argue that small-scale phenomena lose their importance at larger scales. So, is the formation of PFP really relevant for hydrological modelling? Parameters in retrospective modelling of the October 2011 event had to be tweaked to allow for fast runoff processes in order to reproduce observed runoff peaks for this particular event (Rössler et al., 2014, Badoux et al., 2013). This suggests that although the models are generally capable of simulating runoff processes for the respective catchments, the simplified snow cover representations were incapable of addressing the snow cover runoff processes of this particular event. With a generally fast transport of rainwater in snowpacks dominated by PF (Chapter 2 and Juras et al., 2017), the influence of snow height heterogeneity in a catchment decreases, supporting runoff synchronicity. Thus, even a small artificial delay of snowpack runoff by neglecting preferential flow can hinder the successful modelling of ROS events, such as the one that occurred in October 2011. Additionally, water transport in PFP can lead to highly saturated ponding layers, which can lead to lateral flow processes, as discussed in Section 6.1.3.

Installing multiple lysimeters at each of the field sites described in Chapter 2 allowed us to

estimate the effect of preferential flow from snowpack runoff heterogeneity during natural ROS events. However, the dual-domain model validation was mainly conducted on single lysimeters at Weissfluhjoch and Col de Porte (where a second smaller lysimeter served as reference) and simulated structural parameters had to be used to estimate if preferential flow occurred. Both lysimeters measure a relatively large area ($5\,m^2$), but this may not be large enough to measure the range of observed snowpack runoff heterogeneity (up to $20\,m^2$; Kattelmann, 1985, 2000, Yamaguchi et al., 2012a). It would therefore be desirable to establish a sensor network allowing for observing larger scale snowpack runoff heterogeneity. Such a network could incorporate the following sensors: large-scale multi-compartment lysimeters that assess the effect of PFP on snowpack runoff heterogeneity (as in (Yamaguchi et al., 2012a)), and "slope lysimeters" similar to the ones presented in Eiriksson et al. (2013), that could be extended to measure runoff from different snow and soil depths and at their interface. This could improve the quantification of lateral flow processes within the snow cover and at the snow-soil interface. Additionally, a slope-scale array of soil moisture sensors could provide a relatively low cost, wide-scale and spatially distributed way to qualitatively assess timing and heterogeneity of snowpack runoff.

6.1.1 Refreeze processes

If PFP are formed during ROS events, water transport is much more efficient in a limited fraction of the snowpack and rainwater can be released even from a partly sub-freezing snowpack. However, observations of ice columns inside the snowpack clearly show that refreeze of flow fingers cannot be neglected (Kattelmann, 1985, Fierz et al., 2009, Williams et al., 2000). In the PF model presented in Chapter 2, refreeze is a function of a parameter (N) describing the number of PFP, forming the PFP area. This parameter should be seen as a tuning parameter rather than an exact abundance of PFP. For the simulations presented in Chapter 2, however, refreeze in the PF domain was neglected by setting N to zero, since it did not significantly affect the models ability to reproduce measured hourly snowpack runoff, but was found to reproduce ice layer formation best (Wever et al., 2016b). Ideally, this would be attributable to the limited effect of refreeze on PFPs. However, since the PF model incorporated a second tuning parameter, this could also be a problem of equifinality with the parameter Θ_{th}, which describes the threshold for saturation of the preferential flow domain (See Chapter 2 and Wever et al. (2016b)). Unfortunately, there are limited data available on the influence of snowpack properties on area and number of PFP and how these in turn limit refreeze processes in snow. Laboratory experiments on the formation of PFP exist for both homogeneous (Katsushima et al., 2013) and layered snow (Avanzi et al., 2016) and a 3D-water transport model was successfully validated for these datasets (Hirashima et al., 2014, 2017). Results from Katsushima et al. (2013) suggest that for small and rounded grains, 100% of the sample area (diameter of 5 cm) is participating in water transport and therefore represents matrix flow. However, during the sprinkling experiments presented in Chapter 2, PFPs with diameters exceeding 20 cm were forming at ponding layers, representing just 3% of the total area (Figure 1.1). The experiments by Katsushima et al. (2013) and Avanzi et al. (2016) might

not be able to represent for such large PFP, which, however, were only observed in initially cold snow. Recently, Avanzi et al. (2017) used X-ray micro-tomography under constant melt and melt-refreeze conditions to investigate the formation of PFP during non-ROS conditions. Tracer methods presented for use at larger scales (Juras et al., 2017) enabled us to distinguish between snowpack runoff from rain or melt and therefore estimate the dynamics of water storage in snowpack. However, this approach does not allow for determination of the exact area or number of PFP. Despite the recent progress presented in these studies, no experimental or detailed modelling approaches on the formation and persistence of PFP are presented for larger volumes, especially in a layered, sub-freezing snowpack. Hence, experimental and model research should be extended to such scales and conditions. Nonetheless, detailed 3D models and experiments on small scales are a valuable contribution to the understanding of preferential flow in snow and lay the foundation for developing simplified 1D models that account for PFP. Kattelmann (1985) suggests that persistent PFP in terms of macro pores are formed by wet snow metamorphism, and are likely to get "reactivated" in subsequent rain or melt events. Yet, the PF model is not capable of representing the persistence of PFP, since phase changes and snow metamorphism is just represented in the matrix domain. However, reliable data on the persistence of such structures are not available and new preferential flow paths are known to form in subsequent melt cycles (Schneebeli, 1995).

6.1.2 Liquid water retention

Similar to the refreeze, liquid water retention is also reduced if PFP are present and runoff can occur significantly faster than what would be expected when using a classical retention capacity approach (Juras et al., 2017, and Chapter 2). For the sprinkling experiment on nearly dry snow presented in Juras et al. (2017), a retention capacity of 10% of SWE (as used as default in PREVAH (Viviroli et al., 2009)) would have resulted in snowpack runoff after retaining approximately 12.5 mm of rain. For a sprinkling amount of 10.39 mm in the first hour, all water should be retained. However, runoff was already observed after 10 minutes (approximately 3.5 mm) of sprinkling and made in total 8.14 mm in the first hour, hence just 20% of rainwater in the first hour after onset of sprinkling. As shown in the experiments in Chapter 2, only ca. 50 % of rainwater was retained compared to the PREVAH default. Typical water retention values around 5-15% of mass are representing the irreducible water content of a saturated layer of snow, but not of a total snowpack where PFPs are present (Coléou and Lesaffre, 1998, Colbeck, 1974). Therefore, such values might be able to represent liquid water retention for spring snowpacks and low melt rates, where a uniform wetting is more likely.

6.1.3 Formation of preferential lateral flow

There are strong indications that small-scale processes such as PFP do affect catchment scale water transport in addition to speeding up vertical water transport in snow. Structures like rills can often be observed after ROS events on slopes (Figure 6.1) and indicate slope-parallel, lateral down-hill water transport (Higuchi and Tanaka, 1982) in "lanes" initially caused by the

Figure 6.1 – Picture of rills across the snow surface after a ROS event in the Swiss Alps, taken by Michel Bovey

presence of PFP. The remnants of such structures can also occur as slope-parallel ribs (Williams et al., 2000) or might form icy veins at the snow-soil interface (Webb et al., 2017). The latter was found to be continuous along the slope, although underlying soils were not saturated and hence could allow for infiltration (Webb et al., 2017). It is important to note that there is a discrepancy between the correlation length of meltwater flowing through ripe snowpacks (ca. 6 m; Sommerfeld et al., 1994, Williams et al., 1999, Higuchi and Tanaka, 1982) and the much smaller spatial separation of PFP which account for up to 300 PFPs m^{-2} (Kattelmann, 1985, Marsh and Woo, 1985, McGurk and Marsh, 1995). Even if rills are not observed, water in highly saturated ponding layers above capillary barriers can form efficient lateral flow processes (Eiriksson et al., 2013), which decrease travel time in sloped terrain. Such processes were also observed in the lowermost layers at the snow-soil interface. Ponding layers on "coarse-grained" grass were mainly observed during autumn (Mitterer and Schweizer, 2013) and could have been present during the October 2011 event, where capillary barriers and lateral flow within the snowpack were unlikely.

6.2 Snow cover process representation in hydrological models

Simulations with detailed snow cover models have shown that snowpack runoff modelling can benefit significantly from the use of more complex, physically based models (Wever et al., 2014a, and Chapter 2). Nonetheless, hydrological models used for operational flood forecasting purposes (e.g. HBV (Bergstroem, 1995), WASIM (Schulla, 2017), PREVAH) pay little attention to snow cover processes. The complexity of snow cover processes can simply not be reproduced with such models, which in turn leads to a decreased forecast skill for extreme runoff events in snow covered catchments (Orth et al., 2015). Even retrospective modelling, where the uncertainties in meteorological forcing are smaller than forecasted data, often results in surprisingly inaccurate simulations (Badoux et al., 2013, Rössler et al., 2014).

This section shall discuss how these models could be adapted to better predict runoff formation in future ROS events. Rössler et al. (2014) concluded that the October 2011 ROS flood was generally predictable, but required a special hydrological model setup that accounts for fast (lateral) runoff processes, which might also be used for assessing future ROS events. Implicitly, fast transport processes are incorporated in hydrological models by parameter calibration, however, they usually originate from catchment physiography and do not change over time. For snow cover, however, the formation of such structures strongly depends on snowpack properties and therefore can change significantly over short timescales. Compensating limited process representation with such a special setup additionally carries the risk of poor and dangerous extrapolation performance. Based on findings in Chapter 2, such a "ROS setup" should primarily be used if PFP can be expected, and this could be determined by extending simple snow modules of hydrological models with snow density parametrizations. Alternatively, this decision could be based on snowpack stratigraphy measures such as grain size changes, density changes, and the presence of melt forms, which could be derived from SNOWPACK simulations. This approach could to some extent mimic the representation of snow cover-processes, but would require some sort of transfer function describing the relation of snowpack structure and snow module parameters as retention capacity and refreeze and the respective parameters governing fast lateral runoff processes. With generally limited data for extreme events and many unknowns (e.g. dependence on water influx rates, catchment physiography), such a "ROS setup" might only help with estimating a worst-case scenario for respective snow properties and rain intensities/totals.

The above-mentioned limitations of such an approach could be circumvented by coupling distributed hydrological models such as WASIM (which is used by the Swiss hydrological forecast) with distributed versions of detailed snow cover models such as ALPINE3D. ALPINE3D can already be coupled with the semi-distributed hydrological model PREVAH (Viviroli et al., 2009) by providing distributed input parameters for PREVAH. Another approach allows for hydrological modelling using a travel time formulation implemented in ALPINE3D (Comola et al., 2015). Despite the potential coming with accounting for PFP, such an approach allows for the modulating effect of snow cover processes on rainfall, which can lead to increased snowpack runoff rates for longer events (See Chapter 3 and 4). If ALPINE3D would explicitly

account for lateral flow processes, a standard parametrization of the coupled hydrological model could be used. Wever (2014) suggest modelling lateral flow in ALPINE3D by separating the gravitational flow of water in components perpendicular and parallel to the slope, where the slope-parallel component could be routed to the next grid cell. Based on findings in Chapter 2 and Section 6.1, such an approach should also account for increased transport efficiency of water concentrated in ponding layers. Besides the opportunity of accounting for lateral flow outside the hydrological model, this involves the danger of over-fitting by consequently adding further arbitrary parameters which have to be, in absence of reliable measurements, calibrated (See Section 6.1). Most hydrological models used for operational flood forecasting purposes (e.g. HBV, PREVAH) do not account for changes in water transport due to frozen soil and therefore entail frost-related errors in the timing and amount of runoff (Stähli et al., 2001). Using ALPINE3D could account for the formation of basal ice layers during mid-winter ROS events as well as basal ponding zones (See Section 6.1.3). The disadvantages of this approach is that it is computationally expensive and has a higher demand for meteorological forcing data and quality. This limits the applicability for operational hydrological forecasting on larger scales. Particularly in regions lacking a dense meteorological observation network, the actual state of snow cover and it's heterogeneity is difficult to assess. However, with increasing accuracy of meteorological forecast, such data could be used to replace meteorological measurements. Anyhow, the presented research recommends that hydrological models must be able to represent snow cover in a more complex way to be able to predict runoff formation during extreme ROS events.

6.3 Hydroclimatical effects on ROS

The presented research focusses primarily on runoff formation processes during ROS in high elevations in the Swiss Alps. However, if comparing the seasonal occurrence of ROS at a high elevation site in eastern Switzerland (WFJ) and a mid elevation site in the French Alps (CDP), some distinct differences are notable. Whereas most ROS events at CDP occur in mid-winter (December-February), most ROS events at WFJ occur in its late snow season (May-July), when CDP is not covered by snow anymore. Due to their seasonal occurrence in mid-winter, ROS events at CDP entailed lower initial snowpack densities, a lower initial LWC and higher initial cold content, despite the lower elevation of the site. This resulted in a more distinct difference in RE and PF model performance at CDP, if compared to WFJ (Chapter 2). In combination with the sprinkling experiments shown in Chapter 2 and Juras et al. (2017), this suggests a dominating effect of preferential flowpaths at this site. As further shown in Chapter 2, CDP showed lower maximum rain intensities, however the event rainfall extended over a longer period of time. Under such conditions, snow cover was shown to amplify snowpack runoff generation (Figures 3.9 and 4.7). Projections by Schmucki et al. (2015) show a continuous snow cover at WFJ by the end of the 21st century even in a warming climate. Further, Köplin et al. (2014) projected an increase in winter liquid precipitation for a nival alpine catchment in Switzerland by the end of the 21st century. Conditions currently

observed at CDP might therefore be observed in higher elevations in the future. A shift in ROS occurrence is likely to change the flood regime in elevations and regions where such snowpack runoff formation processes are currently exceptional during autumn and mid-winter. According to Köplin et al. (2014), this leads to an unstable state of the hydrological regime with unspecific seasonality and increased mean annual flood peaks. In respect of results shown in Chapter 4, a warming future might entail long-lasting rainfall falling on a widespread snow cover at high elevations in Switzerland during winter. A change in ROS frequency and flood regimes with a warming climate is also shown by results from Surfleet and Tullos (2013), suggesting that for a set of catchments in Oregon both ROS frequency and annual peak flows increase in higher elevations, but decrease in lower elevations. In combination with different physiographic conditions of high elevation catchments (e.g. hypsometry, geology, pedology) this leads to a challenge for flood forecasting. The presented research might give a clue in how snowpack runoff formation processes may change at high elevations in future climate. However, more research is needed in both investigating the effect of climate change as well as in what respect catchment physiography affects catchment runoff formation during ROS.

A further aspect is the effect of large weather phenomena associated with ROS. Trubilowicz and Moore (2017) found that most large ROS events of a total of 286 ROS events in British Columbia were associated with atmosperic rivers (ARs). This is alarming, since the frequency of ARs is projected to increase with climate change in British Columbia (Radić et al., 2015). For some parts of Germany, the frequency of extreme winter floods was shown to change with the frequency and persistence of large scale weather patterns (See Section 1.2.5 and Caspary, 1995). However, to the authors knowledge, no projections on the changing frequency of ARs in the future are available for Europe.

6.4   Final remarks

This chapter shows that there are still several challenges to be addressed before streamflow can be predicted accurately for complex phenomena such as ROS. This results from limited process understanding (e.g. refreeze of liquid water in sub-freezing snow), limited process representation (e.g. preferential flow and lateral flow in hydrological models) and limited representation of small-scale heterogeneity and accuracy in meteorologic forecast.

The sprinkling experiments and simulations with the new dual-domain water transport model presented in Chapter 2 show that classical "bucket approaches", relying on retention capacity, are not capable to address water transport for ROS events on a dry and low density snowpack. Particularly for ROS events where previous snowfall reaches down to low-elevation mountain ridges, little retention can be expected and hydrological models will consequently fail to predict the onset of snowpack runoff accurately. Experiments by Juras et al. (2017) (Section 5.2) revealed that much higher liquid water transport velocities can be expected under such conditions. Moreover, the experiments in Chapter 2 revealed strong ponding on capillary

barriers. Such ponding layers were shown to play an important role in ice layer formation (Wever et al. (2016b), Section 5.1) and are suggested to support fast lateral water transport processes in the catchment. However, little is yet known about the quantities transported by lateral flow processes.

Chapter 3 points out the dominant energy contribution by turbulent fluxes for events showing considerable snowmelt. Hence, if meteorological forecast indicates a strong rise in air temperatures and high wind speeds, hydrological forecasters must expect melt rates significantly higher than determined with TI approaches. Therefore forecasters are encouraged to use energy-balance (EB) models in case of ROS events. Moreover, forecasters should be aware of considerable low bias in quantitative precipitation forecast in case of a predicted AR system. A high initial LWC is associated high runoff excess (Chapter 3), low time-lags (Chapter 3) and high snowpack runoff synchronicity (Chapter 4) during ROS. If a snow with high LWC covers large parts of the catchment, forecasters might consider the high flooding potential involved with such factors.

The research presented in this thesis advances the knowledge of snow cover processes during ROS and increases the accuracy of ROS snowpack runoff predictions by:

- Identifying snowpack and meteorological boundary conductions associated with high runoff formation during ROS through analysis of data from a vast number of point and catchment scale snow cover simulations across Switzerland (Chapter 3 and 4).

- Incorporating the influence of PFP formation on water transport in a 1D snow cover model, which is used operationally (Chapter 2).

- Presenting key factors which entail a increased risk of excessive snow cover runoff formation at the point and catchment scales (Chapter 3 and 4).

Despite better process understanding, better representation of the water transport in the snow cover, and knowing about the factors entailing a high risk for high snowpack runoff and therefore a high flooding potential, a quantitative prediction of streamflow during ROS will be difficult. This is due to the fact that detailed physics-based snow cover models entail a higher level of process representation than hydrological models for catchment scales. Forecasters, however, have to rely on hydrological models, being significantly constrained by limited process representation. Not just snow cover processes, but processes describing water transport in soils or groundwater dynamics are considerably simplified. Fast transport processes, such as macropore flow or fast subsurface lateral flow in slopes are not explicitly represented in such hydrological models. Moreover, most models do not allow for soil freezing and hence will likely underestimate surface runoff. The results presented in this thesis will help to interpret the results of the hydrological forecasting models used by forecasters. The long-term goal should be to adapt snow models in hydrological models to be able to represent processes occurring in rare, but severe situations. However, even with better models and enhanced

process understanding, accurate stream peakflow prediction and flood warnings for such complex phenomena will rely on adequate assessment of the situation by forecasters. This research provides the operational forecast services simple key factors which can be used for a fast assessment of the effect of snow cover situation for an upcoming event, and can be used for plausibility checks of the hydrological model results.

Bibliography

Albert, M., Koh, G., and Perron, F. Radar investigations of melt pathways in a natural snowpack. *Hydrol. Process.*, 13(18):2991–3000, 1999. doi: 10.1002/(SICI)1099-1085(19991230)13:18<2991::AID-HYP10>3.0.CO;2-5.

Armstrong, R. L. and Brodzik, M. J. Recent northern hemisphere snow extent: A comparison of data derived from visible and microwave satellite sensors. *Geophys. Res. Lett.*, 28(19): 3673–3676, 2001. doi: 10.1029/2000GL012556.

Avanzi, F., Hirashima, H., Yamaguchi, S., Katsushima, T., and De Michele, C. Observations of capillary barriers and preferential flow in layered snow during cold laboratory experiments. *The Cryosphere*, 10(5):2013–2026, 2016. doi: 10.5194/tc-10-2013-2016.

Avanzi, F., Petrucci, G., Matzl, M., Schneebeli, M., and De Michele, C. Early formation of preferential flow in a homogeneous snowpack observed by micro-ct. *Water Resources Research*, 53(5):3713–3729, 2017. ISSN 1944-7973. doi: 10.1002/2016WR019502.

Badoux, A., Hofer, M., and Jonas, T. Hydrometeorologische Analyse des Hochwasser-ereignisses vom 10. Oktober 2011. Technical report, WSL/SLF/MeteoSwiss, 2013. in German, available at: http://www. wsl.ch/fe/gebirgshydrologie/wildbaeche/projekte/unwetter2011/Ereignisanalyse _Hochwasser_Oktober_2011.pdf (last access: 13 Sept 2017).

Barnett, T. P., Adam, J. C., and Lettenmaier, D. P. Potential impacts of a warming climate on water availability in snow-dominated regions. *Nature*, 438(7066):303–309, 2005. doi: 10.1038/nature04141.

Bartelt, P. and Lehning, M. A physical SNOWPACK model for the Swiss avalanche warning Part I: Numerical model. *Cold Reg. Sci. Technol.*, 35(3):123–145, 2002. doi: 10.1016/S0165-232X(02)00074-5.

Bavay, M. and Egger, T. MeteoIO 2.4.2: a preprocessing library for meteorological data. *Geosci. Model Dev.*, 7(6):3135–3151, 2014. doi: 10.5194/gmd-7-3135-2014.

Bayard, D., Stähli, M., Parriaux, A., and Flühler, H. The influence of seasonally frozen soil on the snowmelt runoff at two Alpine sites in Southern Switzerland. *J. Hydrol.*, 309(1-4):66–84, 2005. doi: 10.1016/j.jhydrol.2004.11.012.

Beaudry, P. and Golding, D. Snowmelt during rain-on-snow in coastal british columbia. In *Proceedings of the Western Snow Conference*, volume 51, pages 55–66, 1983.

Beniston, M. Mountain climates and climatic change: an overview of processes focusing on the

Bibliography

European Alps. *Pure and Applied Geophysics*, 162(8-9):1587–1606, 2005. doi: 10.1007/s00024-005-2684-9.

Beniston, M. and Stoffel, M. Rain-on-snow events, floods and climate change in the Alps: Events may increase with warming up to 4° c and decrease thereafter. *Science of the Total Environment*, 571:228–236, 2016. doi: 10.1016/j.scitotenv.2016.07.146.

Berg, N., Osterhuber, R., and Bergman, J. Rain-induced outflow from deep snowpacks in the central Sierra Nevada, California. *Hydrol. Sci. J.*, 36(6):611–629, 1991. doi: 10.1080/02626669109492547.

Bergstroem, S. Chapter 13: The hbv model, 1995. Computer models of watershed hydrology, ed. V.P. Singh, Water Resources Publications, Littleton, Colorado.

Berris, S. N. and Harr, R. D. Comparative snow accumulation and melt during rainfall in forested and clear-cut plots in the Western Cascades of Oregon. *Water Resour. Res.*, 23(1): 135–142, 1987. doi: 10.1029/WR023i001p00135.

Biggs, T. W. and Whitaker, T. M. Critical elevation zones of snowmelt during peak discharges in a mountain river basin. *J. Hydrol.*, 438-439:52–65, 2012. doi: 10.1016/j.jhydrol.2012.02.048.

Blöschl, G., Kirnbauer, R., and Gutknecht, D. Modelling snowmelt in a mountainous river basin on an event basis. *J. Hydrol.*, 113(1):207 – 229, 1990. doi: 10.1016/0022-1694(90)90176-X.

Blöschl, G. *Runoff prediction in ungauged basins: synthesis across processes, places and scales*. Cambridge University Press, 2013.

Brands, S., Gutiérrez, J. M., and San-Martín, D. Twentieth-century atmospheric river activity along the west coasts of Europe and North America: algorithm formulation, reanalysis uncertainty and links to atmospheric circulation patterns. *Climate Dynamics*, 48(9):2771–2795, May 2017. doi: 10.1007/s00382-016-3095-6.

Brooks, K. N., Ffolliott, P. F., and Magner, J. A. *Precipitation*, pages 49–79. Blackwell Publishing Ltd., 2012. ISBN 9781118459751. doi: 10.1002/9781118459751.ch3.

Brun, E. Investigation on wet-snow metamorphism in respect of liquid-water content. *Annals of Glaciology*, 13:22–26, 1989. doi: 10.1017/S0260305500007576.

Calonne, N., Geindreau, C., Flin, F., Morin, S., Lesaffre, B., Rolland du Roscoat, S., and Charrier, P. 3-D image-based numerical computations of snow permeability: links to specific surface area, density, and microstructural anisotropy. *Cryosphere*, 6(5):939–951, 2012. doi: 10.5194/tc-6-939-2012.

Caspary, H. Recent winter floods in Germany caused by changes in the atmospheric circulation across Europe. *Physics and Chemistry of the Earth*, 20(5):459 – 462, 1995. ISSN 0079-1946. doi: 10.1016/S0079-1946(96)00006-7.

Cline, D. W. Snow surface energy exchanges and snowmelt at a continental, midlatitude alpine site. *Water Resour. Res.*, 33(4):689–701, 1997. doi: 10.1029/97WR00026.

Colbeck, S. C. Analysis of hydrologic response to rain-on-snow. Technical Report 340, CRREL Research Rep., 1975.

Colbeck, S. C. and Davidson, G. Water percolation through homogeneous snow. In *The Role of Snow and Ice in Hydrology: Proc: Banff Symp*, pages 242–257, 1973.

Colbeck, S. C. A theory of water percolation in snow. *J. Glaciol.*, 11(63):369–385, 1972. doi: 10.3189/S0022143000022346.

Colbeck, S. C. The capillary effects on water percolation in homogeneous snow. *J. Glaciol.*, 13 (67):85–97, 1974. doi: 10.3189/S002214300002339X.

Coléou, C. and Lesaffre, B. Irreducible water saturation in snow: experimental results in a cold laboratory. *Ann. Glaciol.*, 26:64 – 68, 1998. doi: 10.3189/1998AoG26-1-64-68.

Comola, F., Schaefli, B., Rinaldo, A., and Lehning, M. Thermodynamics in the hydrologic response: Travel time formulation and application to Alpine catchments. *Water Resour. Res.*, 51(3):1671–1687, 2015. doi: 10.1002/2014WR016228.

Conway, H. and Benedict, R. Infiltration of water into snow. *Water Resour. Res.*, 30(3):641–649, 1994. doi: 10.1029/93WR03247.

Conway, H. and Raymond, C. F. Snow stability during rain. *J. Glaciol.*, 39(133):635–642, 1993. doi: 10.3189/S0022143000016531.

Dadic, R., Mott, R., Lehning, M., Carenzo, M., Anderson, B., and Mackintosh, A. Sensitivity of turbulent fluxes to wind speed over snow surfaces in different climatic settings. *Advances in Water Resources*, 55:178–189, 2013. doi: 10.1016/j.advwatres.2012.06.010.

D'Amboise, C. J. L., Müller, K., Oxarango, L., Morin, S., and Schuler, T. V. Implementation of a physically based water percolation routine in the crocus (v7) snowpack model. *Geoscientific Model Development Discussions*, 2017:1–32, 2017. doi: 10.5194/gmd-2017-56.

Davies, J. H. and Davies, D. R. Earth's surface heat flux. *Solid Earth*, 1(1):5–24, 2010. doi: 10.5194/se-1-5-2010.

Denoth, A. An electronic device for long-term snow wetness recording. *Ann. Glaciol.*, 19: 104–106, 1994.

DeWalle, D. R. and Rango, A. *Principles of Snow Hydrology*. Cambridge University Press, 2008. doi: 10.1017/CBO9780511535673.

DiCarlo, D. A. Stability of gravity-driven multiphase flow in porous media: 40 years of advancements. *Water Resour. Res.*, 49(8):4531–4544, 2013. doi: 10.1002/wrcr.20359.

Dilley, A. and O'Brien, D. Estimating downward clear sky long-wave irradiance at the surface from screen temperature and precipitable water. *Quarterly Journal of the Royal Meteorological Society*, 124(549):1391–1401, 1998. doi: 10.1002/qj.49712454903.

Dyer, J. L. and Mote, T. L. Role of energy budget components on snow ablation from a mid-latitude prairie snowpack. *Polar Geography*, 26(2):87–115, 2002. doi: 10.1080/789610133.

Eiras-Barca, J., Lorenzo, N., Taboada, J., Robles, A., and Miguez-Macho, G. On the relationship between atmospheric rivers, weather types and floods in galicia (nw spain). *Natural Hazards and Earth System Sciences Discussions*, 2017:1–16, 2017. doi: 10.5194/nhess-2017-145.

Eiriksson, D., Whitson, M., Luce, C. H., Marshall, H. P., Bradford, J., Benner, S. G., Black, T., Hetrick, H., and McNamara, J. P. An evaluation of the hydrologic relevance of lateral flow in snow at hillslope and catchment scales. *Hydrol. Process.*, 27(5):640–654, 2013. doi: 10.1002/hyp.9666.

Fang, X. and Pomeroy, J. W. Impact of antecedent conditions on simulations of a flood in a mountain headwater basin. *Hydrol. Process.*, 30(16):2754–2772, 2016. doi: 10.1002/hyp.10910.

Ferguson, S. A. The spatial and temporal variability of rain-on-snow. In *Proceedings of the International Snow Science Workshop*, pages 1–6, 2000.

Bibliography

Fierz, C., Armstrong, R., Durand, Y., Etchevers, P., Greene, E., McClung, D., Nishimura, K., Satyawali, P., and Sokratov, S. The International Classification for Seasonal Snow on the Ground (ICSSG). Technical report, IHP-VII Technical Documents in Hydrology No. 83, IACS Contribution No. 1, UNESCO-IHP, Paris, 2009.

FOEN, F. Produktinformation Einzugsgebietsgliederung Schweiz EZGG-CH. *Web document in German.(Available at https://www.bafu. admin. ch/dam/bafu/de/dokumente/wasser/fachinfo-daten/produktedokumentationeinzugsgebietsgliederungschweiz .pdf)*, 2015.

Forbes, B. C., Kumpula, T., Meschtyb, N., Laptander, R., Macias-Fauria, M., Zetterberg, P., Verdonen, M., Skarin, A., Kim, K.-Y., Boisvert, L. N., Stroeve, J. C., and Bartsch, A. Sea ice, rain-on-snow and tundra reindeer nomadism in arctic russia. *Biology Letters*, 12(11), 2016. doi: 10.1098/rsbl.2016.0466.

Freudiger, D., Kohn, I., Stahl, K., and Weiler, M. Large-scale analysis of changing frequencies of rain-on-snow events with flood-generation potential. *Hydrol. Earth Syst. Sci.*, 18(7): 2695–2709, 2014. doi: 10.5194/hess-18-2695-2014.

FSO, F. Switzerland's Land Use Statistics (Arealstatistik der Schweiz, in German. *Web document in German.(Available at https://www.bfs.admin.ch/bfsstatic/dam/assets/6813/master)*, 2017.

Garvelmann, J., Pohl, S., and Weiler, M. Variability of observed energy fluxes during rain-on-snow and clear sky snowmelt in a midlatitude mountain environment. *J. Hydrometeorol.*, 15(3):1220–1237, 2014. doi: 10.1175/JHM-D-13-0187.1.

Garvelmann, J., Pohl, S., and Weiler, M. Spatio-temporal controls of snowmelt and runoff generation during rain-on-snow events in a mid-latitude mountain catchment. *Hydrol. Process.*, 29(17):3649–3664, 2015. doi: 10.1002/hyp.10460.

Gerdel, R. W. The transmission of water through snow. *Eos, Transactions American Geophysical Union*, 35(3):475–485, 1954. doi: 10.1029/TR035i003p00475.

Gimeno, L., Nieto, R., Vázquez, M., and Lavers, D. Atmospheric rivers: a mini-review. *Frontiers in Earth Science*, 2:2, 2014. doi: 10.3389/feart.2014.00002.

Glass, R., Steenhuis, T., and Parlange, J. Wetting front instability, 2, experimental determination of relationships between system parameters and two-dimensional unstable flow field behavior in initially dry porous media. *Water Resour. Res*, 25(6):1195–1207, 1989. doi: 10.1029/WR025i006p01195.

Gouttevin, I., Lehning, M., Jonas, T., Gustafsson, D., and Mölder, M. A two-layer canopy model with thermal inertia for an improved snowpack energy balance below needleleaf forest (model snowpack, version 3.2.1, revision 741). *Geoscientific Model Development*, 8(8): 2379–2398, 2015. doi: 10.5194/gmd-8-2379-2015.

Harr, R. D. Some characteristics and consequences of snowmelt during rainfall in Western Oregon. *J. Hydrol.*, 53(3-4):277–304, 1981. doi: 10.1016/0022-1694(81)90006-8.

Harr, R. D. Effects of clearcutting on rain-on-snow runoff in Western Oregon: A new look at old studies. *Water Resour. Res.*, 22(7):1095–1100, 1986. doi: 10.1029/WR022i007p01095.

Harr, R. D. and McCorison, F. M. Initial effects of clearcut logging on size and timing of peak flows in a small watershed in western Oregon. *Water Resources Research*, 15(1):90–94, 1979. ISSN 1944-7973. doi: 10.1029/WR015i001p00090.

Higuchi, K. and Tanaka, Y. Flow pattern of meltwater in mountain snow cover. *in: Hydrological aspects of alpine and high-mountain areas/edited by JW Glen*, 1982. Proceedings of the Exeter Symposium, July 1982, IAHS Publ. no. 138.

Hirashima, H., Avanzi, F., and Yamaguchi, S. Liquid water infiltration into a layered snowpack: evaluation of a 3d water transport model with laboratory experiments. *Hydrology and Earth System Sciences Discussions*, 2017:1–22, 2017. doi: 10.5194/hess-2017-200.

Hirashima, H., Yamaguchi, S., and Katsushima, T. A multi-dimensional water transport model to reproduce preferential flow in the snowpack. *Cold Reg. Sci. Technol.*, 108:80–90, 2014. doi: 10.1016/j.coldregions.2014.09.004.

Hock, R. Temperature index melt modelling in mountain areas. *J. Hydrol.*, 282(1-4):104–115, 2003. doi: 10.1016/S0022-1694(03)00257-9.

Horton, R. E. The melting of snow. *Monthly Weather Review*, 43(12):599–605, 1915.

Il Jeong, D. and Sushama, L. Rain-on-snow events over north america based on two canadian regional climate models. *Climate Dynamics*, pages 1–14, 2017. doi: 10.1007/s00382-017-3609-x.

Illangasekare, T. H., Walter, R. J., Jr., Meier, M. F., and Pfeffer, W. T. Modeling of meltwater infiltration in subfreezing snow. *Water Resour. Res.*, 26(5):1001–1012, 1990. doi: 10.1029/WR026i005p01001.

Jennings, K. and Jones, J. A. Precipitation-snowmelt timing and snowmelt augmentation of large peak flow events, western Cascades, Oregon. *Water Resour. Res.*, 51(9):7649–7661, 2015. doi: 10.1002/2014WR016877.

Jones, J. A. and Perkins, R. M. Extreme flood sensitivity to snow and forest harvest, western Cascades, Oregon, United States. *Water Resour. Res.*, 46(12):W12512–, December 2010. doi: 10.1029/2009WR008632.

Jordan, P. Meltwater movement in a deep snowpack: 1. Field observations. *Water Resour. Res.*, 19(4):971–978, 1983. doi: 10.1029/WR019i004p00971.

Jordan, R. A one-dimensional temperature model for a snow cover: Technical documentation SNTHERM.89. Technical Report Spec. Rep. No. CRREL-SR-91-16, U.S. Army Cold Reg. Res. Eng. Lab., Hanover, NH, 1991.

Jordan, R. E., Albert, M. R., and Brun, E. Physical processes within the snow cover and their parametrization. In Armstrong, R. L. and Brun, E., editors, *Snow and Climate: Physical Processes, Surface Energy Exchange and Modeling*, chapter 2, pages 12–69. Cambridge University Press, 2008. Chapter 2.4.

Juras, R., Pavlásek, J., Děd, P., Tomášek, V., and Máca, P. A portable simulator for investigating rain-on-snow events. *Zeitschrift für Geomorphologie, Supplementary Issues*, 57(1):73–89, 2013.

Juras, R., Würzer, S., Pavlásek, J., Vitvar, T., and Jonas, T. Rainwater propagation through snowpack during rain-on-snow sprinkling experiments under different snow conditions. *Hydrol. Earth Syst. Sci.*, 21(9):4973–4987, 2017. doi: 10.5194/hess-21-4973-2017.

Juras, R., Pavlásek, J., Vitvar, T., Šanda, M., Holub, J., Jankovec, J., and Linda, M. Isotopic tracing of the outflow during artificial rain-on-snow event. *J. Hydrol.*, 541:1145–1154, 2016. doi: 10.1016/j.jhydrol.2016.08.018.

99

Bibliography

Kampf, S., Markus, J., Heath, J., and Moore, C. Snowmelt runoff and soil moisture dynamics on steep subalpine hillslopes. *Hydrol. Process.*, 29(5):712–723, 2015. doi: 10.1002/hyp.10179.

Katsushima, T., Yamaguchi, S., Kumakura, T., and Sato, A. Experimental analysis of preferential flow in dry snowpack. *Cold Reg. Sci. Technol.*, 85:206–216, 2013. doi: 10.1016/j.coldregions.2012.09.012.

Kattelmann, R. Macropores in snowpacks of Sierra Nevada. *Ann. Glaciol.*, 6:272–273, 1985.

Kattelmann, R. Water release from a forested snowpack during rainfall. *Forest Hydrology and Watershed Management*, pages 265–272, 1987a.

Kattelmann, R. Some measurements of water movement and storage in snow. In *Proceedings of the Symposium at Davos 1986: Avalanche formation, movement and effects. IAHS Publications 162:245-254.*, 1987b.

Kattelmann, R. Spatial variability of snow-pack outflow at a site in Sierra Nevada, U.S.A. *Ann. Glaciol.*, 13:124–128, 1989. doi: 10.3189/S0260305500007758.

Kattelmann, R. Flooding from rain-on-snow events in the Sierra Nevada. *IAHS Publications-Series of Proceedings and Reports-Intern Assoc. Hydrological Sciences*, 239:59–66, 1997.

Kattelmann, R. Snowmelt lysimeters in the evaluation of snowmelt models. *Ann. Glaciol.*, 31 (1):406–410, 2000. doi: 10.3189/172756400781820048.

Kattelmann, R. and Dozier, J. Observations of snowpack ripening in the Sierra Nevada, California, USA. *J. Glaciol.*, 45(151):409–416, 1999. doi: 10.3189/S002214300000126X.

Kirchner, J. W. Catchments as simple dynamical systems: Catchment characterization, rainfall-runoff modeling, and doing hydrology backward. *Water Resources Research*, 45(2), 2009. ISSN 1944-7973. doi: 10.1029/2008WR006912.

Kohl, B., Fuchs, M., Markart, G., and Patzelt, G. Heavy rain on snow cover. *Ann. Glaciol.*, 32(1): 33–38, 2001. doi: 10.3189/172756401781819139.

Köplin, N., Schädler, B., Viviroli, D., and Weingartner, R. Seasonality and magnitude of floods in Switzerland under future climate change. *Hydrol. Process.*, 28(4):2567–2578, 2014. doi: 10.1002/hyp.9757.

Kroczynski, S. A comparison of two rain-on-snow events and the subsequent hydrologic responses in three small river basins in central Pennsylvania. *Eastern Region Technical Attachment*, 4:1–21, 2004.

Lavers, D. A. and Villarini, G. The contribution of atmospheric rivers to precipitation in Europe and the United States. *Journal of Hydrology*, 522:382 – 390, 2015. ISSN 0022-1694. doi: 10.1016/j.jhydrol.2014.12.010.

Lavers, D. A., Allan, R. P, Wood, E. F., Villarini, G., Brayshaw, D. J., and Wade, A. J. Winter floods in Britain are connected to atmospheric rivers. *Geophysical Research Letters*, 38(23), 2011. ISSN 1944-8007. doi: 10.1029/2011GL049783.

Lavers, D. A., Pappenberger, F., and Zsoter, E. Extending medium-range predictability of extreme hydrological events in Europe. *Nat. Commun.*, 5(5382), 2014. doi: 10.1038/n-comms6382.

Leathers, D. J., Kluck, D. R., and Kroczynski, S. The severe flooding event of January 1996 across north-central Pennsylvania. *Bulletin of the American Meteorological Society*, 79(5): 785–797, 1998. doi: 10.1175/1520-0477(1998)079<0785:TSFEOJ>2.0.CO;2.

Lehning, M., Bartelt, P., Brown, B., Russi, T., Stöckli, U., and Zimmerli, M. SNOWPACK calculations for avalanche warning based upon a new network of weather and snow stations. *Cold Reg. Sci. Technol.*, 30(1–3):145–157, 1999. doi: 10.1016/S0165-232X(99)00022-1.

Lehning, M., Bartelt, P., Brown, B., and Fierz, C. A physical SNOWPACK model for the Swiss avalanche warning Part III: Meteorological forcing, thin layer formation and evaluation. *Cold Reg. Sci. Technol.*, 35(3):169–184, 2002a. doi: 10.1016/S0165-232X(02)00072-1.

Lehning, M., Bartelt, P., Brown, B., Fierz, C., and Satyawali, P. A physical SNOWPACK model for the Swiss avalanche warning Part II: Snow microstructure. *Cold Reg. Sci. Technol.*, 35(3): 147–167, 2002b. doi: 10.1016/S0165-232X(02)00073-3.

Liston, G. E. and Elder, K. A meteorological distribution system for high-resolution terrestrial modeling (micromet). *J. Hydrometeorol.*, 7(2):217–234, 2006. doi: 10.1175/JHM486.1.

Liu, A. Q., Mooney, C., Szeto, K., Thériault, J. M., Kochtubajda, B., Stewart, R. E., Boodoo, S., Goodson, R., Li, Y., and Pomeroy, J. The june 2013 alberta catastrophic flooding event: Part 1: Climatological aspects and hydrometeorological features. *Hydrol. Process.*, 30(26): 4899–4916, 2016. doi: 10.1002/hyp.10906.

Lundquist, J. D. and Dettinger, M. D. How snowpack heterogeneity affects diurnal streamflow timing. *Water Resour. Res.*, 41(5), 2005. doi: 10.1029/2004WR003649.

Lundquist, J. D., Cayan, D. R., and Dettinger, M. D. Spring onset in the sierra nevada: When is snowmelt independent of elevation? *J. Hydrometeorol.*, 5(2):327–342, 2004. doi: 10.1175/1525-7541(2004)005<0327:SOITSN>2.0.CO;2.

Lundquist, J. D., Dettinger, M. D., and Cayan, D. R. Snow-fed streamflow timing at different basin scales: Case study of the Tuolumne River above Hetch Hetchy, Yosemite, California. *Water Resour. Res.*, 41(7), 2005. doi: 10.1029/2004WR003933.

Marks, D. and Dozier, J. Climate and energy exchange at the snow surface in the alpine region of the Sierra-Nevada .2. snow cover energy-balance. *Water Resour. Res.*, 28(11):3043–3054, 1992. doi: 10.1029/92WR01483.

Marks, D., Kimball, J., Tingey, D., and Link, T. The sensitivity of snowmelt processes to climate conditions and forest cover during rain-on-snow: a case study of the 1996 Pacific Northwest flood. *Hydrol. Process.*, 12(10-11):1569–1587, 1998. doi: 10.1002/(SICI)1099-1085(199808/09)12:10/11<1569::AID-HYP682>3.0.CO;2-L.

Marks, D., Link, T., Winstral, A., and Garen, D. Simulating snowmelt processes during rain-on-snow over a semi-arid mountain basin. *Ann. Glaciol.*, 32(1):195–202, 2001. doi: 10.3189/172756401781819751.

Marsh, P. and Pomeroy, J. The impact of heterogeneous flow paths on snowmelt runoff chemistry. In *Proc. East. Snow. Conf*, volume 61, pages 231–238, 1993.

Marsh, P. and Woo, M.-K. Wetting front advance and freezing of meltwater within a snow cover 1. observations in the Canadian Arctic. *Water Resour. Res.*, 20(12):1853–1864, 1984. doi: 10.1029/WR020i012p01853.

Marsh, P. Snowcover formation and melt: recent advances and future prospects. *Hydrol. Process.*, 13(14-15):2117–2134, 1999. doi: 10.1002/(SICI)1099-1085(199910)13:14/15<2117::AID-HYP869>3.0.CO;2-9.

Bibliography

Marsh, P. and Woo, M.-K. Meltwater movement in natural heterogeneous snow covers. *Water Resour. Res.*, 21(11):1710–1716, 1985. doi: 10.1029/WR021i011p01710.

Marshall, H., Conway, H., and Rasmussen, L. Snow densification during rain. *Cold Reg. Sci. Technol.*, 30(1–3):35–41, 1999. doi: 10.1016/S0165-232X(99)00011-7.

Mazurkiewicz, A. B., Callery, D. G., and McDonnell, J. J. Assessing the controls of the snow energy balance and water available for runoff in a rain-on-snow environment. *J. Hydrol.*, 354(1–4):1–14, 2008. doi: 10.1016/j.jhydrol.2007.12.027.

McCabe, G. J., Clark, M. P., and Hay, L. E. Rain-on-snow events in the Western United States. *Bulletin of the American Meteorological Society*, 88(3):319–328, 2007. doi: 10.1175/BAMS-88-3-319.

McGurk, B. J. and Marsh, P. Flow-finger continuity in serial thick-sections in a melting Sierran snowpack. In Tonnessen K, T. M. e., Williams MW, editor, *Biogeochemistry of Seasonally Snow Covered Catchments. Proceedings of a Boulder Symposium, July 1995. IAHS-AIHS Publ. 228.*, pages 81–88. Intl. Assoc. Hydrol. Sci.: Wallingford, UK, 1995.

Merz, R. and Blöschl, G. A process typology of regional floods. *Water Resour. Res.*, 39(12), 2003. doi: 10.1029/2002WR001952.

MeteoSwiss. Documentation of MeteoSwiss grid-data products, daily precipitation (final analysis): RhiresD. Technical report, Federal Office of Meteorology and Climatology MeteoSwiss, Zürich, Switzerland, 2013.

Michlmayr, G., Lehning, M., Koboltschnig, G., Holzmann, H., Zappa, M., Mott, R., and Schöner, W. Application of the Alpine 3D model for glacier mass balance and glacier runoff studies at Goldbergkees, Austria. *Hydrol. Process.*, 22(19):3941–3949, 2008. doi: 10.1002/hyp.7102.

Mitterer, C. and Schweizer, J. Glide snow avalanches revisited. *Avalanche Journal*, 102:68–71, 2013.

Moeser, D., Roubinek, J., Schleppi, P., Morsdorf, F., and Jonas, T. Canopy closure, LAI and radiation transfer from airborne lidar synthetic images. *Agricultural and Forest Meteorology*, 197:158 – 168, 2014. doi: 10.1016/j.agrformet.2014.06.008.

Molnar, P., Fatichi, S., Gaál, L., Szolgay, J., and Burlando, P. Storm type effects on super clausius-clapeyron scaling of intense rainstorm properties with air temperature. *Hydrol. Earth Syst. Sci.*, 19(4):1753–1766, 2015. doi: 10.5194/hess-19-1753-2015.

Moore, R. D. and Owens, I. F. Controls on advective snowmelt in a maritime alpine basin. *Journal of Climate and applied Meteorology*, 23(1):135–142, 1984. doi: 10.1175/1520-0450(1984)023<0135:COASIA>2.0.CO;2.

Morin, S., Lejeune, Y., Lesaffre, B., Panel, J.-M., Poncet, D., David, P., and Sudul, M. An 18-yr long (1993-2011) snow and meteorological dataset from a mid-altitude mountain site (Col de Porte, France, 1325 m alt.) for driving and evaluating snowpack models. *Earth System Science Data*, 4(1):13–21, 2012. doi: 10.5194/essd-4-13-2012.

Ohmura, A. Physical basis for the temperature-based melt-index method. *Journal of Applied Meteorology*, 40(4):753–761, 2001. doi: 10.1175/1520-0450(2001)040<0753:PBFTTB>2.0.CO;2.

Orth, R., Staudinger, M., Seneviratne, S. I., Seibert, J., and Zappa, M. Does model performance

improve with complexity? a case study with three hydrological models. *Journal of Hydrology*, 523:147 – 159, 2015. ISSN 0022-1694. doi: 10.1016/j.jhydrol.2015.01.044.

Osterhuber, R. Precipitation intensity during rain-on-snow. In *67th Annual Western Snow Conference*, Proceedings of the 67th Annual Western Snow Conference, pages 153–155, South Lake Tahoe California, 1999.

Osterhuber, R. and Kattelmann, R. Warm storms associated with avalanche hazard in the sierra nevada. In *Proceedings of the International Snow Science Workshop, 27 September–1 October 1998, Sunriver, Oregon*, pages 526–533, 1998.

Parajka, J., Kohnová, S., Bálint, G., Barbuc, M., Borga, M., Claps, P., Cheval, S., Dumitrescu, A., Gaume, E., Hlavčová, K., Merz, R., Pfaundler, M., Stancalie, G., Szolgay, J., and Blöschl, G. Seasonal characteristics of flood regimes across the alpine–carpathian range. *J. Hydrol.*, 394(1):78 – 89, 2010. doi: 10.1016/j.jhydrol.2010.05.015. Flash Floods: Observations and Analysis of Hydrometeorological Controls.

Pfeffer, W. and Humphrey, N. Formation of ice layers by infiltration and refreezing of meltwater. *Ann. Glaciol.*, 26:83–91, 1998. doi: 10.1017/S0260305500014610.

Piaget, N., Froidevaux, P., Giannakaki, P., Gierth, F., Martius, O., Riemer, M., Wolf, G., and Grams, C. M. Dynamics of a local alpine flooding event in october 2011: moisture source and large-scale circulation. *Quarterly Journal of the Royal Meteorological Society*, 141(690): 1922–1937, 2015. ISSN 1477-870X. doi: 10.1002/qj.2496.

Pollack, H. N., Hurter, S. J., and Johnson, J. R. Heat flow from the Earth's interior: analysis of the global data set. *Reviews of Geophysics*, 31(3):267–280, 1993. doi: 10.1029/93RG01249.

Pomeroy, J. W., Fang, X., and Marks, D. G. The cold rain-on-snow event of june 2013 in the canadian rockies - characteristics and diagnosis. *Hydrol. Process.*, 30(17):2899–2914, 2016. doi: 10.1002/hyp.10905.

Prowse, T. D. and Owens, I. F. Energy balance over melting snow, Craigieburn Range, New Zealand. *J. Hydrol. (N.Z.)*, 21(2):133–147, 1982.

Putkonen, J. and Roe, G. Rain-on-snow events impact soil temperatures and affect ungulate survival. *Geophys. Res. Lett.*, 30(4), 2003. doi: 10.1029/2002GL016326. 1188.

R Development Core Team. R: A language and environment for statistical computing, 2016. available at: http://www.R-project.org/ (last access: 6 February 2017).

Radić, V., Cannon, A. J., Menounos, B., and Gi, N. Future changes in autumn atmospheric river events in British Columbia, Canada, as projected by CMIP5 global climate models. *Journal of Geophysical Research: Atmospheres*, 120(18):9279–9302, 2015. doi: 10.1002/2015JD023279. 2015JD023279.

Ralph, F. M., Neiman, P. J., Wick, G. A., Gutman, S. I., Dettinger, M. D., Cayan, D. R., and White, A. B. Flooding on California's Russian River: Role of atmospheric rivers. *Geophysical Research Letters*, 33(13), 2006. ISSN 1944-8007. doi: 10.1029/2006GL026689.

Ralph, F. M., Neiman, P. J., Kiladis, G. N., Weickmann, K., and Reynolds, D. W. A multiscale observational case study of a pacific atmospheric river exhibiting tropical–extratropical connections and a mesoscale frontal wave. *Monthly Weather Review*, 139(4):1169–1189, 2011. doi: 10.1175/2010MWR3596.1.

Bibliography

Richards, L. Capillary conduction of liquids through porous mediums. *J. Appl. Phys.*, 1(5): 318–333, 1931. doi: 10.1063/1.1745010.

Rössler, O., Froidevaux, P., Börst, U., Rickli, R., Martius, O., and Weingartner, R. Retrospective analysis of a nonforecasted rain-on-snow flood in the Alps-a matter of model limitations or unpredictable nature? *Hydrol. Earth Syst. Sci.*, 18(6):2265–2285, 2014. doi: 10.5194/hess-18-2265-2014.

Sandersen, F., Bakkehøi, S., Hestnes, E., and Lied, K. The influence of meteorological factors on the initiation of debris flows, rockfalls, rockslides and rockmass stability. *Publikasjon-Norges Geotekniske Institutt*, 201:97–114, 1997.

Schmucki, E., Marty, C., Fierz, C., and Lehning, M. Evaluation of modelled snow depth and snow water equivalent at three contrasting sites in Switzerland using SNOWPACK simulations driven by different meteorological data input. *Cold Reg. Sci. Technol.*, 99(0): 27–37, 2014. doi: 10.1016/j.coldregions.2013.12.004.

Schmucki, E., Marty, C., Fierz, C., and Lehning, M. Simulations of 21st century snow response to climate change in Switzerland from a set of rcms. *International Journal of Climatology*, 35(11):3262–3273, 2015. doi: 10.1002/joc.4205.

Schneebeli, M. Development and stability of preferential flow paths in a layered snowpack. In Tonnessen, K., Williams, M., and Tranter, M., editors, *Biogeochemistry of Seasonally Snow-Covered Catchments (Proceedings of a Boulder Symposium July 1995)*, pages 89–95, 1995. AHS Publ. no. 228.

Schulla, J. Model description wasim, 2017. available at: www.wasim.ch (last access: 12 Sept 2017).

Seyednasrollah, B. and Kumar, M. Net radiation in a snow-covered discontinuous forest gap for a range of gap sizes and topographic configurations. *Journal of Geophysical Research: Atmospheres*, 119(17):10,323–10,342, 2014. ISSN 2169-8996. doi: 10.1002/2014JD021809.

Singh, P., Spitzbart, G., Hübl, H., and Weinmeister, H. Hydrological response of snowpack under rain-on-snow events: a field study. *J. Hydrol.*, 202(1–4):1–20, 1997. doi: 10.1016/S0022-1694(97)00004-8.

Sommerfeld, R. A., Bales, R. C., and Mast, A. Spatial statistics of snowmelt flow: Data from lysimeters and aerial photos. *Geophys. Res. Lett.*, 21(25):2821–2824, 1994. doi: 10.1029/94GL02493.

Stähli, M., Nyberg, L., Mellander, P.-E., Jansson, P.-E., and Bishop, K. H. Soil frost effects on soil water and runoff dynamics along a boreal transect: 2. simulations. *Hydrol. Process.*, 15(6): 927–941, 2001. doi: 10.1002/hyp.232.

Stearns, C. R. and Weidner, G. A. Sensible and latent heat flux estimates in Antarctica. In Bromwich, D. and Stearns, C. R., editors, *Antarctic Meteorology and Climatology: Studies Based on Automatic Weather Stations*, Antarctic Research Series, pages 109–138. American Geophysical Union, 1993. doi: 10.1029/AR061p0109.

Stimberis, J. and Rubin, C. M. Glide avalanche response to an extreme rain-on-snow event, Snoqualmie Pass, Washington, USA. *J. Glaciol.*, 57(203):468–474, 2011. doi: 10.3189/002214311796905686.

Sturm, M., Holmgren, J., and Liston, G. E. A seasonal snow cover classification system for local to global applications. *Journal of Climate*, 8(5):1261–1283, 1995. doi: 10.1175/1520-0442(1995)008<1261:ASSCCS>2.0.CO;2.

Sturm, M., Goldstein, M. A., and Parr, C. Water and life from snow: A trillion dollar science question. *Water Resour. Res.*, 2017. doi: 10.1002/2017WR020840.

Sui, J. and Koehler, G. Rain-on-snow induced flood events in Southern Germany. *J. Hydrol.*, 252(1-4):205–220, 2001. doi: 10.1016/S0022-1694(01)00460-7.

Sui, J. and Koehler, G. Impacts of snowmelt on peak flows in a forest watershed. *Water resources management*, 21(8):1263–1275, 2007. doi: 10.1007/s11269-006-9080-9.

Surfleet, C. G. and Tullos, D. Variability in effect of climate change on rain-on-snow peak flow events in a temperate climate. *J. Hydrol.*, 479:24–34, 2013. doi: 10.1016/j.jhydrol.2012.11.021.

Techel, F. and Pielmeier, C. Point observations of liquid water content in wet snow – investigating methodical, spatial and temporal aspects. *Cryosphere*, 5(2):405–418, 2011. doi: 10.5194/tc-5-405-2011.

Teufel, B., Diro, G. T., Whan, K., Milrad, S. M., Jeong, D. I., Ganji, A., Huziy, O., Winger, K., Gyakum, J. R., de Elia, R., Zwiers, F. W., and Sushama, L. Investigation of the 2013 alberta flood from weather and climate perspectives. *Climate Dynamics*, 48(9):2881–2899, 2017. doi: 10.1007/s00382-016-3239-8.

Trubilowicz, J. W. and Moore, R. Quantifying the role of the snowpack in generating water available for runoff during rain-on-snow events from snow pillow records. *Hydrological Processes*, 2017. ISSN 1099-1085. doi: 10.1002/hyp.11310.

Unsworth, M. H. and Monteith, J. L. Long-wave radiation at the ground I. Angular distribution of incoming radiation. *Q. J. Roy. Meteor. Soc.*, 101(427):13–24, 1975. doi: 10.1002/qj.49710142703.

Vikhamar-Schuler, D., Hanssen-Bauer, I., Schuler, T., Mathiesen, S., and Lehning, M. Use of a multilayer snow model to assess grazing conditions for reindeer. *Ann. Glaciol.*, 54(62): 214–226, 2013. doi: 10.3189/2013AoG62A306.

Vionnet, V., Brun, E., Morin, S., Boone, A., Faroux, S., Le Moigne, P., Martin, E., and Willemet, J.-M. The detailed snowpack scheme Crocus and its implementation in SURFEX v7.2. *Geosci. Model Dev.*, 5(3):773–791, 2012. doi: 10.5194/gmd-5-773-2012.

Viviroli, D., Zappa, M., Gurtz, J., and Weingartner, R. An introduction to the hydrological modelling system prevah and its pre- and post-processing-tools. *Environmental Modelling & Software*, 24(10):1209 – 1222, 2009. ISSN 1364-8152. doi: 10.1016/j.envsoft.2009.04.001.

Waldner, P. A., Schneebeli, M., Schultze-Zimmermann, U., and Flühler, H. Effect of snow structure on water flow and solute transport. *Hydrol. Process.*, 18(7):1271–1290, 2004. doi: 10.1002/hyp.1401.

Walter, B., Horender, S., Gromke, C., and Lehning, M. Measurements of the pore-scale water flow through snow using Fluorescent Particle Tracking Velocimetry. *Water Resour. Res.*, 49 (11):7448–7456, 2013. doi: 10.1002/2013WR013960.

Wayand, N. E., Lundquist, J. D., and Clark, M. P. Modeling the influence of hypsometry, vegetation, and storm energy on snowmelt contributions to basins during rain-on-snow floods. *Water Resour. Res.*, 51(10):8551–8569, 2015. doi: 10.1002/2014WR016576.

Bibliography

Webb, R. W., Fassnacht, S. R., and Gooseff, M. N. Hydrologic flowpath development varies by aspect during spring snowmelt in complex subalpine terrain. *The Cryosphere Discussions*, 2017:1–24, 2017. doi: 10.5194/tc-2017-12.

Webb, R. W., Fassnacht, S. R., and Gooseff, M. N. Wetting and drying variability of the shallow subsurface beneath a snowpack in California's southern Sierra Nevada. *Vadose Zone Journal*, 14(8), 2015. doi: 10.2136/vzj2014.12.0182.

Westrick, K. J. and Mass, C. F. An evaluation of a high-resolution hydrometeorological modeling system for prediction of a cool-season flood event in a coastal mountainous watershed. *J. Hydrometeorol.*, 2(2):161–180, 2001. doi: 10.1175/1525-7541(2001)002<0161:AEOAHR>2.0.CO;2.

Wever, N., Jonas, T., Fierz, C., and Lehning, M. Model simulations of the modulating effect of the snow cover in a rain-on-snow event. *Hydrology and Earth System Sciences*, 18(11): 4657–4669, 2014a. doi: 10.5194/hess-18-4657-2014.

Wever, N., Schmid, L., Heilig, A., Eisen, O., Fierz, C., and Lehning, M. Verification of the multi-layer snowpack model with different water transport schemes. *Cryosphere*, 9(6):2271–2293, 2015. doi: 10.5194/tc-9-2271-2015.

Wever, N., Vera Valero, C., and Fierz, C. Assessing wet snow avalanche activity using detailed physics based snowpack simulations. *Geophysical Research Letters*, 43(11):5732–5740, 2016a. ISSN 1944-8007. doi: 10.1002/2016GL068428.

Wever, N., Würzer, S., Fierz, C., and Lehning, M. Simulating ice layer formation under the presence of preferential flow in layered snowpacks. *Cryosphere*, 10(6):2731–2744, 2016b. doi: 10.5194/tc-10-2731-2016.

Wever, N., Comola, F., Bavay, M., and Lehning, M. Simulating the influence of snow surface processes on soil moisture dynamics and streamflow generation in an alpine catchment. *Hydrology and Earth System Sciences*, 21(8):4053–4071, 2017. doi: 10.5194/hess-21-4053-2017.

Wever, N. *Liquid water flow in snow and hydrological implications.* PhD thesis, École Polytechnique Fédérale de Lausanne (EPFL), School of Architecture, Civil and Environmental Engineering, Lausanne, Switzerland, 2014.

Wever, N., Fierz, C., Mitterer, C., Hirashima, H., and Lehning, M. Solving richards equation for snow improves snowpack meltwater runoff estimations in detailed multi-layer snowpack model. *Cryosphere*, 8(1):257–274, 2014b. doi: 10.5194/tc-8-257-2014.

White, A. B., Gottas, D. J., Strem, E. T., Ralph, F. M., and Neiman, P. J. An automated brightband height detection algorithm for use with doppler radar spectral moments. *Journal of Atmospheric and Oceanic Technology*, 19(5):687–697, 2002. doi: 10.1175/1520-0426(2002)019<0687:AABHDA>2.0.CO;2.

Whitfield, P. H. and Pomeroy, J. W. Changes to flood peaks of a mountain river: implications for analysis of the 2013 flood in the upper bow river, canada. *Hydrol. Process.*, 30(25):4657–4673, 2016. doi: 10.1002/hyp.10957.

Wickham, H. *ggplot2: Elegant Graphics for Data Analysis.* Use R! Springer-Verlag New York, 2009.

Williams, M. W., Sommerfeld, R., Massman, S., and Rikkers, M. Correlation lengths of meltwater flow through ripe snowpacks, Colorado Front Range, USA. *Hydrol. Process.*, 13(12-13):1807–1826, 1999. doi: 10.1002/(SICI)1099-1085(199909)13:12/13<1807::AID-HYP891>3.0.CO;2-U.

Williams, M. W., Rikkers, M., and Pfeffer, W. T. Ice columns and frozen rills in a warm snowpack, Green Lakes Valley, Colorado, USA. *Hydrology Research*, 31(3):169–186, 2000.

Williams, M. W., Erickson, T. A., and Petrzelka, J. L. Visualizing meltwater flow through snow at the centimetre-to-metre scale using a snow guillotine. *Hydrol. Process.*, 24(15):2098–2110, 2010. doi: 10.1002/hyp.7630.

Winther, J.-G. and Hall, D. K. Satellite-derived snow coverage related to hydropower production in norway: Present and future. *International Journal of Remote Sensing*, 20(15-16):2991–3008, 1999. doi: 10.1080/014311699211570.

WSL Institute for Snow and Avalanche Research SLF. *Meteorological and snowpack measurements from Weissfluhjoch, Davos, Switzerland*. WSL Institute for Snow and Avalanche Research SLF, 2015. doi: 10.16904/1. Dataset.

Würzer, S., Wever, N., Juras, R., Lehning, M., and Jonas, T. Modelling liquid water transport in snow under rain-on-snow conditions - considering preferential flow. *Hydrol. Earth Syst. Sci.*, 21(3):1741–1756, 2017. doi: 10.5194/hess-21-1741-2017.

Würzer, S. and Jonas, T. Der Einfluss von Schneedeckeneigenschaften auf die Abflussgenerierung während Regen-auf-Schnee Ereignissen in der Schweiz. *Wasser Energie Luft*, 3: 197–202, 2017.

Würzer, S., Jonas, T., Wever, N., and Lehning, M. Influence of initial snowpack properties on runoff formation during rain-on-snow events. *J. Hydrometeorol.*, 17(6):1801–1815, 2016. doi: 10.1175/JHM-D-15-0181.1.

Yamaguchi, S., Hirashima, H., Sato, A., and Adachi, S. The relationship between preferential flow in snow cover and weather conditions. In *Proceedings of the 2012 International Snow Science Workshop*, 2012a.

Yamaguchi, S., Watanabe, K., Katsushima, T., Sato, A., and Kumakura, T. Dependence of the water retention curve of snow on snow characteristics. *Ann. Glaciol.*, 53(61):6–12, 2012b. doi: 10.3189/2012AoG61A001.

Ye, H., Yang, D., and Robinson, D. Winter rain on snow and its association with air temperature in northern Eurasia. *Hydrol. Process.*, 22(15):2728–2736, 2008. doi: 10.1002/hyp.7094.

Curriculum Vitae

PERSONAL INFORMATION	**Sebastian Würzer**

Adress: Flüelapassstrasse 5, 7260 Davos Dorf (Switzerland)

Phone: +49 1631639889

E-Mail: sebastian.wuerzer@gmail.com

Sex: male | Date of birth: 14. Mai 1985 | Nationality: German

EDUCATION AND TRAINING

Sep 2001 – Jul 2004 Grammar School (Abitur), Technisches Gymnasium Leutkirch, Leutkirch i.A. (Germany)

Oct 2006 – Sep 2009 Bachelor of Science in Geoecology, Universität Bayreuth (Germany)
Thesis at the department of hydrology: *"Charakterisierung der Anbindung eines Baches an ein Niedermoor (Schlöppnerbrunnen) im Wassereinzugsgebiet des Lehstenbachs"*

Sep 2009 – May 2013 Master of Science in Hydrology, Albert-Ludwigs-Universität Freiburg (Germany)
Thesis: *„Der Einfluss von Klimaveränderungen auf Regen-auf-Schnee Ereignisse: Eine modellbasierte Attribution"*

Jan 2011 – Jul 2011 ERASMUS student exchange program, Universitetet i Oslo, Oslo (Norway),
Department of Geosciences

Oct 2013 till now PhD student in Environmental Engineering
École Polytechnique Fédérale de Lausanne (EPFL), Lausanne, Switzerland

EMPLOYMENT

Sep 2004 – Dec 2005 Civil service and nursing assistant, Seniorenzentrum Carl-Josef, Leutkirch

Mar 2006 – Jun 2006 Naturschutzwart at Mellumrat e.V., Varel-Dangast

May 2008 – Aug 2008 Student assistant, Limnological Research Station, Department of Hydrology, University of Bayreuth
Fieldwork, installation of measurement systems, laboratory work

Feb 2009 – May 2009 Internship, Planungsbüro OPUS, Bayreuth (Germany)
River habitat surveys, ArcGIS, watercourse development plans.

Jul 2010 – Sep 2010 Internship, Dr. Ebel & Co. Ingenieurs-GmbH, Bad Wurzach - Arnach (Germany)
Dynamic soil probing, core soundings, groundwater observations.

Oct 2011 – Aug 2013 Research Assistant
Forstliche Versuchs- und Forschungsanstalt Baden-Württemberg (FVA), Freiburg (Germany)
data bases, user support (library)

Oct 2013 till now PhD student
Snow Hydrology Research Group, WSL Institute for Snow and Avalanche Research SLF, Davos (Switzerland)

PERSONAL SKILLS

Mother tongue(s)	German	
Other Languages	English	Proficient User
	Norwegian (Bokmål)	Basic User
	French	Basic User

Organisational work   Event management at the public charities Glashaus e.V. Bayreuth and Förderkreis-Kultur-Reichenhofen e.V. for several years.

Computer skills   Technical software: SNOWPACK, GIS (ArcGIS 9.x und 10).
Programming languages R, MATLAB, C/C++, Python and Bash Script.
OS etc.: MS Windows, Linux, MS Office, LaTeX

Hobbies   Skiing, hiking, mountain biking and music (guitar and bass)

PUBLICATIONS

Juras, R., **Würzer, S.**, Pavlásek, J., Vitvar, T., and Jonas, T. (2017): Rainwater propagation through snowpack during rain-on-snow sprinkling experiments under different snow conditions, Hydrol. Earth Syst. Sci., 21(9):4973–4987, 2017. doi: 10.5194/hess-21-4973-2017

Wever, N., **Würzer, S.**, Fierz, C., and Lehning, M (2016).: Simulating ice layer formation under the presence of preferential flow in layered snow covers, Cryosphere, doi:10.5194/tc-10-2731-2016.

Würzer, S., Jonas, T., Wever, N., and Lehning, M. (2016): Influence of initial snowpack properties on runoff formation during rain-on-snow events, J. Hydrometeorol., 17, 1801-1815, doi: 10.1175/JHM-D-15-0181.1.

Würzer, S., Wever, N., Juras, R., Lehning, M., and Jonas, T (2017).: Modeling liquid water transport in snow under rain-on-snow conditions - considering preferential flow, Hydrol. Earth Syst. Sci., 21, 1741-1756, doi:10.5194/hess-21-1741-2017.

Würzer, S., and Jonas, T (2017).: Spatio-temporal aspects of snowpack runoff formation during rain-on-snow, Submitted to Hydrological Processes.

Würzer, S., and Jonas, T (2017).: Der Einfluss von Schneedeckeneigenschaften auf die Abflussgenerierung während Regen-auf-Schnee-Ereignissen, Fachzeitschrift <<Wasser Energie Luft>>, 3,197-202.

CONFERENCE PRESENTATIONS

Würzer, S., Jonas, T.: **Rain-on-snow: An analysis of 1300 events at various meteorological and snowpack conditions** (Oral presentation), European Geosciences Union General Assembly, Vienna, Austria, April 2015.

Würzer, S., Wever, N., Juras, R., Lehning, M., Jonas, T.: **Modeling liquid water transport in snow under rain-on-snow conditions considering preferential flow** (Poster)**,** European Geosciences Union General Assembly, Vienna, Austria, April 2016.

Würzer, S., Wever, N., Juras, R., Fierz, C., Lehning, M., Jonas, T.: **The role of preferential flow in modeling liquid water transport and ice layer formation in snow** (Poster), American Geophysical Union Fall Meeting, San Francisco, USA, December 2016.